2014

Proliferation and Survival Mechanisms in Soft Tissue Sarcoma and Glioblastoma Tumors

Vera Mucaj
University of Pennsylvania, vera.mucaj@gmail.com

www.manaraa.com

Proliferation and Survival Mechanisms in Soft Tissue Sarcoma and Glioblastoma Tumors

Abstract

Soft tissue sarcomas and glioblastomas are two deadly tumors that are characterized by aggressive overproliferation, and regions of severe intratumoral nutrient and oxygen deprivation. The mechanisms by which tumors evade proliferation control signals and survive in a hostile microenvironment are active areas of investigation. This work describes two projects investigating loss of proliferation control in soft tissue sarcoma, as a result of Hippo pathway deregulation, and mechanisms of survival under stress in glioblastoma, as a result of decreased microRNA-124 (miR-124) levels. First, we demonstrate that the Hippo pathway is deregulated in soft tissue sarcoma patient samples, leading to overexpression of the Hippo effector YAP. YAP, a transcriptional coactivator, binds to TEAD proteins in the nucleus and controls the transcription of multiple pro-proliferation and anti-apoptosis targets, including the transcription factor FOXM1. Interestingly, we show that FOXM1 physically interacts with the TEAD/YAP complex, creating a powerful pro-proliferation complex. FOXM1 genetic deletion and pharmacologic inhibition resulted in decreased sarcoma tumor size, suggesting that FOXM1 inhibition is a viable potential sarcoma treatment. Second, we show that ectopically expressing miR-124 in glioblastoma cells leads to increased cell death. We identify three factors (SERP1, TEAD1, and MAPK14) as direct miR-124 targets and partial effectors of cell survival under stress. Inhibition of these targets recapitulates the miR-124 cell death phenotype under stress, and decreased glioma growth in vivo. Importantly, miR-124 ectopic expression results in increased survival in an in vivo orthotopic intracranial glioma model, suggesting that expression of miR-124, or inhibition of its downstream targets, is an attractive way of targeting glioblastoma cells residing in hypoxic/ischemic regions, and ultimately a method of investigating novel glioblastoma treatments.

Degree Type
Dissertation

Degree Name
Doctor of Philosophy (PhD)

Graduate Group
Cell & Molecular Biology

First Advisor
Celeste Simon

Keywords
cancer, glioblastoma, hippo, hypoxia, micro-RNA, sarcoma

Subject Categories
Cell Biology | Molecular Biology

PROLIFERATION AND SURVIVAL MECHANISMS IN SOFT TISSUE

SARCOMA AND GLIOBLASTOMA TUMORS

Vera Mucaj

A DISSERTATION

in

Cell and Molecular Biology

Presented to the Faculties of the University of Pennsylvania

in

Partial Fulfillment of the Requirements for the

Degree of Doctor of Philosophy

2014

Supervisor of Dissertation

_____

M. Celeste Simon, PhD
Scientific Director and Investigator
Abramson Family Cancer Research Institute
Professor of Cell and Developmental Biology

Graduate Group Chairperson

_____

Daniel S. Kessler, PhD
Associate Professor of Cell and Developmental Biology

Dissertation Committee

Ben Z. Stanger, MD, PhD (Chair)
Associate Professor of Medicine and Cell and Developmental Biology
Morris J. Birnbaum, MD, PhD
Emeritus Professor of Medicine
Sarah Millar, PhD
Professor of Dermatology
Eric W. Witze, PhD
Assistant Professor of Cancer Biology

ACKNOWLEDGMENT

I am indebted to my mentor, Celeste Simon, for giving me the opportunity and freedom to ask scientific questions that were important to me, and for providing me with the support and encouragement to see my projects to completion. Her enthusiasm, perseverance, incredible management skills, and immense love of science are qualities I deeply admire. Brian Keith – thank you for helping me learn how to effectively turn incongruent thoughts in my head into concise and comprehensible grants and manuscripts.

I have been privileged to have a group of incredibly insightful scientists as part of my dissertation committee. Ben Stanger, who chaired our meetings, Morrie Birnbaum, Sarah Millar and Eric Witze provided me with thoughtful supervision and good advice, and I am deeply grateful for their insights and support.

I would like to thank every member of the Simon Laboratory past and present – you have been inspiring colleagues and even better friends. Michael Nakazawa, Bo Qiu, Bo Li, Dion Giannoukos, Nicolas Skuli, Sam Lee, Jess Shay, and Kevin Biju – thank you for your time, your technical expertise, and your enthusiasm for my projects. A special acknowledgment goes to Lijoy Mathew and Karin Eisinger, with whom I have worked closely in the past five years. You taught me how to think critically about scientific discoveries related to glioblastoma and soft tissue sarcoma, and your devotion to helping me succeed has not been overlooked or ignored. I am incredibly indebted to both of you, and wish you most successful careers in your next adventures.

Finally, I am forever appreciative for my family: Arturo, Silvia, and Elvis Mucaj. They have sacrificed to support me in more ways than I even deserve, across both sides of the Atlantic. I have been the luckiest – thank you.

ABSTRACT

PROLIFERATION AND SURVIVAL MECHANISMS IN SOFT TISSUE SARCOMA AND GLIOBLASTOMA TUMORS.

Vera Mucaj

M. Celeste Simon

Soft tissue sarcomas and glioblastomas are two deadly tumors that are characterized by aggressive overproliferation, and regions of severe intratumoral nutrient and oxygen deprivation. The mechanisms by which tumors evade proliferation control signals and survive in a hostile microenvironment are active areas of investigation. This work describes two projects investigating loss of proliferation control in soft tissue sarcoma, as a result of Hippo pathway deregulation, and mechanisms of survival under stress in glioblastoma, as a result of decreased *microRNA-124* (*miR-124*) levels. First, we demonstrate that the Hippo pathway is deregulated in soft tissue sarcoma patient samples, leading to overexpression of the Hippo effector YAP. YAP, a transcriptional coactivator, binds to TEAD proteins in the nucleus and controls the transcription of multiple pro-proliferation and anti-apoptosis targets, including the transcription factor FOXM1. Interestingly, we show that FOXM1 physically interacts with the TEAD/YAP complex, creating a powerful pro-proliferation complex. FOXM1 genetic deletion and pharmacologic inhibition resulted in decreased sarcoma tumor size, suggesting that FOXM1 inhibition is a viable potential sarcoma treatment. Second, we show that ectopically expressing *miR-124* in glioblastoma cells leads to increased cell death. We identify three factors (*SERP1*, *TEAD1*, and *MAPK14*) as direct *miR-124* targets and partial effectors of cell survival under stress. Inhibition of these targets recapitulates the *miR-124* cell death phenotype under stress, and decreased glioma growth in vivo. Importantly, miR-124 ectopic expression results in increased survival in an in vivo orthotopic intracranial glioma model, suggesting that expression of miR-124, or inhibition of its downstream targets, is an attractive way of targeting glioblastoma cells residing in hypoxic/ischemic regions, and ultimately a method of investigating novel glioblastoma treatments.

iii

TABLE OF CONTENTS

LIST OF TABLES

LIST OF ILLUSTRATIONS

CHAPTER 1

Growth control and survival in soft tissue sarcoma and glioblastoma.

INTRODUCTION

Proliferation and cell survival are two key processes required for all living cells. Appropriate control of the mechanisms governing proliferation and survival is necessary for proper cellular and organismic homeostasis. Malignant tumors are characterized by their ability to overcome restrictions on growth and proliferation and by their ability to survive the microenvironment arising as a result of abnormal proliferation. These properties have been extensively reviewed in the cancer biology literature, and are tightly connected to the "hallmarks" of cancer characterized by Hanahan and Weinberg, which generally define our current understanding of tumor initiation and progression. (Hanahan and Weinberg, 2000, 2011).

How tumor cells evade signals that restrict proliferation and how they survive under stress are two important phenomena in the field of cancer research. These are complex phenotypes, resulting in part due to universal mechanisms co-opted by cancer cells. However, some mechanisms are specific to a subset of cancers, depending on the oncogenic and tumor suppressive networks aberrantly regulated in a particular tumor. Of particular interest are the mechanisms that govern proliferation and survival in the highly aggressive mesenchymal glioblastoma multiforme and soft tissue sarcoma tumors. While these tumors have disparate etiologies and treatment modalities, they also possess some remarkably similar tissue architecture and molecular signatures. Besides the common expression of genes associated with mesenchymal tissues, both glioblastomas and soft tissue sarcomas (i.e. Undifferentiated Pleomorphic Sarcoma (UPS)) are characterized by high rates of proliferation, and perhaps subsequent to hyperproliferation, the presence of a very hypoxic/ischemic microenvironment (Eisinger-Mathason et al., 2013; Mathew et al., 2014b; Mucaj et al., 2014). This body of work

1

aims to answer the following two questions (1) which pathways drive proliferation and (2) how is survival under an aggressive microenvironment achieved in mesenchymal tumors?

One important pathway involved in proliferation control is the Hippo pathway. In this chapter, I will introduce background information on the Hippo pathway and its roles in regulating cell proliferation and tissue size determination (Part I). Additionally, I will outline how microRNA expression changes can modulate cellular survival, especially under nutrient, growth factor and oxygen deprivation (Part II). As the work comprising this dissertation has been conducted in the soft tissue sarcoma and glioblastoma models, two types of tumors expressing a mesenchymal signature, background information on sarcoma/glioblastoma will follow in Chapters II and III, where I describe how the Hippo pathway is deregulated in soft tissue sarcoma, and how microRNA-*124* loss leads to glioblastoma survival under nutrient and oxygen deprivation (Mucaj et al., 2014).

PART I. THE HIPPO PATHWAY AND PROLIFERATION CONTROL

A. Hippo Pathway Overview

Tissue size control is an intriguing developmental biology puzzle. Through tight control of proliferation signals, the Hippo pathway is currently thought to be a key regulator of tissue and organ size (Mo et al., 2014; Pan, 2010). Originally delineated in the *Drosophila Melanogaster* model, the Hippo pathway is evolutionarily conserved from premetazoan ameboid species to mammalians (Sebe-Pedros et al., 2012). The role of the Hippo pathway has been studied extensively in the past two decades, starting from the original discovery of the Yes Associated Protein (YAP) in a screen for proteins binding to the Yes kinase (Sudol, 1994). It took more than a decade between YAP description and the discovery that the conserved Hippo pathway kinase cascade inhibited YAP, as well as YAP homolog Transcription coactivator with PDZ motif (TAZ), to blunt proliferation signaling within a cell (Dong et al., 2007; Varelas, 2014).

2

In mammals, the pathway is thought to respond to contact inhibition or diffusible extracellular signals by activating the Mammalian sterile 20-like kinases 1 and 2 (MST1/MST2). While these upstream events are still incompletely understood and are an area of active investigation (Park and Guan, 2013), intracellular proteins including Neurofibromatosis II (NF2, also known as Merlin), Expanded (Ex) and Kidney and Brain Protein (KIBRA, also known as WWC1) have been shown to be crucial mediators linking the extracellular signals to YAP inhibition (Genevet et al., 2010; Hamaratoglu et al., 2006; Yu et al., 2010; Zhang et al., 2010). MST1/2 are dependent upon the Salvador homolog 1 (SAV1, also called WW45) adaptor for their kinase activity (Callus et al., 2006; Pan, 2010). In turn, the MST/SAV1 complex phosphorylates and activates the Large Tumor Suppressor kinases 1 and 2 (LATS1/2), which are bound by the MOB1 adaptor complex (Chan et al., 2005). The LATS complex phosphorylates YAP, leading to recognition and binding by 14-3-3 proteins, and resulting in YAP cytoplasmic sequestration or proteasomal degradation (Hao et al., 2008; Zhao et al., 2010b; Zhao et al., 2007). Upon pro-proliferation signaling, the Hippo pathway is inactivated, allowing unphosphorylated YAP to translocate into the nucleus, where it binds the Tea Domain Family of transcription factors (TEAD1-4) and directs the transcription of multiple factors required for proliferation (Zhao et al., 2008c) and survival (Dong et al., 2007).

B. Hippo pathway members and regulation

Many factors are implicated in the overarching Hippo signaling pathway. This section highlights the importance of many Hippo components in cellular homeostasis maintenance, and underscores the importance of an intact Hippo pathway in preventing deregulation that may result in tumorigenesis. Table 1 provides an overview of the players currently linked to the Hippo pathway. Below, I outline some key players involved in the Hippo core kinase complex, the upstream Hippo regulators, as well as the downstream nuclear effectors. These players are delineated in the schematic of the Hippo pathway in Fig. 1.

The Hippo core kinase complex.

3

The Drosophila Hippo pathway is composed of a kinase cascade including the Hippo (Hpo) kinase and its adaptor Salvador, as well as the Drosophila LATS (dLATS) or Warts (Wts) kinase and its adaptor Mob as tumor suppressor (MATS or MOB1) (Pan, 2007). The drosophila kinases were discovered in screens for pro-proliferation factors. Hpo and Wts mutants led to hyperproliferation of the Drosphila imaginal disc (Harvey et al., 2003; Jia et al., 2003; Udan et al., 2003; Wu et al., 2003). These studies and others demonstrated that Hpo and Wts controlled the function of Yorkie (Yki), a transcriptional coactivator whose loss leads to decreased tissue proliferation in drosophila (Huang et al., 2005). The Ser/Thre kinases MST1 and 2 were identified as the Hpo counterparts in mammals, whereas YAP was identified as the Yki ortholog, and MST1/2 – mediated phosphorylation of the mammalian Wts homologs Lats1 and 2 was found to be necessary for YAP cytoplasmic retention (Dong et al., 2007; Pan, 2007).

Mst kinase activation is mediated through autophosphorylation (Praskova et al., 2004), but adaptor proteins are necessary for this activation to occur. Using biochemistry and molecular biology approaches, Callus and colleagues showed that human SAV1 binds to MST1/2 at the Mst C-terminal coiled-coiled domain and this association causes both MST and SAV1 phosphorylation. The phosphorylated complex is considered activated, and SAV1 loss abrogates MST activation (Callus et al., 2006). In addition to autophosophorylation, the MST/SAV1 complex separately phosophorylates the MOB1 complex as well as the LATS kinases. Similarly to Mst/Sav1, human MOB1 has been shown to be necessary for LATS activation (Hergovich et al., 2006). Further studies have suggested that Mst/Sav/Lats/Mob1 all bind as part of a complex which dynamically controls cell proliferation fate (Sudol and Harvey, 2010).

While there have been instances where MST1/2-mediated LATS phosphorylation is not necessary for YAP inhibition, particularly in Mouse Embryonal Fibroblasts (MEFs) (Zhou et al., 2009), the MST/SAV1-LATS/MOB signaling is considered the core of the Hippo pathway, and is the best understood signaling module within the pathway (Pan, 2010; Park and Guan, 2013; Yu and Guan, 2013)

4

Upstream regulators and intracellular mediators.

To date, the full spectrum of events leading to Hippo pathway activation remains incompletely understood. *In vitro*, high cell density/confluency has been repeatedly shown to affect YAP phosphorylation and cytoplasmic retention, suggesting that cell contact inhibition activates the Hippo pathway (Dupont et al., 2011; Overholtzer et al., 2006; Zhao et al., 2007). It is possible that this phenotype is mediated through polarity/tight junction regulation and mechanotransduction.

Drosophila genetic screens have provided some early insight into regulators upstream of the core kinase cassette, implicating key players involved in cell polarity (Yu and Guan, 2013). Several parallel studies identified the Fat (Ft) and Dachsous (Ds) tumor suppressors, two membrane proteins involved in the establishment of Planar Cell Polarity (PCP), as well as their downstream effectors, as YAP negative regulators (Bennett and Harvey, 2006; Feng and Irvine, 2007; Silva et al., 2006). While the PCP is largely considered a property of epithelial cells, this network is also present in mesenchymal cells. In fact, the PCP is thought to be important during gastrulation and the formation of the mesenchyme (Mlodzik, 2002), for cellular interchalation (Simons and Mlodzik, 2008), directed movement (Tada and Kai, 2012), neural crest migration (Clay and Halloran, 2011) and myogenesis (Gros et al., 2009). The current understanding is that Ft/Ds signaling affects the Hippo pathway through activating the core kinase cassette, either directly by activating Wts or through Dachs, an atypical myosin (Yu and Guan, 2013). The mammalian PCP complex is more complicated, with several Ft and Ds orthologs (Bossuyt et al., 2014). Nonetheless, the upstream regulation of Hippo by PCP components seems to be conserved in mammalian cells.

In addition to PCP, the apical-basal polarity complexes are also significant for Hippo pathway activity. Apical-basal polarity is determined by the localization of tight and adherens junctions (TJ, AJ) (McCaffrey and Macara, 2011). TJ and AJ complexes are important for maintaining epithelial tissue organization, and disruption of TJ and AJ is one of the key steps in

5

Epithelial-to-Mesenchymal transition, both in development and tumorigenesis (Lamouille et al., 2014). Varelas and colleagues showed that perturbation of TJ or AJs leads to nuclear YAP localization (Varelas et al., 2010). This finding is supported by the fact that key components of TJ and AJ complexes have been associated with Hippo pathway activation. Three of these components are NF2/Merlin, Expanded (Ex) and Kibra.

NF2, Ex and Kibra are intracellular mediators thought to localize at the apical side of the cell membrane of polarized epithelial cells (Genevet et al., 2010; Hamaratoglu et al., 2006; Yu and Guan, 2013). The localization of NF2/Ex/Kibra in mesenchymal cells is unclear, but the expression of at least NF2 has been described in mesenchymal tissues (den Bakker et al., 1995; McClatchey et al., 1998; Shaw et al., 1998). NF2, Ex and Kibra have been shown to control proliferation rates in normal cells (Baumgartner et al., 2010; Genevet et al., 2010; Ji et al., 2012; McCartney et al., 2000) and are considered to be tumor suppressors (Yi et al., 2011; Yu et al., 2010; Zhang et al., 2010).

Other players of TJ and AJ complexes have been associated with physical restriction of YAP into the cytoplasm. YAP has been shown to interact with Angiomotin proteins (AMOT, AMOTL1 and AMOTL2, which are considered AJ members) and possibly with Zona Occludens proteins (ZO1, ZO2, TJ members) as well as non-receptor tyrosine phosphatase 14 (PTPN14, also found at the TJ) (Wang et al., 2012; Yi et al., 2013; Zhao et al., 2011a). Initial studies identified AMOTs as negative regulators of YAP, which functioned by sequestering YAP to the AJ. However, the relationship between YAP and AMOT proteins is more nuanced, as a further study has demonstrated cooperation between YAP and AMOT as a transcriptional complex in the nucleus (Yi et al., 2013)

As hinted by the *in vitro* observation that cell density affects YAP localization, mechanical cues are crucial to Hippo pathway function. Cells modify shape in response to stiffness changes caused by the extracellular matrix (ECM) as well as in response to contact with neighboring cells, and these changes get transduced into signaling via cytoskeleton alterations. Pointedly, contact

6

inhibition loss is a key property of cancer cells (Hanahan and Weinberg, 2011). Various studies have linked YAP and TAZ nuclear/cytoplasmic transolcation to mechanotransduction, whereby stiffer surfaces lead to more nuclear YAP and TAZ localization, and, vice versa, decreased stiffness causing YAP/TAZ cytoplasmic retention (Calvo et al., 2013; Dupont et al., 2011; Wada et al., 2011; Zhao et al., 2012). Interestingly, Dupont and colleagues showed that modulating stiffness *in vitro* is sufficient to cause mesenchymal stem cell (MSC) differentiation into adipogenic or osteogenic lineages in a YAP/TAZ dependent manner (Dupont et al., 2011).

In addition to responding to mechanical cues, it has been hypothesized that the Hippo pathway could be modulated by diffusible signals (ie ligand-receptor interactions). Recently, G-protein coupled receptor (GPCR) ligands have been identified as the first extracellular factors responsible for Hippo pathway activation (Miller et al., 2012; Mo et al., 2012; Yu et al., 2012). These ligands include sphingosine 1 phosphate (S1P) phosphate and lipophosphatidic acid (LPA), which signal to activate multiple GPCRs (Yu and Guan, 2013). GPCR signaling-mediated YAP control is complex, as some GPCRs are thought to inhibit YAP, whereas others activate it (Yu et al., 2012). These recent discoveries have introduced a series of new questions about normal Hippo pathway regulation that are currently under investigation by several groups. Proper identification of the role for each GPCR Ligand/Receptor pair in YAP regulation is necessary before these insights are translated into cancer biology studies, especially considering that many of these receptors are expressed in both epithelial and mesenchymal cancer cells.

While above regulators have focused on Hippo pathway activation/YAP negative regulation, it is increasingly appreciated that growth factor signaling can also affect YAP activation either directly or by inhibiting the Hippo pathway (Fan et al., 2013). The current understanding is that growth factor signaling (for example, EGFR signaling) affects Hippo pathway function by engaging the Ras/MAP kinase and the PI3 kinase signal transduction wings (Gumbiner and Kim, 2014).

7
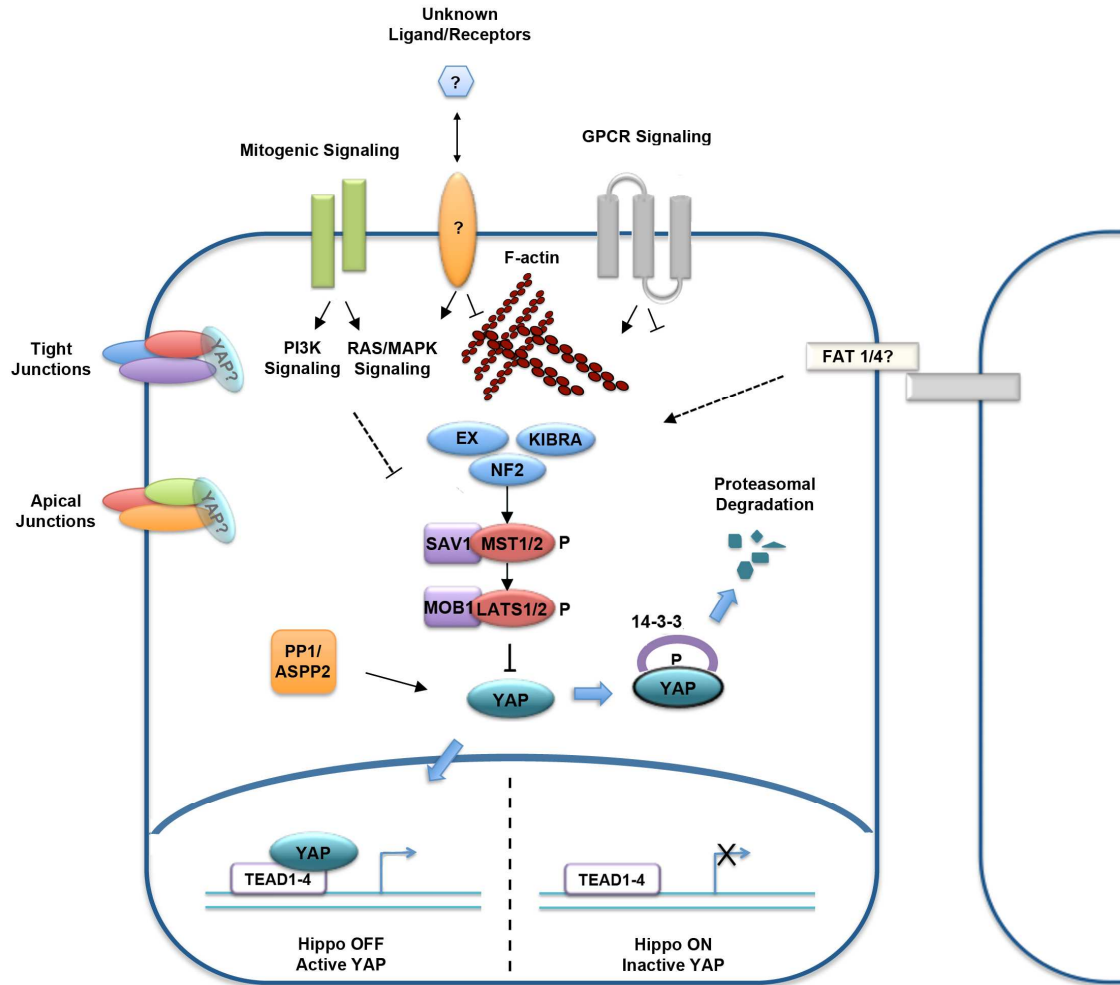
Figure 1. A schematic of the mammalian Hippo Pathway. The Hippo pathway is regulated by an extensive group of upstream signals, including factors involved in apicobasal polarity (tight and adherens junction), planar cell polarity (Fat signaling), GPCR and mitogenic signals, and mechanic cues leading to F-actin/cytoskeletal rearrangements. These upstream signals either activate or inhibit the Hippo core kinase cassette, frequently involving intracellular mediators such as NF2, KIBRA and EX. The core kinase cassette includes MST1/2, SAV1, LATS1/2 and the MOB1 complex. Upon of phosphorylation-mediated kinase activation, LATS1/2 phosphorylate and inhibit YAP. Phospho-YAP is recognized by 14-3-3 adaptor proteins and sequestered to the cytoplasm, where it can further be targeted for proteasomal-mediated degradation. Phosphatases such as PP1/ASPP2 can counteract YAP inhibition. Unphosphorylated YAP translocates into the nucleus, binds to transcription factors such as TEAD1-4 and promotes the transcription of many pro-proliferation and anti-apoptotic targets. Many members of the Hippo pathway remain unknown (designated by a question mark). Arrows indicate activation whereas blunted lines indicate inhibition. A more detailed look at known Hippo pathway members can be found in Table 1.

Drosophila	Mammals	Protein type	Hippo pathway role
Hpo (Hippo)	MST1/2	Kinase	Core kinase casette
Sav (Salvador	Sav1	Adaptor	Core kinase casette
Wts (Warts)	Lats1/2	Kinase	Core kinase casette
Mats	Mob1 (a and b)	Adaptor	Core kinase casette
Yki (Yorkie)	YAP/TAZ	Transcriptional coactivator/WW domain protein	Downstream effector
Sd (Scalloped)	TEAD1-4	Transcription factor	Downstream effector
Crb (Crumbs)	Crb1–3	Transmembrane protein	Upstream component - Apical-basal polarity
Ex (Expanded)	Frmd6	FERM-domain protein	Upstream component - Apical-basal polarity
Mer (Merlin)	NF2 (Mer)	FERM-domain protein	Upstream component - Apical-basal polarity
Kibra	Kibra	WW domain protein	Upstream component - Apical-basal polarity
aPKC	aPKC	atypical Ser/Thr kinase	Upstream component - Apical-basal polarity
Baz (Bazooka)	PAR 3	Scaffold protein	Upstream component - Apical-basal polarity
Par6	PAR 6	Scaffold protein	Upstream component - Apical-basal polarity
Sdt (Stardust)	PALS1	Membrane-associated guanylate kinase homologs	Upstream component - Apical-basal polarity
Scrib (Scribble)	Scrib	Scaffold protein	Upstream component - Apical-basal polarity
Dlg	Dlg	Membrane-associated guanylate kinase homologs	Upstream component - Apical-basal polarity
Lgl (Discs large)	Lgl	Scaffold protein	Upstream component - Apical-basal polarity
?	AMOT (angiomotin)	Peripheral membrane protein	Upstream component - Apical-basal polarity
Pez	PTPN14	Phosphatase	Upstream component - Apical-basal polarity
Jub	Ajuba/LIMD1/WTIP	LIM-domain protein	Upstream component - Apical-basal polarity
α-Catenin	α-Catenin	Linking protein/transcription factor	Upstream component - Apical-basal polarity
β-Catenin	β-Catenin	Linking protein/transcription factor	Upstream component - Apical-basal polarity
ZO-1	ZO-1	Scaffold protein	Upstream component - Apical-basal polarity
ZO-2	ZO-2	Scaffold protein	Upstream component - Apical-basal polarity
E-cad	E-cad (E-cadherin)	Transmembrane protein	Upstream component - Apical-basal polarity
Fat	Fat1-4	Atypical Cadherin	Upstream component - PCP
Ds (Dachsous)	Dchs1/2	Atypical Cadherin	Upstream component - PCP
Fj (four-jointed)	Fjx1	Ser/Thr kinase	Upstream component - PCP
Dachs	?	Atypical Myosin	Upstream component - PCP
Zyx (zyxin)	Zyxin/Lpp/Trip6	Focal Adhesion protein	Upstream component - PCP
Lft (lowfat)	Lix1, Lix1L	Unknown (Ft/Ds regulator)	Upstream component - PCP
Dco (Discs overgrowth)	CK1δ/ε	Ser/Thr kinase	Upstream component - PCP
App (approximated)	ZDHHCs	Palmytoyltransferase	Upstream component - PCP
Tao	Taok1-3	Kinase	Upstream component - Other
RASSF	RASSF1-6	Adaptor	Upstream component - Other
STRIPAK (PP2A)	PP2A (STRIPAK)	Phosphatase	Downstream effector - Other
Slimb	βTRCP	Ubiquitin ligase	Downstream effector - Other
14-3-3	14-3-3	Adaptor	Downstream effector - Other

Table 1. Hippo pathway members. Table adapted form (Yu and Guan, 2013) and (Grusche et al., 2010)

Taken together, the variety of factors and the complex interactions involved in the activation or inhibition of the Hippo pathway underscores the importance of YAP/TAZ regulation for proper cellular homeostasis.

Downstream nuclear effectors.

As mentioned, the role of the Hippo pathway is to inactivate YAP or its homolog TAZ, two transcriptional coactivators (Zhao et al., 2010a). YAP is expressed ubiquitously, whereas TAZ exhibits more restricted tissue expression. As our work in sarcoma demonstrated aberrant YAP (but not TAZ) expression, I am focusing the majority of the description below on YAP.

As a modular protein, YAP contains several binding motifs, which allow for interaction with multiple protein structures (reviewed in Figure 2). However, YAP does not contain a DNA binding domain, and is considered a transcriptional coactivator (Sudol and Harvey, 2010). YAP functions by enhancing the output of several transcription factors, most notably the TEAD1-4 proteins. Other known YAP binding partners include the Runx and Smad family members, p73, beta catenin, GLI2, and FOXO1 (Shao et al., 2014). Negative regulation of YAP is mainly mediated through post-transcriptional modifications and protein-protein interaction mediated cytoplasmic sequestration (Zhao et al., 2011b). The Lats/Mob1 kinase complex phosphorylates YAP at five different Serine residues. YAP phosphorylation at Serine 127 is the most important site, as it creates a docking site for the 14-3-3 adaptor proteins (Zhao et al., 2007). Phospho-YAP bound to 14-3-3 can be exported from the nucleus and kept sequestered in the cytoplasm. Subsequently, YAP can be phosphorylated by CK1 (Casein Kinase 1). This second phosphorylation leads to βTRCP (SCF)-mediated proteasomal degradation. (Zhao et al., 2010b) Yap an also be localized at tight junction complexes (Oka et al., 2010; Zhao et al., 2011a) or other complexes associated with the cell membrane (Badouel et al., 2009; Oh et al., 2009) in a Hippo pathway-dependent, phosphorylation-independent manner.
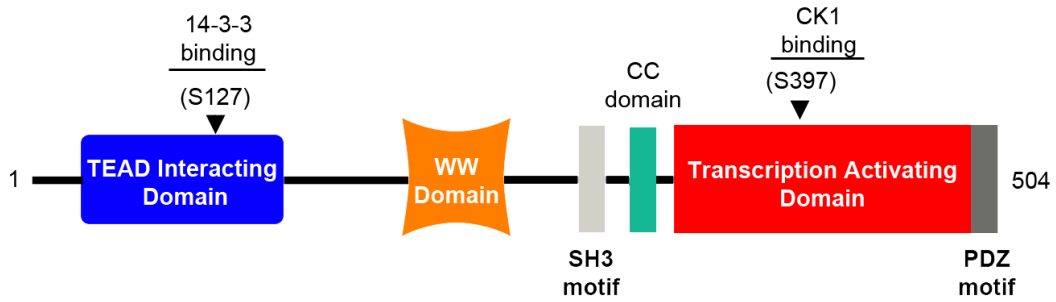
10

Figure 2. Schematic of YAP interacting and regulatory domains. (Modified from (Varelas 2014) and (Sudol et al., 2012)). YAP can be phosphorylated by LATS1/2 at multiple Serine sites. Importantly, phospho-S127 is necessary for 14-3-3 binding and cytoplasmic retention, and S397 for CK1 recognition. Further CK1 phosphorylation leads to YAP degradation.

The best understood role for YAP is in directing transcription of genes involved in promoting cellular proliferation. To date, multiple players have been identified as direct YAP targets, including Cyclin D1 (Cao et al., 2008), Amphiregulin (AREG) (Zhang et al., 2009), Connective Tissue Growth Factor (CTGF) (Zhao et al., 2008b), Gli2 (Fernandez et al., 2009), and Survivin/Birc5 (Muramatsu et al., 2011), all targets that have been associated with promoting tumor growth.

While the majority of studies have focused on investigating pro-proliferative roles of YAP in the nucleus, there is evidence that YAP (particularly the YAP2 isoform) might be promoting cell death when binding and consequently stabilizing p73 in the nucleus (Oka et al., 2008). It is thought that the YAP-p73 complex is promoted via LATS2 inactivation of the c-Abl kinase (Reuven et al., 2013). However, the precise conditions leading to a pro-apoptotic YAP function, as well as the downstream targets that mediate apoptotic signaling remain unclear.

C. The Hippo pathway in cancer

The propensity for tumorigenesis upon Hippo pathway modulation has been described through various animal models. As mentioned earlier, Drosophila screens for proliferation inhibitors have been crucial in the delineation of many Hippo pathway members. The tumor-like phenotypes in those screens have been described previously (Pan, 2007). In mice, organ-specific YAP overexpression or constitutive activation (through a mutation in Serine 127, a LATS phosphorylation site) causes tissue overproliferation and consequent carcinogenesis notably in liver (Camargo et al., 2007), colon (Avruch et al., 2012), skin (Schlegelmilch et al., 2011), and pancreas (Zhang et al., 2014). Additionally, deletions in upstream Hippo pathway factors have faithfully recapitulated the tumor phenotypes observed with YAP overexpression. AlbCre; NF2$^{fl/fl}$ mice result in hepatocellular carcinoma (HCC), a phenotype that can be abrogated when the mice are crossed to YAP1$^{fl/fl}$ mice (Zhang et al., 2010). Mst1/Mst2 deletions as well as Sav1 deletions induce liver hypertrophy and eventual HCC progression as well (Lu et al., 2010; Zhou et al., 2009). LATS1 global deletion showed one of the first instances of spontaneous sarcoma

12

formation (St John et al., 1999). (LATS2$^{fl/fl}$ mice result in embryonic lethality (Yabuta et al., 2007)). Recently, Tremblay and colleagues showed that YAP overexpression in muscle can lead to spontaneous Embryonal Rhabdomyosarcoma formation (Tremblay et al., 2014).

D. Targeting the Hippo pathway: YAP inhibition.

Due to its functions in cell growth, regeneration and tumor promotion, finding appropriate targeting modalities against the Hippo pathway is a highly studied field. Hippo pathway activators and inhibitors have been recently surveyed by Johnson and Halder (Johnson and Halder, 2014). Inhibiting the upstream Hippo pathway members, or alternatively activating YAP, could be an attractive method for inducing tissue regeneration. However, such activation would have to be tightly controlled, due to the potent tumorigenic properties of YAP. In cancer, conversely, Hippo upstream activators or alternatively YAP inhibitors are sought after, especially in the cases where YAP overexpression/activation is thought to drive tumor progression. However, most small molecules that target kinases tend to be inhibitory, which would be counterproductive in this particular pathway, as it would lead to further YAP activity (Stanger, 2012). While inhibiting transcription factor/coactivator complexes poses its own challenges, due to the lack of a druggable pocket between protein-DNA interactions, emerging studies are identifying promising proof-of-concept YAP inhibitors. In fact, directly inhibiting YAP/TEAD function is preferable, as upstream Hippo members are involved in crosstalks with multiple pathways. Table 2 summarizes many of these putative YAP inhibitors.

Part I conclusion

While the Hippo pathway key effectors have been extensively studied, the aberrant activation or inactivation of Hippo members in the context of cancer is still an evolving field of study. Several *in vitro*, mouse models and patient data studies have demonstrated the propensity for tumorigenesis associated with loss of upstream Hippo members, or aberrant YAP activation. Many of these studies have focused on epithelial tumors, particularly modeling liver

13

tumorigenesis. Tumors considered mesenchymal in nature however also may rely on aberrant

Hippo pathway regulation to promote progression. Chapter II describes a new role for Hippo

Name	Mechanism	References
Adrenergic Agonists (Dobutamine)	YAP cytoplasmic retention. Unknown mechanism but possibly function as $G\alpha_s$-coupled GPCR agonists	(Bao et al., 2011), (Park and Guan, 2013)
Benzophyrins (Verteporfin)	Inhibit YAP-TEAD interaction, possibly by binding to YAP and changing its conformation	(Liu-Chittenden et al., 2012)
Statins (Cerivastatin)	YAP/TAZ inactivation by inhibitiing HMG-CoA reductase, a key upstream enzyme in the mevalonate pathway. Ultimately Rho inactivation	(Sorrentino et al., 2014)
VGLL4 peptide mimic	VGLL4 mimic binds to and titrates TEAD away from YAP binding	(Jiao et al., 2014)
Indirect inhibitors	Rho/Rock inhibitors that affect cytoskeleton dynamics and GPCR signaling	(Johnson and Halder, 2014)

Table 2. Summary of potential YAP inhibitors. Partially adapted from Johnson and Halder, 2014.

inactivation/YAP activation in sarcomagenesis, emphasizing on FOXM1 as an attractive target for sarcoma treatment.

PART II. MIRNA ROLE IN CELLULAR SURVIVAL UNDER STRESS.

While uncontrolled proliferation is a key hallmark of tumorigenesis, evading pro-apoptotic signals is equally important for tumor progression (Hanahan and Weinberg, 2000). Uncontrolled proliferation creates a microenvironment that is depleted of nutrients and oxygen (O_2), or "hypoxic" (Semenza, 2007). The angiogenesis switch is necessary for tumor growth (Folkman, 2002), however, tumor-associated blood vessels are leaky and disorganized (Carmeliet and Jain, 2011), resulting in heterogeneous availability of nutrients/O_2. Tumor cells have managed to co-opt normal cellular mechanisms to be able to survive under those metabolic stresses (Mucaj et al., 2012). Some of these mechanisms include the stabilization of the Hypoxia Inducible factors (HIFs) (Keith and Simon, 2007), the activation of the Unfolded Protein Response (UPR) as a result of ER stress (Hetz et al., 2013), and various other means of metabolic adaptation (such as activation of autophagy, or mutations leading to changed metabolic enzyme functions) which are still being elucidated (Cheong et al., 2012). Glioblastoma multiforme tumors experience heterogeneous microenvironments with sharp changes in O_2 gradients (Vartanian et al., 2014). In the next section, I am outlining how cells adapt to low O_2, focusing on the Hypoxia Inducible Factors (HIFs).

A. Hypoxia Inducible factors

Healthy tissues experience a range of 2% to 9% O_2. Tissues grown in less than 2% O_2 are considered to experience hypoxia (Bertout et al., 2008). Hypoxia may occur secondary to necrosis or aberrant neovascularization resulting in poor perfusion. Additionally, cancer cells may proliferate rapidly enough to outstrip their blood supply (Majmundar et al., 2010). Cells adapt to changes in O_2 availability by altering gene expression of crucial metabolic enzymes in order to counter changes in nutrient availability and redox status. This response is mediated, in part, by

15

O_2 – labile transcription factors hypoxia-inducible factors HIF-1α and HIF-2α, key regulators of cellular adaptation to hypoxic stress (Keith et al., 2012).

Comprised of an O_2 -sensitive α subunit and constitutively expressed β subunit, HIFs are primarily regulated through post-translational modification and stabilization. Under normal O2 tensions, prolyl hydroxylase domain enzymes (PHDs) hydroxylate two conserved proline residues in the HIF-α subunits. Upon hydroxylation, the HIFα subunit is poly-ubiquitinated for proteasomal degradation via the von Hippel-Lindau (VHL) tumor suppressor E3 ligase complex (Cockman et al., 2000; Jaakkola et al., 2001). Upon low O_2 levels, PHDs no longer hydroxylate the HIFα subunit, which leads to HIFα stabilization and nuclear translocation. In the nucleus, HIFα transcription factors dimerize with their obligate binding partner, HIFβ (also known as ARNT), and the HIFα/ARNT complex drives the transcription of numerous factors important for survival under low O_2, as well as for migration/invasion away from low O_2 areas. These factors include, but are not limited to: VEGFA, CA9, BNIP3, LOX, SERPINE, PGK1, GLUT1 (Dayan et al., 2006; Pouyssegur et al., 2006).

Increased HIF activity is evident in cancer, as cancer cells maintain rapid proliferation, even in the absence of adequate O_2 and nutrient availability. Adaptive metabolic changes allow continued biosynthesis and cell growth in the setting of decreased access to O_2. As cancer cells divide and outstrip O_2 and nutrient supplies, HIF activation allows modulation of cell metabolism and gene expression to adapt to the ever-changing landscape of the tumor microenvironment. HIF expression is an important prognostic factor, as levels associate closely with poor patient outcomes in a variety of cancers (Semenza, 2007).

B. MiRNA biology.

While only ~22 nucleotides in length, mature miRNAs control a wide-spanning array of targets, whose modulation can cause profound changes within a cell (Ambros, 2004). These

16

small noncoding RNAs originate from genomic DNA and function by negatively regulating their targets in a post-transcriptional manner. First described in *C. elegans* as controller of developmental cues (Lee et al., 1993), miRNAs are now thought to modulate a range of cellular functions, including proliferation, differentiation, and cell death. Fig. 3 summarizes miRNA biogenesis, and the concept that aberrant over and underexpression of miRNAs can lead to deleterious consequences, including tumor progression (Esquela-Kerscher and Slack, 2006b).

Yi and Fuchs compare miRNA function to that of a rheostat, which modulates and fine-tunes signals in the cell, potentially to achieve homeostasis, or a particular goal, such as stem cell maintenance, proliferation control, or differentiation (Yi and Fuchs, 2011). This notion is supported by the fact that, while miRNAs only slightly attenuate their target levels, it is estimated that they may regulate more than 30% of the mammalian genome (Bartel, 2009; Esquela-Kerscher and Slack, 2006b). It is thus tempting to hypothesize that miRNAs are key players in stress response signaling. In fact, several miRNAs have been implicated in responses to stress. For example, *miR-210* is considered the "master hypoxamiR" as low O_2 can upregulate *miR-210* expression. In turn, *miR-210* targets a wide range of factors involved in cell cycle, mitochondrial respiration, angiogenesis, and DNA repair, ultimately giving rise to cellular changes that allow for hypoxic adaptation (Chan et al., 2012). Similarly, *miR-451* has been implicated in metabolic stress adaptation (Godlewski et al., 2010) while miR-211 has been shown to elicit pro-survival mechanisms under ER stress (Chitnis et al., 2012).

While miRNA expression can be regulated to respond to stress, similar effects can be observed when miRNAs are aberrantly expressed, as in the case of many cancers. Recently, our lab has shown that clear renal cell carcinomas (ccRCC) express low levels of *miR-30c-2-3p* and *miR-30a-3p* in order to enhance HIF-2α expression, and elevating the oncogenic potential of ccRCC (Mathew et al., 2014a). Similarly, investigating the effects of diminished miRNA levels on glioblastoma survival under hypoxia, our laboratory has shown that mesenchymal subtype glioblastomas express the lowest levels of *miR-218*, even when compared to other glioblastoma

17

subtypes. As *miR-218* targets a series of proteins involved in a Receptor-Tyrosine Kinase/HIF signaling cascade, low *miR-218* levels allow for uncontrolled expression of that signaling axis, which promotes survival under a hypoxic/ischemic microenvironment (Mathew et al., 2014b).

Among miRNAs differentially regulated in glioblastoma, *miR-124* is one of the most decreased at the tissue level, both when comparing glioblastoma tissue to adjacent normal tissue, as well as when we compare glioblastomas (grade IV gliomas) to lower grade gliomas or to gliosis tissues (Silber et al., 2008b). *miR-124* is one of the best studied miRNAs in the brain, and a key modulator of neuronal differentiation (Makeyev et al., 2007a). Thus, differentially expressed *miR-124* in the context of the brain has important consequences, and in the case of glioblastoma, *miR-124* can become an attractive tool for identifying key factors involved in glioma progression. Several studies have ectopically expressed miR-124 in glioblastoma cells and demonstrated changes in proliferation, migration, invasion, and inflammation. The previously examined roles of *miR-124* in normal development and in glioblastoma are summarized in Fig. 4.

Part II conclusion

Solid tumors have adopted multiple mechanisms to survive stressful microenvironments, including the modulation of miRNA levels. While multiple roles for *miR-124* in glioblastoma have been previously addressed, very little is known about how *miR-124* affects cells grown under limiting O_2 and nutrients. To that end, Chapter III introduces a new phenotype where *miR-124* elicits increased death in cells grown under hypoxic/ischemic conditions, thereby counteracting glioblastoma pro-survival responses to stress.

Normal tissue

1. Neuronal Differentiation
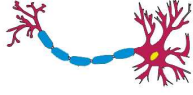
(Makeyev et al., 2007)
(Yoo et al., 2011)

2. Migration in ES cell differentiation

(Fang et al, 2014)

3. Neural Tube formation

(Cao et al., 2007)

miR-124
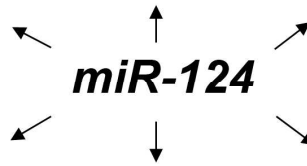
(Silber et al., 2008)
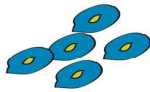
(Fowler et al., 2011)

(Mucaj et al., 2014)

1. Proliferation

2. Migration/Invasion

3. Cell survival under stress

Glioblastoma

Figure 4. Multiple roles for miR-124 in normal brain tissues and in glioblastoma.

CHAPTER 2

Deregulation of the Hippo Pathway in soft tissue sarcoma promotes tumorigenesis via YAP/FOXM1 signaling

SUMMARY

The role of the Hippo pathway is unclear in most soft tissue sarcomas (STS). Recent studies have suggested that inactivation of the Hippo pathway, resulting in over-expression of the transcriptional co-activator Yes-activated protein (YAP), may drive proliferation in these tumors but the mechanism is unclear. In other tumor contexts increased YAP expression has been shown to facilitate expression of the pro-proliferation transcription factor, FOXM1. FOXM1 and many of its transcription targets including MYC, LOX, and VEGF have been directly associated with tumorigenesis. In this chapter, I present data gathered from human sarcoma patients and a novel autochthonous mouse sarcoma model to show that YAP-mediated FOXM1 expression is necessary for sarcoma proliferation and tumorigenesis. Additionally, we have uncovered a previously unknown mechanism wherein FOXM1 directly interacts with the YAP transcriptional complex via TEAD1, resulting in potential co-regulation of a variety of pro-proliferation transcription targets. Finally, we have found that pharmacologic inhibition of FOXM1 decreases tumor size *in vivo*, suggesting that FOXM1 may be an attractive therapeutic target for the treatment of sarcomas.

INTRODUCTION

Soft tissue sarcomas (STS) are heterogeneous mesenchymal tumors detected annually in more than 200,000 people worldwide (Taylor et al., 2011). STS are comprised of a large subset of histologically distinct tumor types with fibrosarcoma, liposarcoma, and undifferentiated pleomorphic sarcoma (UPS) among the most commonly diagnosed in adults. UPS in particular is an aggressive metastatic STS subtype. As its etiology is currently unknown, UPS is a diagnosis of exclusion, and the lack of elucidated complex genetic drivers underlying human UPS has made therapeutic intervention difficult (Kelleher and Viterbo, 2013; Taylor et al., 2011). Metastasis in UPS patients likely occurs due to hyper-proliferation of the primary tumor, which results in a hypoxic microenvironment that promotes tumor cell dissemination (Eisinger-Mathason et al., 2013). An improved understanding of genetic aberrations responsible for sarcoma initiation and progression is essential for the future development of effective targeted therapies.

To date, there are few disease-specific treatments to offer sarcoma patients. Current therapeutic modalities include surgery, radiotherapy and cytotoxic chemotherapy (Taylor et al., 2011). Among these, radical surgeries are the most effective means of treating sarcoma (Linehan et al., 2000). However, in some cases, tumor-ablating surgery is not possible and local recurrences appear. Furthermore, primary tumor resections do not eliminate cells that may have disseminated prior to surgery. More conservative surgeries, combined with effective targeted inhibitors of proliferation and/or migration would significantly improve patient prognosis and quality of life.

The mesenchymal origins of sarcoma present an inherent challenge to the development of sarcoma-specific therapeutics. Compared with epithelial tumors, sarcomas are significantly understudied. As a result, mesenchymal tumor initiation and progression are poorly understood. Recent efforts by The Cancer Genome Atlas (TCGA) and other tissue banking resources that accumulate and process patient samples have provided invaluable tools for probing molecular

21

pathways underlying sarcomagenesis. Using these tools, we have uncovered a role for aberrant

Hippo pathway signaling in fibrosarcoma, UPS, and potentially several other sub-types of STS.

Given the importance of this conserved pathway in organogenesis, Hippo inactivation

and constitutively active YAP could be potent tumor promoting mechanisms. In fact, NF2

mutation or loss of function have been reported in Neurofibromatosis type II lesions

(schwannomas, meningiomas, ependymomas), malignant mesothelioma, and infrequently in

other carcinomas, albeit infrequently (Harvey et al., 2013; Mizuno et al., 2012; Sekido et al., 1995;

Yoo et al., 2012). With the exception of NF2 mutations, no other Hippo pathway mutational

events have been reported in cancer (Harvey et al., 2013). However, genomic

deletions/amplifications and gene expression changes have been detected throughout Hippo

signaling. For example, decreased SAV1 activity has been implicated in clear cell renal cell

carcinoma progression (Matsuura et al., 2011)**.** In breast cancer, 11q22 chromosomal

amplifications lead to YAP overexpression, thereby bypassing Hippo upstream control

(Overholtzer et al., 2006). Amplifications at the *YAP* locus have also been described in

medulloblastomas (Fernandez et al., 2009). However, little is known about the status of the Hippo

pathway in STS, although MST1/2 appear to be epigenetically silenced through promoter

hypermethylation in a limited number of sarcoma patient samples (Seidel et al., 2007). Of note,

YAP overexpression has recently been reported in both alveolar and embryonic

rhabdomyosarcoma (Crose et al., 2014; Tremblay et al., 2014).

YAP modulation is a powerful regulator of tumor cell proliferation due to the

transcriptional changes associated with its activity. Many YAP/TEAD targets have been

previously associated with tumor progression, including BIRC5, CCND1, and FOXM1 (Kim et al.,

2013; Mizuno et al., 2012; Pan, 2010; Zhao et al., 2011b; Zhao et al., 2008c). In particular,

YAP/TEAD directly bind the *FOXM1* promoter, inducing its expression in a model of malignant

mesothelioma (where upstream NF2 mutations are common) (Mizuno et al., 2012). FOXM1 is a

winged helix-turn-helix transcription factor important for cell cycle progression and proliferation

22

(Wierstra, 2013). FOXM1 is required for tumor formation in multiple epithelial cancers, including hepatocellular carcinoma (HCC), wherein FOXM1 increases cell proliferation by enhancing Cdc25b phosphatase expression (Kalinichenko et al., 2004). FOXM1 activity is inhibited by direct interaction with p19^{ARF}, whereby p19^{ARF} targets FOXM1 and other signaling molecules to the nucleolus preventing them from engaging in transcriptional upregulation of factors involved in proliferation (Kalinichenko et al., 2004). In addition, FOXM1 is negatively regulated through the p53 (Pandit et al., 2009) and RB pathways (Wierstra and Alves, 2006). Therefore, FOXM1 is highly expressed in a variety of human cancer cells due to loss of tumor suppressive proteins, and aberrant expression of pro-mitogenic factors (Halasi and Gartel, 2013) leading to overproliferation and metastasis (Park et al., 2011).

To probe the relationship between the Hippo pathway and FOXM1 in sarcomagenesis, we employed a variety of approaches, including multiple mouse models of UPS and cell lines derived from these tumors. LSL *Kras*$^{G12D/+}$; *Trp53*$^{fl/fl}$ (KP) and LSL *Kras*$^{G12D/+}$; *Ink4*/Arf$^{fl/fl}$ mice recapitulate UPS (Eisinger-Mathason et al., 2013; Kirsch et al., 2007) allowing the study of downstream molecular signaling factors that control sarcomagenesis. Coupled with patient data, we have identified pro-proliferation factors and pathways aberrantly regulated in UPS, which can be targets for therapeutic intervention.

While previous studies have implicated YAP and FOXM1 as critical factors promoting epithelial tumorigenesis, little evidence has suggested that the Hippo pathway and its downstream effectors are aberrantly regulated in STS. Here, we identify key Hippo pathway members whose levels are decreased in TCGA sarcoma patient samples. We show that YAP is nuclear and highly overexpressed in UPS and liposarcomas leading to elevated FOXM1 across these subtypes. Both genetic and pharmacologic inhibition of YAP/TEAD and FOXM1 result in sarcoma cell proliferation defects, suggesting that these targets represent a promising therapeutic intervention for this mesenchymal disease.

MATERIALS AND METHODS

23

Cell culture, drug treatment, and lentiviral transduction

HT-1080 and HEK-293T cell lines were purchased from ATCC (Manassas, VA, USA). KP and KIA cells were derived from KP and KIA tumors, as previously described (Eisinger-Mathason et al., 2013; Kirsch et al., 2007). Cells were treated with 1-2 µM Thiostrepton or 1 µM Verteporfin (Sigma-Aldrich, St. Louis, MO, USA), in dimethyl sulfoxide, diluted in DMEM culture media. Verteporfin was replenished every 24 hours. For shRNA-mediated knockdown of *Yap1*, *YAP1*, *Foxm1*, and *FOXM1* constructs in the pLKO.1 background vector was used (GE lifesciences). Scramble shRNA was obtained from Addgene. shRNA plasmids were packaged using the third-generation lentivector system (VSV-G, p-MDLG, and pRSV-REV) and expressed in HEK-293T cells. TRCN: *Yap1:0000095867* , *YAP1: 0000107268*, *Foxm1:0000084776*, and *FOXM1: 0000015546* Supernatant was collected at 24 and 48 hours post transfection, and subsequently concentrated using 10-kDa Amicon Ultra-15 centrifugal filter units (Millipore, Billerica, MA, USA). Over-expression plasmids used were pPGS-3HA-TEAD1 (plasmid 33055, Addgene), pcDNA3-Flag-FOXM1 (MJ Reginato, Drexel University) and pcDNA3 was used as the empty vector control.

Bioinformatics analysis

Level 3 data comprising regions/segments with altered copy number were downloaded from the TCGA Data portal (data last updated as of May 15, 2014, (https://tcga-data.nci.nih.gov/tcga/tcgaCancerDetails.jsp?diseaseType=SARC&diseaseName=Sarcoma)). The data was analyzed using the Partek 6.6 software (St. Louis, Missouri, USA). Briefly, sample files were lined up and concatenated. Subsequently, the thresholds for amplification/deletion were set at 0.55 and -0.4, for amplification and deletion, respectively. These cutoffs were based on previously published literature. Tumor samples for copy number analysis consisted of 152 samples total, with 150 primary samples and 2 recurrences. The results obtained from blood samples and normal controls were eliminated from the analysis as they contained no amplifications or deletions. The Venn diagram was generated using the BioVenn web application (http://www.cmbi.ru.nl/cdd/biovenn/). Microarray data were downloaded through the Oncomine™

24

Research premium edition (Life Technologies, Carlsbad, CA, USA) software version 4.5 (https://www.oncomine.org) Data was downloaded form microarrays associated with the Nakayama et al., 2007 (Nakayama et al., 2007) and Detwiller et al. 2005, (Detwiller et al., 2005) manuscripts. GIST tumors were excluded from our analysis due to their distinct histological and genetic features as well as their unique tissue of origin.

Immunoblots and qRT-PCR

Protein lysate prepared in SDS/Tris pH 7.6 lysis buffer, separated by electrophoresis in 10% SDS–PAGE gels, transferred to nitrocellulose membrane and probed with the following antibodies: rabbit anti-YAP1, rabbit anti-GAPDH, rabbit anti-HA (Cell Signaling Technology, Inc., Danvers, MA, USA), rabbit anti-FOXM1 (Santa Cruz Biotechnology, Inc., Dallas, TX, USA). Representative immunoblots from multiple independent experiments are presented. Total RNA was isolated from tissues and cells using the RNeasy Mini Kit (Qiagen, Germantown, MD, USA) or the TRIzol reagent protocol (Life Technologies, Carlsbad, CA). Reverse transcription of mRNA was performed using the High-Capacity RNA-to-cDNA Kit (Life Technologies, Carlsbad, CA). qRT-PCR was performed using a ViiA7 apparatus and Taq-Man "best coverage" primers (Life Technologies, Carlsbad, CA).

Immunostaining and Imaging

Immunohistochemistry assays were performed on 5-µm sections according to standard protocols. The following antibody concentrations were used: YAP 1:100 (Cell Signaling Technology, Inc., Danvers, MA, USA), FOXM1 1:100 and TEAD1 (Novus Biologicals, Littleton CO), Ki67 1:100 (Abcam, Cambridge, UK). Images were taken using a Leica 500 microscope (Leica, Solms, Germany) and analyzed using Photoshop CS3 (Adobe Systems, San Jose, CA). IHC of human sarcoma samples was done using core biopsy arrays (US Biomax Inc, Rockville, MD) array #s SO801a and SF961.

Proliferation assays

25

For drug studies cells were plated and incubated overnight in tissue culture dishes. The next day the appropriate drug diluted in growth media was added to the cells. Cells were trypsonized, re-suspended, in PBS and counted daily for 4 days using a hemocytometer. For shRNA studies cells were incubated with virus for 48 hours then trypsonized and re-plated followed by daily counting for four days. Cells were analyzed for shRNA efficacy by immunoblot analysis or qRT-PCR.

Immunoprecipitation

HT-1080 cells were transiently transfected using Fugene 6 (Life Technologies, Carlsbad, CA) with Flag-FOXM1 and either pcDNA3vector control, V5-YAP, or HA-TEAD1 (8 µg total DNA). After 48 hours of incubation cells were washed with PBS, scraped, spun, and re-suspended in lysis buffer containing 1% Triton-X and protease inhibitors. Equal amounts of input lysate were added to 75 µL of anti-Flag M2 coated magnetic beads (Sigma-Aldrich, St. Louis, MO, USA). Beads and lysate were incubated overnight with rocking at $4^{o}C$. Beads were washed, and then boiling with loading buffer for 5 minutes eluted the protein. The sample was removed from the beads by magnetic separation and then run on a 10% SDS-PAGE gel for immunoblot analysis.

Mouse Models

All experiments were performed in accordance with the National Institutes of Health guidelines and approved by the University of Pennsylvania Institutional Animal Care and Use Committee. FOXM1^{fl/fl} mice were crossed with KP mice to create KPF mice. Foxm1^{fl/fl} (Kalinichenko et al., 2002) and KP (Kirsch et al., 2007) mouse generation has been previously described. Tumors were generated by intramuscular injection of a calcium phosphate precipitate of Ad-Cre (Gene Transfer Vector Core; University of Iowa, Iowa City, IA, USA) into the left gastrocnemious muscle of 8-16 week old mice. Mice were sacrificed at maximal permitted tumor burden. For sub-cutaneous transplant tumors 1×10^{6} KP or HT1080 cells were injected subcutaneously into the flanks of 6 weeks old nu/nu mice (Charles River Laboratories, Malvern, PA). In each experiment, ~10 mice per experimental group were used with each mouse bearing two subcutaneous tumors. Animals were euthanized within 20-30 days of injection. Tumor

26

volume was calculated using the formula $(ab^2)\pi/6$, where a is the longest caliper measurement, and b is the shortest.

In vivo drug treatment

Thiostrepton was encapsulated into micelles assembled from amphiphilic lipid-PEG (polyethylene glycol) molecules as previously described (Wang and Gartel, 2011). Anaesthetized mice were retro-orbitally injected with PBS, 7.5 mg/kg, or 15 mg/kg Thiostrepton encapsulated micelles every third day for 3.5 weeks.

Statistical analysis

All statistical analyses were performed using the GraphPad Prism software (La Jolla, CA, USA). Data are represented as mean±s.e.m. Student's *t*-test was performed to establish whether a difference between two values is statistically significant, with statistical significance are designated with a * an defined as $p < 0.05$.

RESULTS

Deregulation of the Hippo pathway in human sarcomas

Abnormal regulation of Hippo pathway activity can lead to increased cell proliferation and tumorigenesis. To determine whether Hippo pathway genetic aberrations occur in STS, we queried the TCGA sarcoma database for copy number variations in the upstream drivers of Hippo signaling. Our analysis revealed that 41% of sarcoma samples deposited in the TCGA database contain deletions in one or more of these Hippo pathway components, including NF2, SAV1, and LATS2 (Fig. 5A). Most of the genetic deletions were in LATS2, while 20% of affected tumors contained deletions of multiple Hippo regulators (Fig. 5B). Such genetic changes would be anticipated to result in stabilization and nuclear translocation of the Hippo pathway downstream effector, YAP. Immunohistochemical (IHC) analysis of human tissue samples showed that YAP levels are dramatically increased in UPS tumors, compared with normal skeletal and arterial tissue (Fig. 6A). Transcriptionally active YAP is localized to the nucleus, and high magnification analyses of human tissue cores (Fig. 6A) clearly demonstrated active YAP in the nuclei of UPS

27

and liposarcoma (LS) samples compared to normal arterial muscle tissue (Fig. 6B). These data suggest that Hippo pathway inhibition and subsequent stabilization of active YAP may be an important mechanism in sarcomagenesis.

YAP inhibition results in decreased sarcoma cell proliferation in vitro and in vivo

To determine the role of YAP in STS we initiated cell-based proliferation studies in murine and human sarcoma cell lines.   Murine sarcoma cells were derived from the autochthonous $Kras^{G12D/+}$;$Trp53^{fl/fl}$ (KP) and $Kras^{G12D/+}$;$Ink4a/Arf^{fl/fl}$ (KIA) models of UPS. Tumors that develop in these mice, following Adeno-Cre virus injection into the left gastrocnemius muscle, recapitulate human UPS morphologically and histologically, while harboring similar gene expression profiles (Eisinger-Mathason et al., 2013; Kirsch et al., 2007; Mito et al., 2009).

A.

N=150 Soft Tissue Sarcomas (TCGA)

B.

N= 62 sarcoma patient samples with Hippo pathway deletions (TCGA)
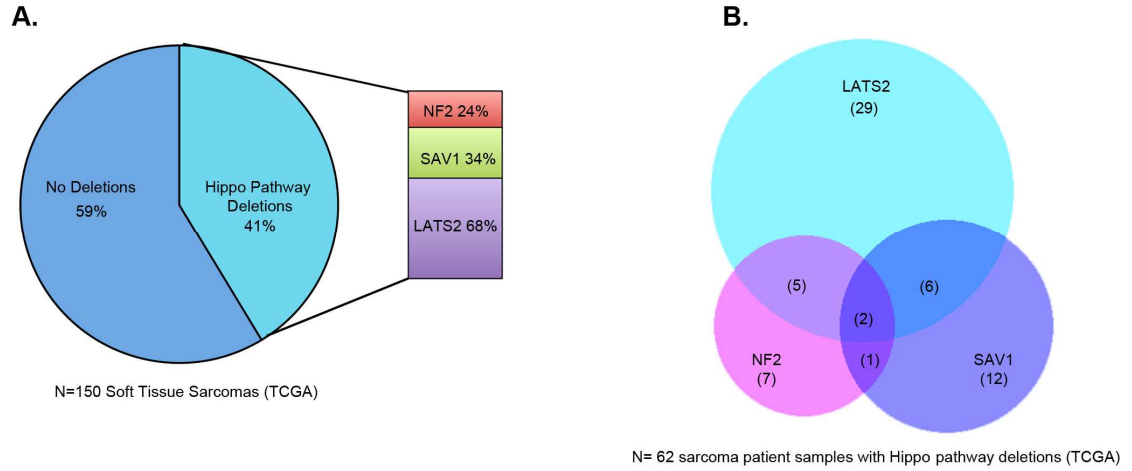
Figure 5. Hippo pathway deregulation in human sarcoma. A) TCGA STS copy number data showing percentage of Hippo pathway deletions. N=150 STS patients. B) Venn diagram delineating number of common and unique deletions in the 62 STS patient samples containing LATS2, SAV1, or NF2 deletions.

A.
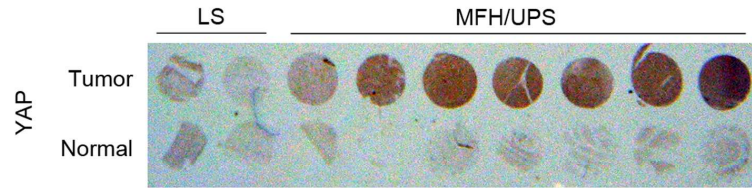
Tumor (Stage)	Lipo (IIB)	Lipo (IIB)	MFH/UPS (III)	MFH/UPS (IIB)	MFH/UPS (III)	MFH/UPS (IIA)	MFH/UPS (IIA)	MFH/UPS (IIA)	MFH/UPS (IIA)
Normal Tissue	Large Artery	Large Artery	Large Artery	Skeletal Muscle	Skeletal Muscle	Skeletal Muscle	Skeletal Muscle	Skeletal Muscle	Skeletal Muscle

B.
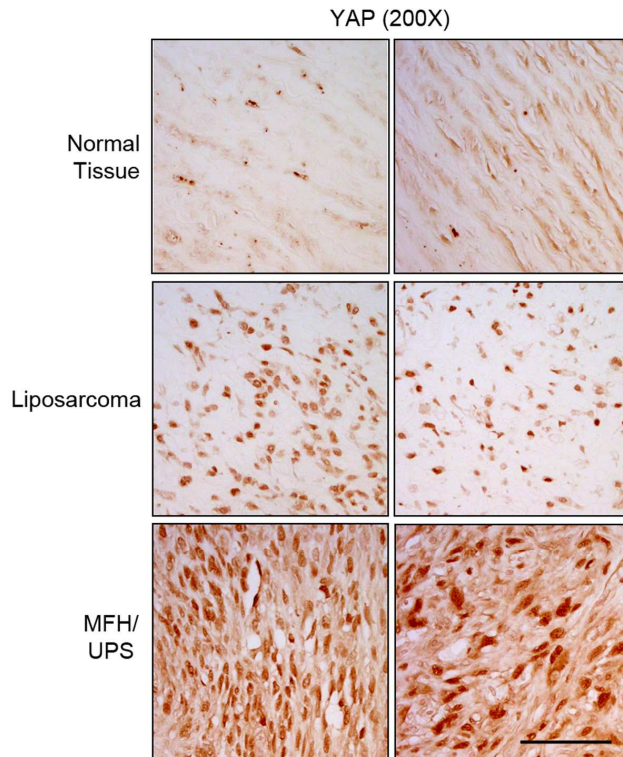
Figure 6. Deregulated YAP expression in human sarcoma. A) Immunohistochemical staining for YAP levels in normal and STS patient sample biopsy cores. B) Magnification showing YAP localization in biopsy cores from D. Scale bar=100 μM. *Karin Eisinger contributed this figure.*

Additionally, hind limb tumors successfully metastasize to the lung, mirroring human UPS. To determine the role of YAP in sarcoma cell proliferation we employed specific lentiviral shRNAs. *Yap* depletion significantly reduced KP and KIA cell proliferation *in vitro* (Fig. 7A), with similar results obtained for human HT-1080 fibrosarcoma cells using an independent shRNA (Fig. 7B). Based on these findings we proceeded to define the role of YAP in tumor formation. We injected 1×10^6 KP cells, transduced with control or *YAP-* specific shRNA, into the flanks of nude mice in order to generate allograft tumors. *YAP* deletion resulted in significantly decreased tumor volume (Fig. 7C) and final tumor weight (Fig. 7D). IHC analysis of control and *Yap*-silenced tumors showed that *Yap* ablation decreases the number of Ki67+ cells by ~40% (n=4 samples per condition, *P*=0.0005), indicating decreased proliferation (Fig. 7E) consistent with our *in vitro* findings (Fig. 7A,B). The YAP inhibitor Verteporfin (VP) prevents its interaction with constitutively nuclear binding partners, TEAD1-4, thereby inhibiting transcriptional activation of YAP/TEAD targets (Liu-Chittenden et al., 2012). Consistent with *Yap* inhibition via shRNA, treatment with 1µM VP dramatically reduced sarcoma cell proliferation (Fig. 8A-C). qRT-PCR analyses of VP treated KP cells revealed that Yap targets including, *Lox*, *Cdkn3*, *Plk1*, *Foxm1*, and *Birc5,* exhibited decreased expression 48 hours later (Fig. 8D). Similar results were obtained by VP treatment of KIA cells (Fig. 8E) as well as shRNA-mediated *Yap* inhibition, although, surprisingly *FOXM1* mRNA levels show a trend in decrease that is not statistical significant (Fig. 8F). From these data we noted that many of the downregulated mRNAs (*Lox*, *Cdkn3*, *Plk1*, and *Birc5*) were also targets of FOXM1-mediated transcription, in addition to being YAP targets. Based on this finding, we investigated the possibility that FOXM1 is an essential component of the YAP transcriptional program wherein YAP activation controls FOXM1 expression, and as a result, impacts FOXM1 transcriptional output (i.e. *LOX, CDKN3, PLK1, BIRC5*). Initially, we confirmed that YAP regulates FOXM1 protein expression. Inhibition of YAP by VP treatment (Fig. 9A) and with *YAP-* specific shRNA (Fig. 9B) decreased FOXM1 protein levels in HT-1080, KIA, and KP cells. Consistent with previous reports, VP had no reproducible effect on YAP protein levels (Liu-Chittenden et al., 2012). We conclude that YAP is a major regulator of FOXM1 expression in

31
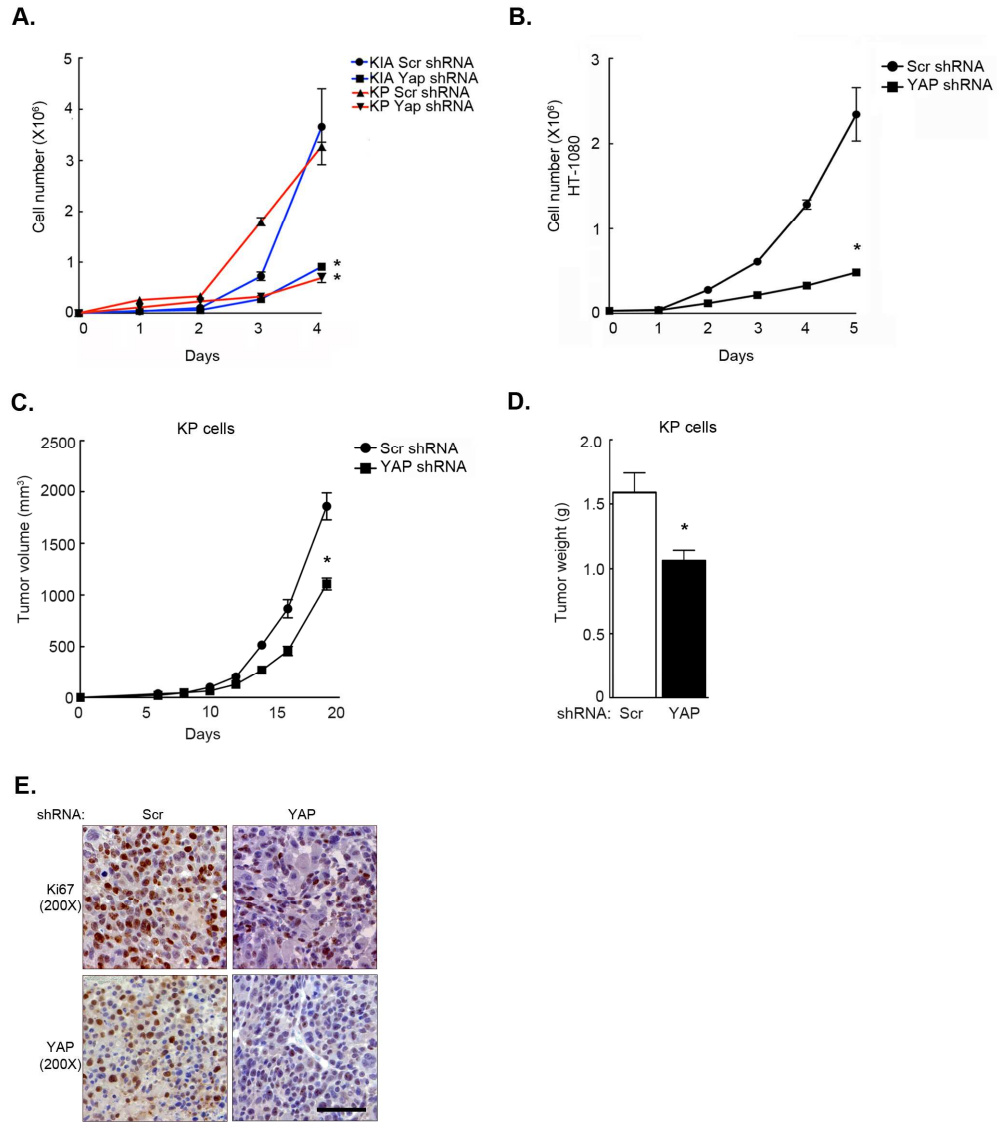
Figure 7. YAP inhibition decreases proliferation *in vitro* and *in vivo.* A) Yap knockdown via shRNA transduction inhibits proliferation in KIA and KP cells *P*<0.0006 for both cell types at day 4. B) *YAP* silencing in human sarcoma (HT-1080 cells) inhibits proliferation as in (A) *P*<0.005 at day 4. C) We subcutaneously injected 1X10^6 KP cells bearing control or control shRNA into nu/nu mice. YAP deletion inhibits tumor growth. Scr shRNA n=9; *Yap* shRNA n=8; *P*<0.0002 at day 18. D) Tumor weight is decreased in *Yap*-deleted tumors *P*=0.009. E) IHC of YAP and Ki67 in control and *Yap*-deleted tumors showing a loss of proliferation associated with *Yap* silencing. Scale bar=100 μM. *Karin Eisinger and Kevin Biju assisted with the completion of this figure.*
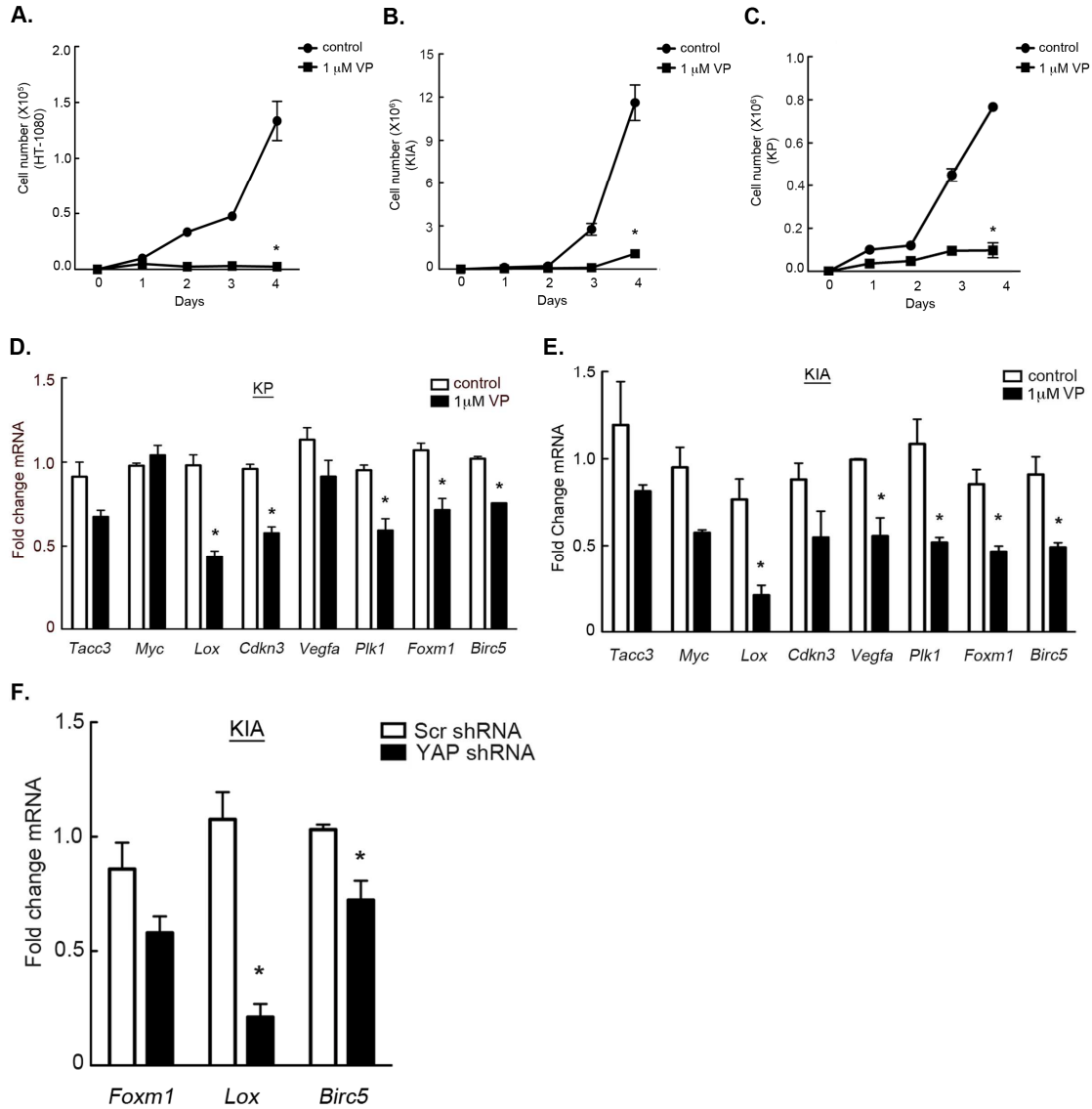
Figure 8. VP treatment affects cell count and decreases pro-proliferation targets. A) Treatment of HT-1080 cells with 1 μM VP for four days inhibited proliferation *P*=0.017 at day 4**.** B) KIA cells treated as in (A) *P*=0.013 at day 4. C) KP cells treated as in (A) *P*=0.003 at day 4. D) qRT-PCR analysis of KP cells 1 μM VP for 48 hours shows that VP treatment decreases mRNA levels of YAP transcriptional targets: *Lox P*=0.007*; Cdkn3 P*=0.001*; Plk1 P*=0.009*; Foxm1 P*=0.017*; Birc5 P*=0.0003. E) KIA cells treated with 1μM VP for 48 hours showed decreases in FOXM1 target mRNA expression including *Lox P*=0.013*; Cdkn3 P*=0.001*; Vegfa P*=0.047; *Plk1 P*=0.012*; Foxm1 P*=0.05*; Birc5 P*=0.004. F) KP cells treated with *Yap* shRNA show decreases in mRNA expression of *Foxm1* and FOXM1 targets including *Lox P*=0.003 and *Birc5 P*=.009. *Karin Eisinger and Kevin Biju assisted with the completion of this figure.*

33

A.
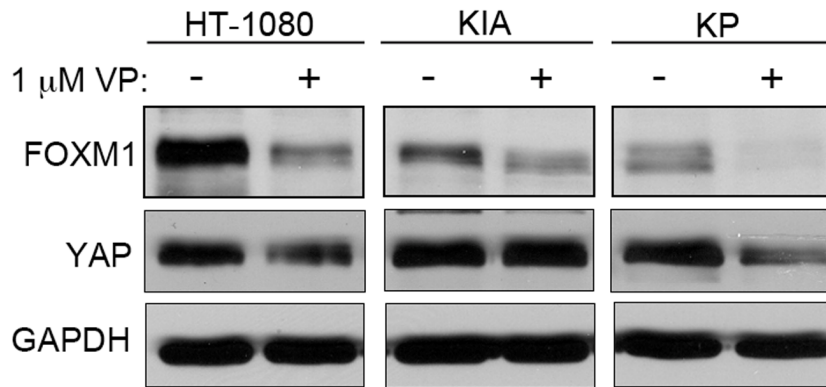
B.
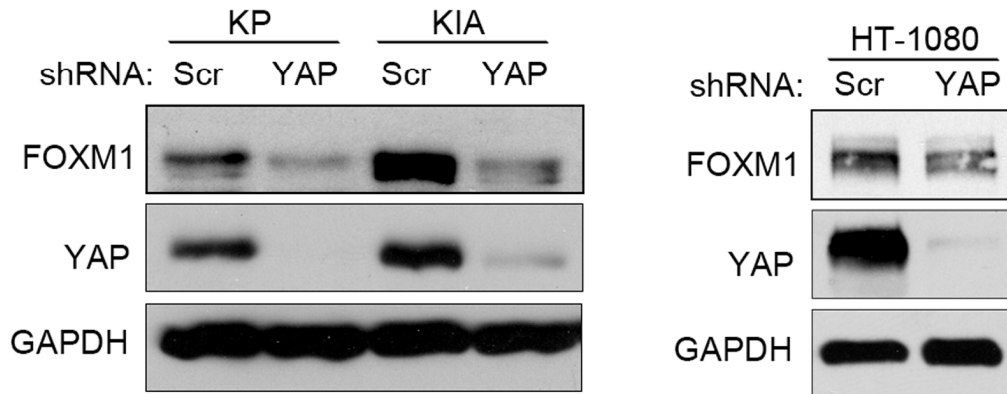
Figure 9. YAP inhibition decreases FOXM1 expression. A) Immunoblot analysis of HT-1080, KIA, and KP cells treated with 1 μM VP for 4 days. B) Immunoblot analysis of FOXM1 expression in *YAP* deleted KP, KIA and HT1080 cells.

sarcoma cells and that mechanisms by which YAP promotes sarcoma cell proliferation and tumorigenesis may require FOXM1.

FOXM1 is highly expressed in human sarcomas

In order to determine the importance of FOXM1 as a downstream effector of the Hippo pathway in human sarcoma, we investigated *FOXM1* expression levels in human tumor samples. Based on the observation that the Hippo pathway is deregulated in STS (Fig.5) we predicted that YAP target gene levels, specifically *FOXM1,* would be elevated in patient samples. Using publically available microarray analyses of STS from Detwiller et al. (Detwiller et al., 2005) and Nakayama et al. (Nakayama et al., 2007) we compared the levels of *FOXM1* mRNA in normal and STS tissues (Fig. 10A,B). The list of individual tumor subtypes and associated *FOXM1* levels can be found in Table 3. *FOXM1* was dramatically upregulated in a variety of human sarcoma subtypes including fibrosarcoma, leiomyosarcoma, UPS, and liposarcoma relative to normal tissues. Interestingly, *FOXM1* levels in synovial sarcoma are less uniform suggesting that synovial sarcomas may employ alternate mechanisms of proliferation control. We used the Oncomine™ co-expression analysis tool to identify genes whose expression paralleled *FOXM1* in STS, and we compared the top 40 genes with known and potential YAP targets identified in the literature and a publically available microarray dataset of genes downregulated upon YAP inhibition in human malignant mesothelioma cells (Mizuno et al., 2012). Of the top 40 genes co-expressed with *FOXM1* in the Detwiller et al. database, 13 are also putative YAP targets (Fig. 11A,B). Similarly, 15 these top 40 genes identified in the Nakayama et al. database are putative YAP targets (Fig. 12A,B). 60% of these top targets are identical between the two databases. These results are consistent with the hypothesis that YAP/TEAD targets are upregulated in STS, most likely as a result of Hippo pathway dysregulation. Importantly, we showed that *FOXM1* is consistently upregulated in a variety of STS subtypes, suggesting that increased FOXM1 may be a common driver of proliferation in sarcoma.

FOXM1 promotes proliferation in sarcoma cells

35

Figure 10. *FOXM1* is highly expressed in human sarcoma. A) *FOXM1* levels obtained from Oncomine™ analysis of the Detwiller et al., 2005 microarray showed elevated FOXM1 mRNA levels in the indicated sarcomas compared with normal tissue all $P < 1 \times 10^{-7}$. B) Oncomine™ analysis of the Nakayama et al., 2007 microarray all $P < 0.014$.
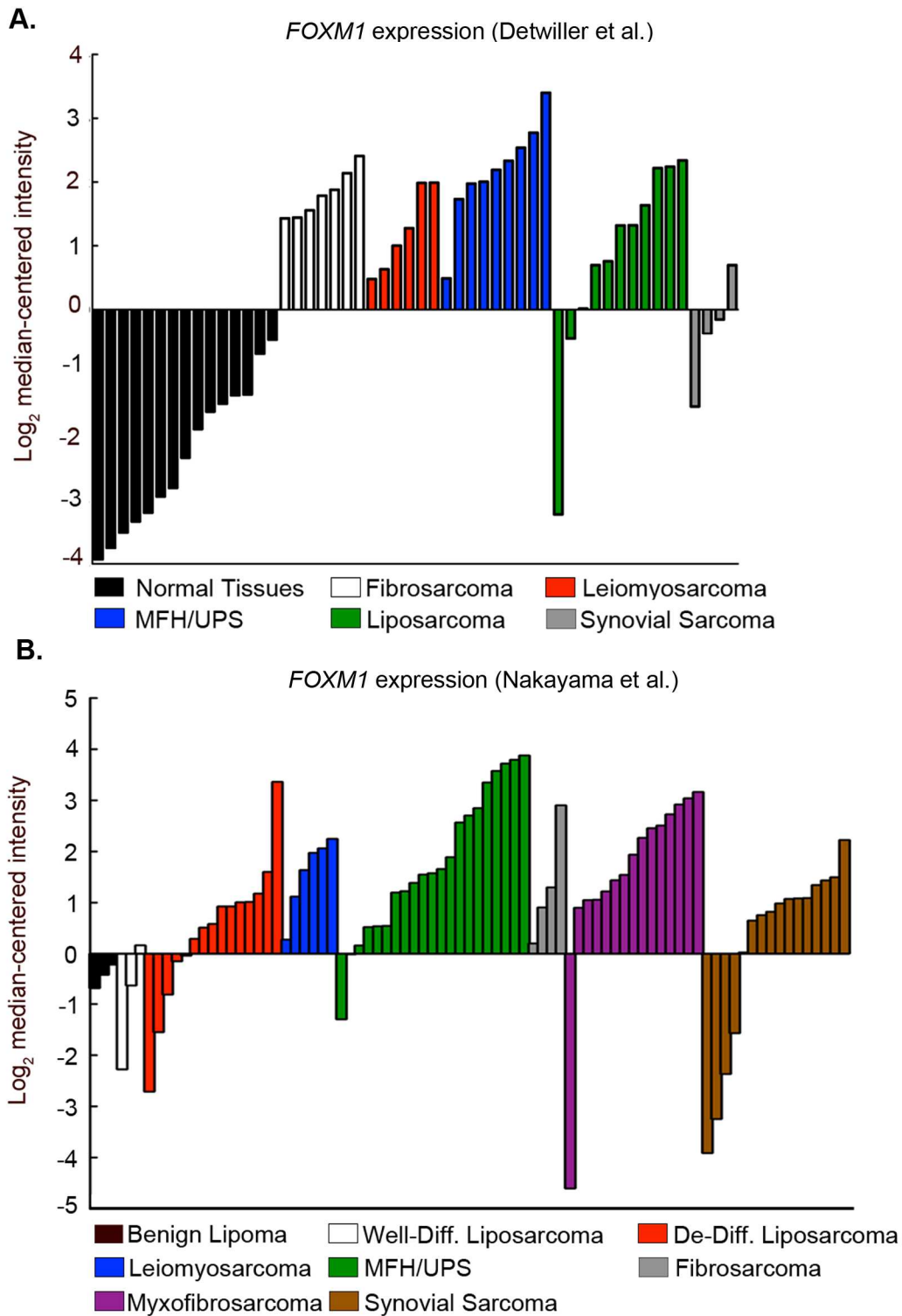
36

Detwiller et al.

Column #	Tissue Type	Normalized Intensity
1	Kidney	-3.92842
2	Adrenal Gland	-3.74958
3	Small Intestine	-3.50922
4	Heart	-3.3358
5	Skeletal Muscle Tissue	-3.19776
6	Pancreas	-2.94417
7	Prostate Gland	-2.81019
8	Stomach	-2.33698
9	Brain	-1.88706
10	Lung	-1.61363
11	Liver	-1.48872
12	Spleen	-1.35685
13	Skin	-1.34489
14	Colon	-0.70539
15	Connective Tissue	-0.48413
16	Fibrosarcoma	1.4324
17	Fibrosarcoma	1.44374
18	Fibrosarcoma	1.55673
19	Fibrosarcoma	1.78611
20	Fibrosarcoma	1.87935
21	Fibrosarcoma	2.13839
22	Fibrosarcoma	2.408
23	Leiomyosarcoma	0.47794
24	Leiomyosarcoma	0.63129
25	Leiomyosarcoma	1.00139
26	Leiomyosarcoma	1.27687
27	Leiomyosarcoma	1.98587
28	Leiomyosarcoma	1.99259
29	Malignant Fibrous Histiocytoma	0.4886
30	Malignant Fibrous Histiocytoma	1.73152
31	Malignant Fibrous Histiocytoma	1.97631
32	Malignant Fibrous Histiocytoma	2.00468
33	Malignant Fibrous Histiocytoma	2.19205
34	Malignant Fibrous Histiocytoma	2.33345
35	Malignant Fibrous Histiocytoma	2.53805
36	Malignant Fibrous Histiocytoma	2.77366
37	Malignant Fibrous Histiocytoma	3.4014
38	Dedifferentiated Liposarcoma	-3.22454
39	Dedifferentiated Liposarcoma	-0.46493
40	Dedifferentiated Liposarcoma	0.01509
41	Dedifferentiated Liposarcoma	0.6968
42	Pleomorphic Liposarcoma	0.75839
43	Pleomorphic Liposarcoma	1.32208
44	Pleomorphic Liposarcoma	1.32214
45	Round Cell Liposarcoma	1.63755
46	Round Cell Liposarcoma	2.21822
47	Round Cell Liposarcoma	2.23949
48	Round Cell Liposarcoma	2.34115
49	Synovial Sarcoma	-1.53243
50	Synovial Sarcoma	-0.38127
51	Synovial Sarcoma	-0.15588
52	Synovial Sarcoma	0.69625

Nakayama et al.

Column #	Tissue Type	Normalized Intensity
1	Lipoma	-0.67173
2	Lipoma	-0.41024
3	Lipoma	-0.20969
4	Well Differentiated Liposarcoma	-2.27397
5	Well Differentiated Liposarcoma	-0.61795
6	Well Differentiated Liposarcoma	0.16911
7	Dedifferentiated Liposarcoma	-2.71199
8	Dedifferentiated Liposarcoma	-1.54724
9	Dedifferentiated Liposarcoma	-0.8147
10	Dedifferentiated Liposarcoma	-0.1467
11	Dedifferentiated Liposarcoma	-0.03368
12	Dedifferentiated Liposarcoma	0.29518
13	Dedifferentiated Liposarcoma	0.51241
14	Dedifferentiated Liposarcoma	0.58496
15	Dedifferentiated Liposarcoma	0.92851
16	Dedifferentiated Liposarcoma	0.92926
17	Dedifferentiated Liposarcoma	1.00929
18	Dedifferentiated Liposarcoma	1.01446
19	Dedifferentiated Liposarcoma	1.17874
20	Dedifferentiated Liposarcoma	1.60416
21	Dedifferentiated Liposarcoma	3.36317
22	Leiomyosarcoma	0.2783
23	Leiomyosarcoma	1.12029
24	Leiomyosarcoma	1.63869
25	Leiomyosarcoma	1.97388
26	Leiomyosarcoma	2.06272
27	Leiomyosarcoma	2.24881
28	Malignant Fibrous Histiocytoma	-1.29653
29	Malignant Fibrous Histiocytoma	-0.00707
30	Malignant Fibrous Histiocytoma	0.16585
31	Malignant Fibrous Histiocytoma	0.52202
32	Malignant Fibrous Histiocytoma	0.53087
33	Malignant Fibrous Histiocytoma	0.54749
34	Malignant Fibrous Histiocytoma	1.1985
35	Malignant Fibrous Histiocytoma	1.22331
36	Malignant Fibrous Histiocytoma	1.38793
37	Malignant Fibrous Histiocytoma	1.54993
38	Malignant Fibrous Histiocytoma	1.57633
39	Malignant Fibrous Histiocytoma	1.65737
40	Malignant Fibrous Histiocytoma	1.89055
41	Malignant Fibrous Histiocytoma	2.56957
42	Malignant Fibrous Histiocytoma	2.70532
43	Malignant Fibrous Histiocytoma	2.84767
44	Malignant Fibrous Histiocytoma	3.35101
45	Malignant Fibrous Histiocytoma	3.57774
46	Malignant Fibrous Histiocytoma	3.71836
47	Malignant Fibrous Histiocytoma	3.79479
48	Malignant Fibrous Histiocytoma	3.88006
49	Fibrosarcoma	0.20492
50	Fibrosarcoma	0.90997
51	Fibrosarcoma	1.30021
52	Fibrosarcoma	2.90502
53	Myxofibrosarcoma	-4.60363
54	Myxofibrosarcoma	0.90215
55	Myxofibrosarcoma	1.0513
56	Myxofibrosarcoma	1.05858
57	Myxofibrosarcoma	1.22107
58	Myxofibrosarcoma	1.44075
59	Myxofibrosarcoma	1.54292
60	Myxofibrosarcoma	1.93743
61	Myxofibrosarcoma	2.26795
62	Myxofibrosarcoma	2.45743
63	Myxofibrosarcoma	2.51022
64	Myxofibrosarcoma	2.72841
65	Myxofibrosarcoma	2.92078
66	Myxofibrosarcoma	3.04032
67	Myxofibrosarcoma	3.16631
68	Synovial Sarcoma	-3.91238
69	Synovial Sarcoma	-3.24793
70	Synovial Sarcoma	-2.36712
71	Synovial Sarcoma	-1.56819
72	Synovial Sarcoma	0.02785
73	Synovial Sarcoma	0.65047
74	Synovial Sarcoma	0.75931
75	Synovial Sarcoma	0.82271
76	Synovial Sarcoma	0.98579
77	Synovial Sarcoma	1.07552
78	Synovial Sarcoma	1.08517
79	Synovial Sarcoma	1.08964
80	Synovial Sarcoma	1.34534
81	Synovial Sarcoma	1.43625
82	Synovial Sarcoma	1.49765
83	Synovial Sarcoma	2.22582

Table 3. Sarcoma subtypes included in expression analysis. Lists of the sarcoma subtypes (in order) included in Oncomine-based gene expression analysis from Detwiller et al., and Nakayama et al.
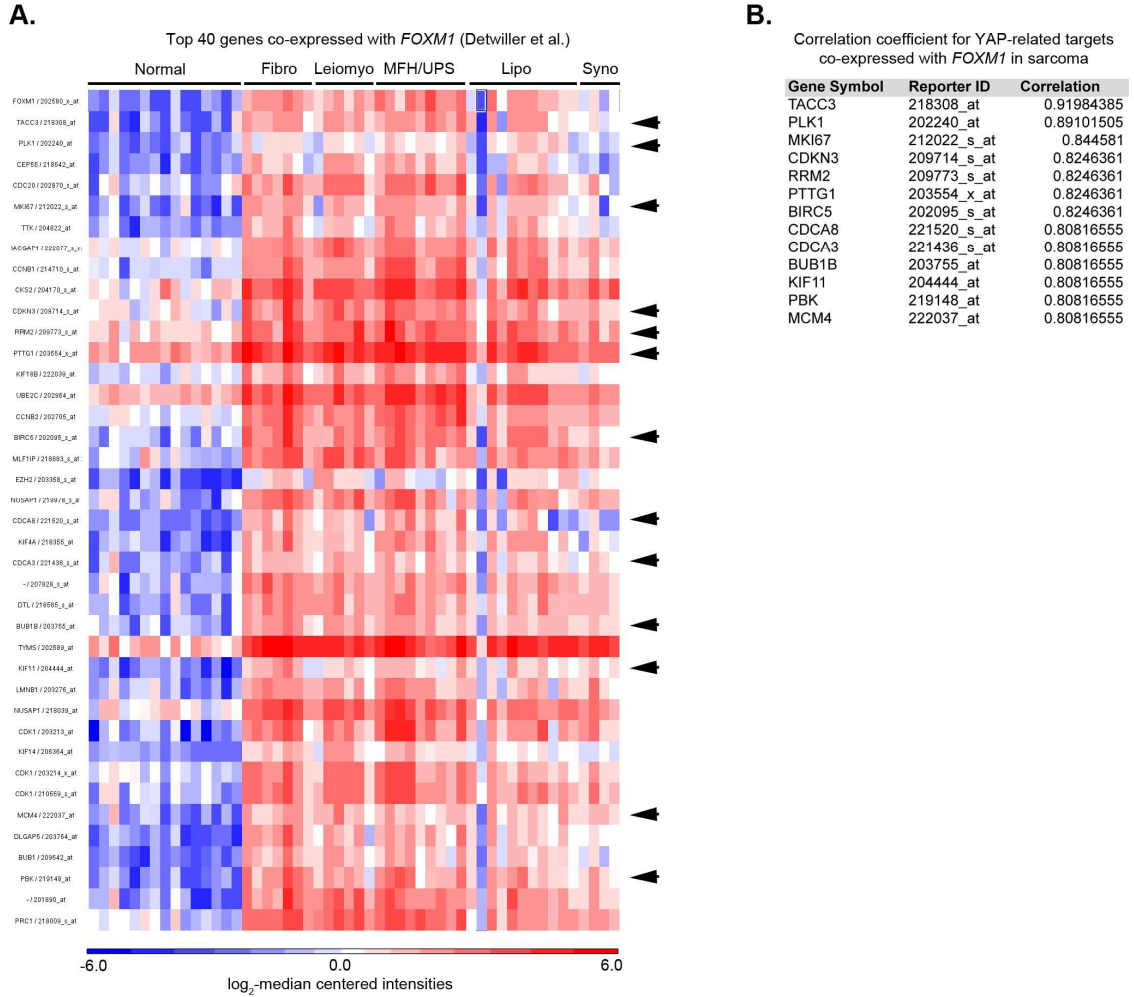
A.

Top 40 genes co-expressed with *FOXM1* (Detwiller et al.)

Normal | Fibro | Leiomyo | MFH/UPS | Lipo | Syno

FOXM1 / 202580_x_at
TACC3 / 218308_at
PLK1 / 202240_at
CEP55 / 218542_at
CDC20 / 202870_s_at
MKI67 / 212022_s_at
TTK / 204822_at
RACGAP1 / 222077_s_at
CCNB1 / 214710_s_at
CKS2 / 204170_s_at
CDKN3 / 209714_s_at
RRM2 / 209773_s_at
PTTG1 / 203554_x_at
KIF18B / 222039_at
UBE2C / 202954_at
CCNB2 / 202705_at
BIRC5 / 202095_s_at
MLF1IP / 218883_s_at
EZH2 / 203358_s_at
NUSAP1 / 219978_s_at
CDCA8 / 221520_s_at
KIF4A / 218355_at
CDCA3 / 221436_s_at
- / 207828_s_at
DTL / 218585_s_at
BUB1B / 203755_at
TYMS / 202589_at
KIF11 / 204444_at
LMNB1 / 203276_at
NUSAP1 / 218039_at
CDK1 / 203213_at
KIF14 / 206364_at
CDK1 / 203214_x_at
CDK1 / 210559_s_at
MCM4 / 222037_at
DLGAP5 / 203764_at
BUB1 / 209642_at
PBK / 219148_at
- / 201890_at
PRC1 / 218009_s_at

-6.0 | 0.0 | 6.0
log$_2$-median centered intensities

B.

Correlation coefficient for YAP-related targets co-expressed with *FOXM1* in sarcoma

Gene Symbol	Reporter ID	Correlation
TACC3	218308_at	0.91984385
PLK1	202240_at	0.89101505
MKI67	212022_s_at	0.844581
CDKN3	209714_s_at	0.8246361
RRM2	209773_s_at	0.8246361
PTTG1	203554_x_at	0.8246361
BIRC5	202095_s_at	0.8246361
CDCA8	221520_s_at	0.80816555
CDCA3	221436_s_at	0.80816555
BUB1B	203755_at	0.80816555
KIF11	204444_at	0.80816555
PBK	219148_at	0.80816555
MCM4	222037_at	0.80816555

Figure 11. YAP target co-expression with *FOXM1* in Detwiller et al. A) Oncomine analysis of targets co-expressing with *FOXM1* in the Detwiller et al., 2005 microarray. Arrows indicate targets that are also controlled by YAP; targets summarized in (B). B) Table delineating YAP targets co-expressed with FOXM1 in the Detwiller et al., 2006 microarray in sarcoma, including correlation coefficients of co-expression.

A.

Top 40 genes co-expressed with *FOXM1* (Nakayama et al.)
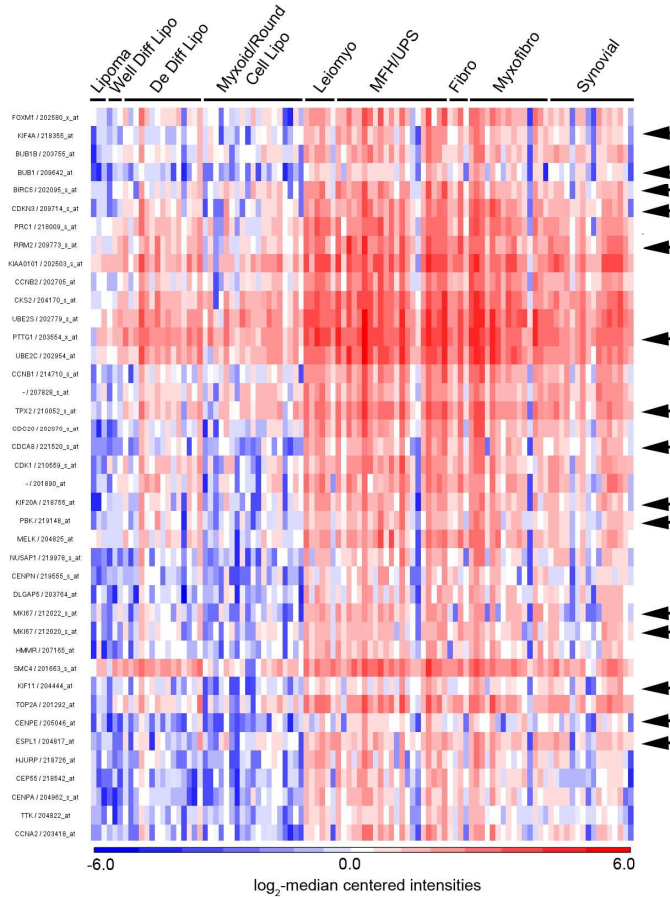
B.

Correlation coefficient for YAP-related targets
co-expressed with *FOXM1* in sarcoma

Gene Symbol	Reporter ID	Correlation
KIF4A	218355_at	0.76150566
BUB1B	203755_at	0.707797
BIRC5	202095_s_at	0.7030443
CDKN3	209714_s_at	0.7030443
RRM2	209773_s_at	0.7030443
PTTG1	203554_x_at	0.7030443
TPX2	210052_s_at	0.7030443
CDCA8	221520_s_at	0.7030443
KIF20A	218755_at	0.7030443
PBK	219148_at	0.7030443
MKI67	212022_s_at	0.6816478
MKI67	212020_s_at	0.67982805
KIF11	204444_at	0.6728878
CENPE	205046_at	0.6728878
ESPL1	204817_at	0.66259366

Figure 12. YAP target co-expression with *FOXM1* in Nakayama et al. A) Oncomine analysis of targets co-expressing with *FOXM1* in the Nakayama et al., 2007 microarray. Arrows indicate targets that are also controlled by YAP; targets summarized in (B). B) Table delineating YAP targets co-expressed with FOXM1 in the Nakayama et al., 2007 microarray in sarcoma, including correlation coefficients of co-expression.
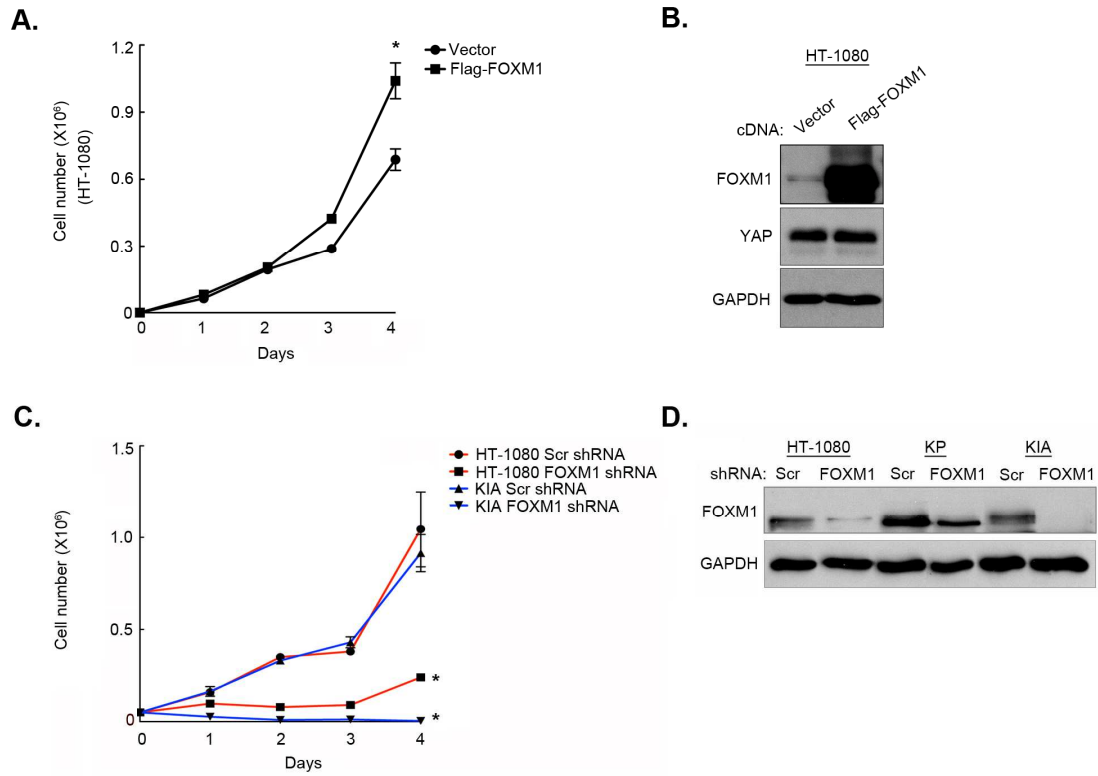
39

Figure 13. *FOXM1* drives proliferation in sarcoma cells. A) Proliferation assay of HT-1080 cells expressing empty vector or Flag-FOXM1 constructs. *P* = 0.019. B) Immunoblot of FOXM1 and YAP levels 4 days post Flag-FOXM1 overexpression. C) Proliferation analysis of HT-1080 and KIA cells expressing scrambled (Scr) or FOXM1 shRNA: HT-1080 *P* =0.042 at day 4; KIA *P*=0.012 at day 4. D) Immunoblot of FOXM1 and YAP levels 4 days post FOXM1 knockdown. *Karin Eisinger contributed this figure.*

As a key transcriptional output of the Hippo pathway and a known driver or proliferation in a variety of cancer models, we investigated the role of FOXM1 in sarcoma cell growth. We performed a combination of over-expression and shRNA-mediated *FOXM1* ablation experiments. Human Flag-FOXM1was introduced into HT-1080 cells, which exhibit a slower rate of proliferation and lack p53 mutations or deletions that could elevate endogenous FOXM1 levels. Expression of Flag-FOXM1 increased proliferation in these cells (Fig. 13A) while having no effect on endogenous YAP expression levels (Fig. 13B). Consistent with these findings, shRNA-mediated silencing of *FOXM1* significantly inhibited proliferation of both human and murine sarcoma cells (Fig. 13C,D). We hypothesized that reintroduction of Flag-FOXM1 might partially rescue YAP-dependent growth defects in sarcoma cells. However, exogenous FOXM1 had no effect on proliferation of sarcoma cells expressing a YAP-specific shRNA (Fig. 14A,B). Based on these data the overlap of YAP and FOXM1 target genes, we investigated the possibility that FOXM1 interacts directly with the YAP complex to promote transcription in sarcoma cells. If a physical interaction between FOXM1 and YAP were essential for YAP/TEAD activity then exogenous FOXM1 would not be able to "rescue" proliferation in the absence of YAP. We performed Flag-FOXM1 IP studies in HT-1080 cells expressing empty vector, V5-YAP, or HA-TEAD1 (Fig. 14C). While FOXM1 failed to bind YAP, it interacted strongly with TEAD1. This observation suggests that a physical association between FOXM1 and the YAP/TEAD complex occurs at the promoters of target genes, providing a likely explanation for the inability of FOXM1 to rescue YAP-deficient cell proliferation. To determine if FOXM1 can interact with the YAP/TEAD complex at target gene promoters in humans, we queried ChIP-seq data available through the Encyclopedia of DNA Elements (ENCODE) project and UCSC Genome Browser (http://genome.ucsc.edu/ENCODE/). Sequence analyses of up to 20 kilobases upstream of the transcriptional start sites (TSS) of 24 independent putative YAP/TEAD or FOXM1 targets was performed, and queried for TEAD or FOXM1 consensus binding sites. FOXM1 and TEAD binding sites were considered adjacent if they were within 200 bases of each other. Target genes containing both FOXM1 and TEAD consensus sites were assessed to determine if the sites were adjacent, suggesting direct
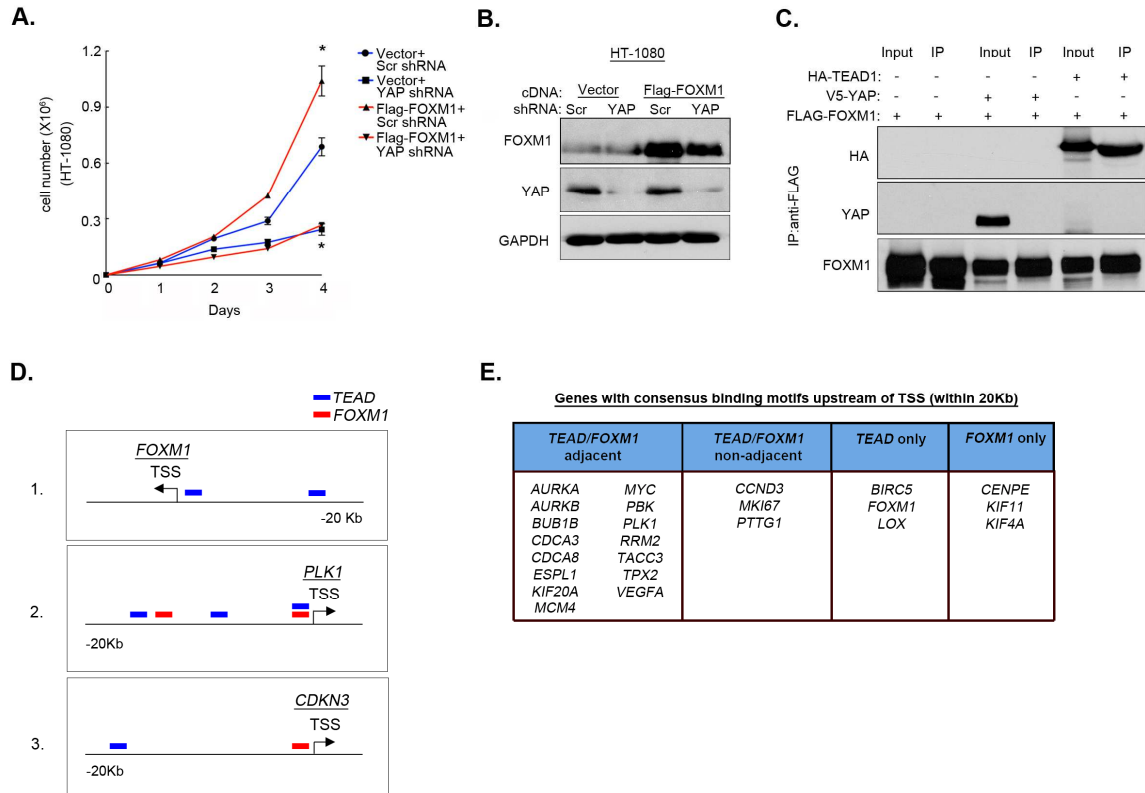
41

Figure 14. Evidence for YAP/TEAD/FOXM1 interaction. A) Rescue Proliferation analysis of HT-1080 cells expressing *YAP* shRNA or Scr shRNA as well either a Flag-FOXM1 over-expression constructor empty vector Scr/vector shRNA vs. *YAP* shRNA/vector P <0.02 at day 4; Scr/vector vs. Scr/Flag-FOXM1 P <0.02 at day 4. B) Immunoblot showing YAP and FOXM1 levels from day 4 of proliferation assay in (A). C). Immunoblot showing HA, YAP, and Flag-FOXM1 levels upon immunoprecipitation with anti-Flag antibody-coated beads. D) Schematic of TEAD and FOXM1 binding sites upstream of the transcription start sites (TSS) for *FOXM1* (1), *PLK1* (2), and *CDKN3* (3). Each schematic represents an example of TEAD1 only binding site presence (1), adjacent TEAD/FOXM1 sites (2) and non-adjacent TEAD/FOXM1 sites (3). Blue = TEAD binding site. Red = FOXM1 binding site. E) Table dividing 24 FOXM1 or YAP/TEAD targets into groups based on location and identity of the binding sites (adjacent TEAD/FOXM1 binding sites, non-adjacent TEAD/FOXM1 binding sites, TEAD sites only, and FOXM1 sites only). *Karin Eisinger assisted with the completion of this figure.*

interaction of FOXM1 with TEAD, or non-adjacent indicating potentially independent regulation by both factors. A schematic of this study can be found in Fig. 14D. Out of 24 targets, 15 contained adjacent TEAD/FOXM1 binding sites, 3 contained TEAD and FOXM1 binding sites that were not adjacent, and 3 contained exclusively TEAD sites or FOXM1 sites (Fig. 14E). These results were based solely on the published ChIP-seq data from ENCODE. Expanding the search to more remote distances away from TSS could yield additional adjacent TEAD/FOXM1 binding sites in the future. These results, taken together with the IP data, suggest that a YAP/TEAD/FOXM1 complex binding at regulatory regions of genes promoting cell growth impacts proliferation.

FOXM1 is required for sarcomagenesis in vivo

We evaluated the contribution of FOXM1 to sarcomagenesis in vivo using human HT-1080 xenografts as well as a novel autochthonous murine model. Deletion of *FOXM1* dramatically reduced tumor volume (Fig. 15A) and tumor volume (Fig. 15B) in HT-1080 xenografts. In order to assess the requirement for FOXM1 during sarcoma initiation and tumorigenesis in a physiological model that accurately recapitulates human disease, we conditionally deleted *Foxm1* in our autochthonous KP murine system. We generated $Kras^{G12D/+}$; $Trp53^{fl/fl}$; $Foxm1^{fl/fl}$ (KPF) mice by crossing $Kras^{G12D/+}$; $Trp53^{fl/fl}$ (KP) and $Foxm1^{fl/fl}$ animals. KPF mice developed very few tumors compared with KP (Fig. 15C) and the tumors that did form were significantly smaller (Fig. 15D,E). Of note, KP tumors contained a heterogeneous population of multinucleated, irregular, enlarged tumor cells compared with KPF tumors, suggesting the *Foxm1*-deleted tumors may undergo less proliferation-associated damage to the genome and accumulate fewer mutations (Fig. 15F). We confirmed recombination at the *Foxm1* locus in KPF tumors (Fig. 15G), which was consistent with IHC showing loss of Foxm1 protein levels in KPF tumors (Fig. 15H). We also showed that YAP and TEAD1 are expressed in the nucleus of KP tumors, indicating that the Hippo pathway may be inactive in this model (Fig. 16). The lack of FOXM1 expression in the existing KPF tumors suggests that Foxm1 may not be required for tumor initiation in this model, but is necessary for
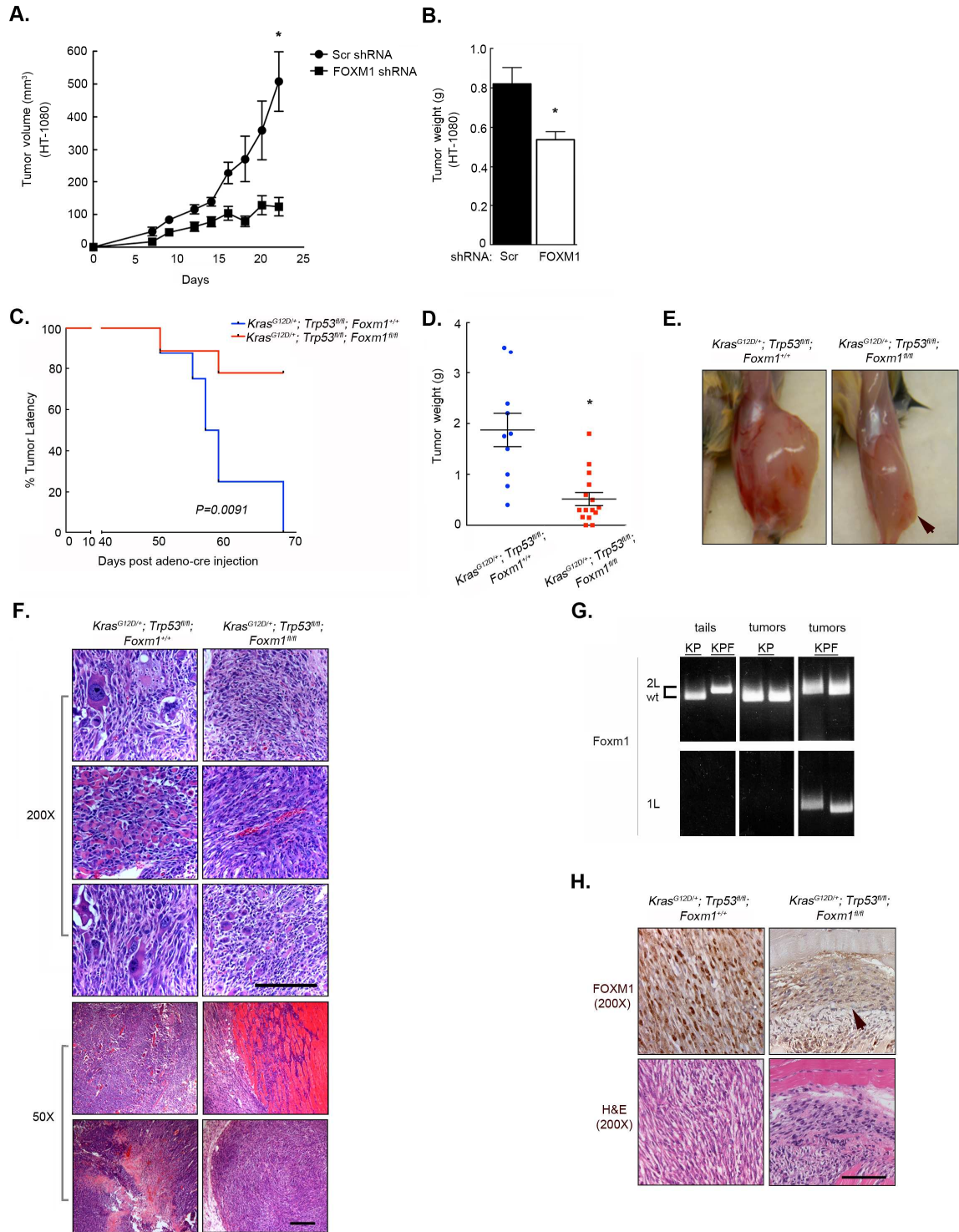
43

Figure 15. FOXM1 is required for sarcomagenesis *in vivo*. A) FOXM1 was depleted in HT-1080 cells and 1×10^6 cells were injected subcutaneously in a xenograft model. Knockdown of FOXM1 significantly inhibited tumor growth n= 5 mice per group, *P*=0.04. **B)** Tumor weight from xenografts in (A) was also decreased in *FOXM1*-depleted cells *P*=0.0091. **C)** Autochthonous

mouse model of UPS, $Kras^{G12D/+}$; $Trp53^{fl/fl}$ (KP) was crossed with $Foxm1^{fl/fl}$ mice to create $Kras^{G12D/+}$; $Trp53^{fl/fl}$; $Foxm1^{fl/fl}$ (KPF). Deletion of Foxm1 inhibited sarcomagenesis n= 10 (KP); n=115 (KPF). P=0.0091. **D)** Tumor weight was significantly decreased in KPF tumors compared with KP P=0.0002. **E)** Images of KP and KPF tumor bearing mice. **F)** H&E images from KP and KPF tumors showing the prevalence of irregular and heterogeneous tumor cells in the KP animals as well as the less of necrotic and stromal compartments due to *Foxm1* deletion. Scale bar=100 µM. **G)** Genotyping of KP and KPF animals and tumors showing recombination at the *Foxm1* locus in KPF tumors**. H)** IHC of Foxm1 and H&E in KP and KPF tumors showing that Foxm1 protein expression is lost in the small KPF tumors. Scale bar=100 µM. *Karin Eisinger contributed this figure.*
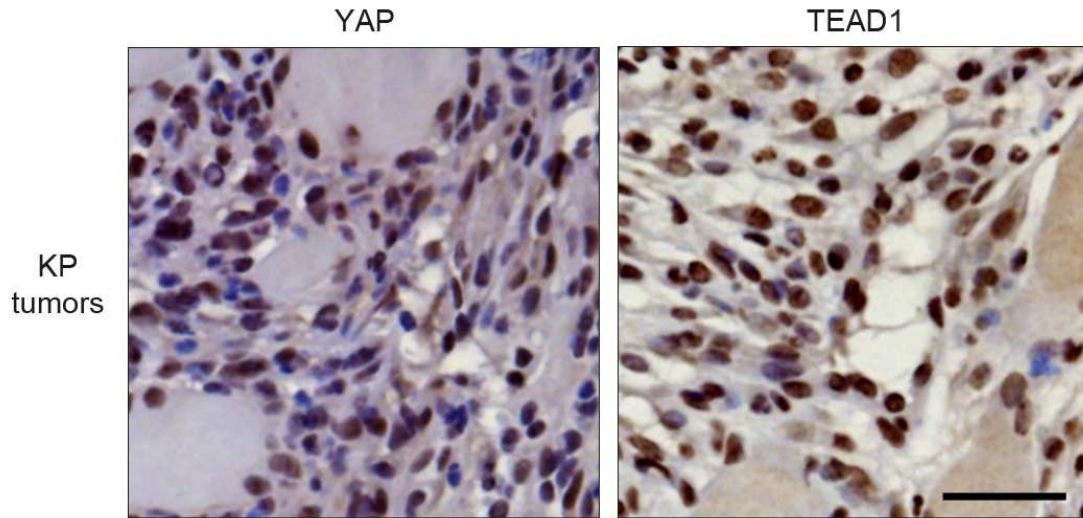
45

YAP   TEAD1

KP
tumors

Figure 16. YAP and TEAD1 are expressed in the nucleus of KP tumors. Tumors were embedded in paraffin, sectioned, and stained for YAP and TEAD1. Scale bar=50 μM.

tumor growth and progression. Together, these data clearly indicate that FOXM1 promotes sarcomagenesis, making it an attractive target for therapeutic intervention in STS.

FOXM1 pharmacological inhibition decreases cell proliferation and tumor formation

To investigate the potential of FOXM1 as an STS therapeutic target, we employed a previously described inhibitor of FOXM1 expression, Thiostrepton (Bhat et al., 2009). Thiostrepton is a proteasomal inhibitor that has been shown to decrease FOXM1 protein expression in multiple cancer cell types (Bhat et al., 2009; Halasi and Gartel, 2009). We found that Thiostrepton is indeed an effective inhibitor of FOXM1 protein accumulation (Fig. 17A) while having no effect on *FOXM1* mRNA levels, compared to shRNA (Fig. 17B). These findings are consistent with previous studies utilizing Thiostrepton. Of note, we successfully decreased FOXM1 expressing using 1 µM Thiostrepton, whereas in a breast cancer model 10 µM Thiostrepton was required to achieve similar levels of inhibition (Wang and Gartel, 2011), suggesting that sarcoma cells may be particularly sensitive to Thiostrepton. FOXM1 inhibition significantly decreased sarcoma cell proliferation *in vitro* (Fig. 17C,D), consistent with results obtained using *FOXM1* shRNA (Fig. 13C). Thiostrepton treatment (48 hours) also inhibited many of the same targets transcriptional targets sensitive to VP treatment, including *Tacc3*, *Lox*, *Cdkn3*, and *Plk1* (Fig. 6E,F). These findings suggest that YAP inhibition via VP, and FOXM1 inhibition through Thiostrepton has similar effects on transcriptional output in sarcoma cells. To determine if FOXM1 could be an effective therapeutic target we performed *in vivo* studies using lipid encapsulated Thiostrepton micelles. Lipid encapsulation, as previously described (Wang and Gartel, 2011), allows for enhanced solubility and delivery of Thiostrepton. We treated nude mice bearing KP allograft tumors with vehicle control, 7.5 mg/kg or 15 mg/kg micelle-encapsulated Thiostrepton retro-orbitally every third day for 2.5 weeks. The higher of the two Thiostrepton doses significantly decreased tumor volume (Fig. 18A) and weight (Fig. 18B) while having no effect on overall animal health and activity. Loss of FOXM1 reduced proliferation (Ki67 IHC) (Fig. 18C,D), consistent with loss of proliferation in YAP and FOXM1 silenced tumors. Together, these
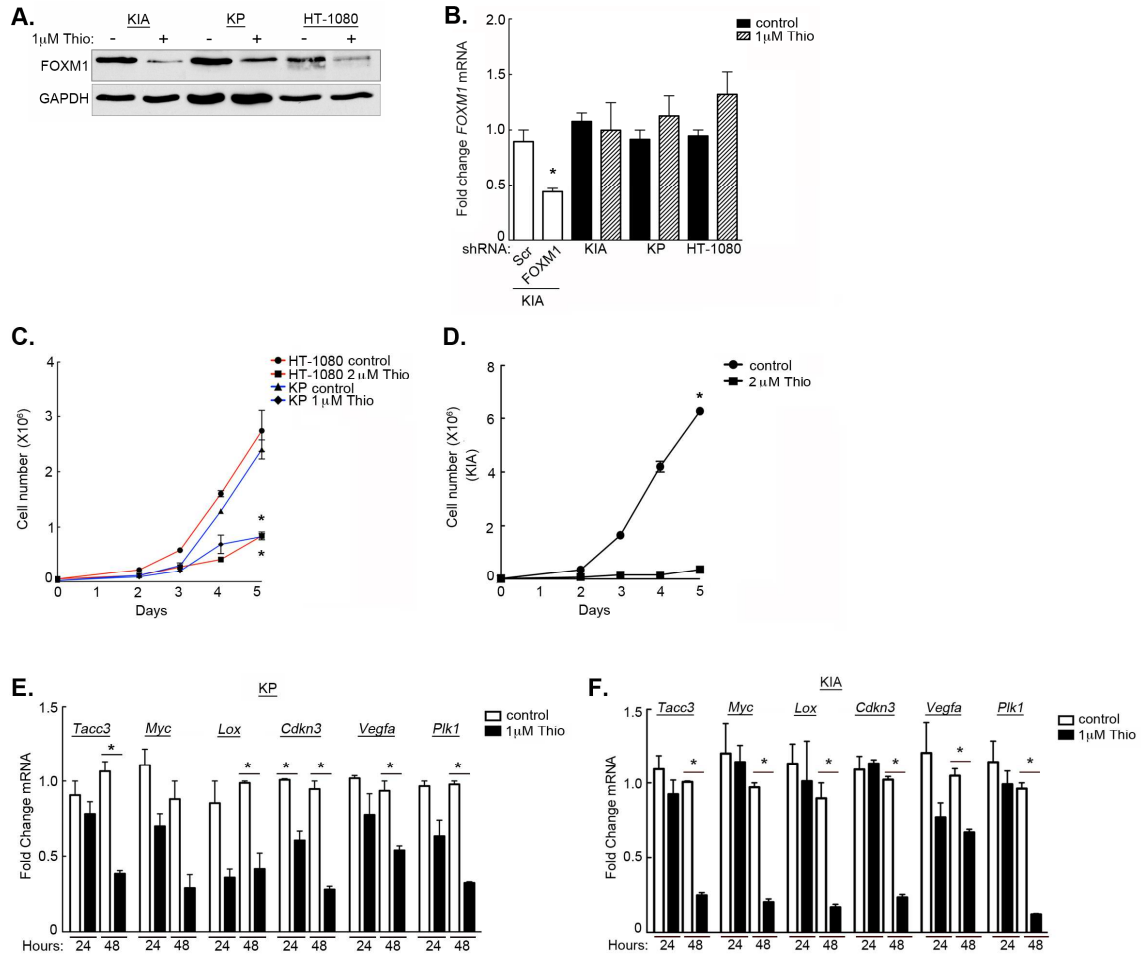
47

Figure 17. Thiostrepton-mediated FOXM1 inhibition decreases proliferation *in vitro.* A) Immunoblot of FOXM1 levels in KIA, KP and HT-1080 cells upon 48 hours of 1μM Thiostrepton (Thio) or DMSO control (-). B) *Foxm1* mRNA levels in KIA cells infected with scramble (Scr) or *FOXM1* shRNA and KIA, KP and HT-1080 cells treated with Control DMSO or 1 μM Thiostrepton. *FOXM1* mRNA is decreased upon shRNA infection but unchanged with Thiostrepton treatment. * P-value = 0.0134. C) Proliferation analysis of HT-1080 cells (red lines) treated with DMSO control or 2 μM Thiostrepton and KP cells (blue lines) treated with DMSO control or 1μM Thiostrepton. P-value = 0.0007 for HT-1080 cells; P-value < 3.57×10^{-5} for KP cells. D) Proliferation analysis of KIA cells treated with DMSO control or 2 μM Thiostrepton. P-value = 0.0009. E) mRNA levels of Foxm1 targets after 24 and 48 hours of control DMSO and 1 μM Thiostrepton treatment. KP cells treated with 1 μM Thiostrepton showed decreases in Foxm1 target mRNA expression including *TACC3* (P = 0.010), *LOX* (P = 0.032), *CDKN3* (P = 0.023 at 24 hours, P = 0.0075 at 48 hours), *VEGFA* (P = 0.030), *PLK1* (P = 0.00133). F) KIA cells were treated with 1μM Thiostrepton for 24 or 48 hours. FOXM1 transcriptional targets decreased include *Tacc3 P=.0007; Myc P=.023; Lox P=0.020; Cdkn3 P=0.001; Vegfa P=0.019*; and *Plk1 P=0.002. Kevin Biju and Karin Eisinger contributed to this figure.*
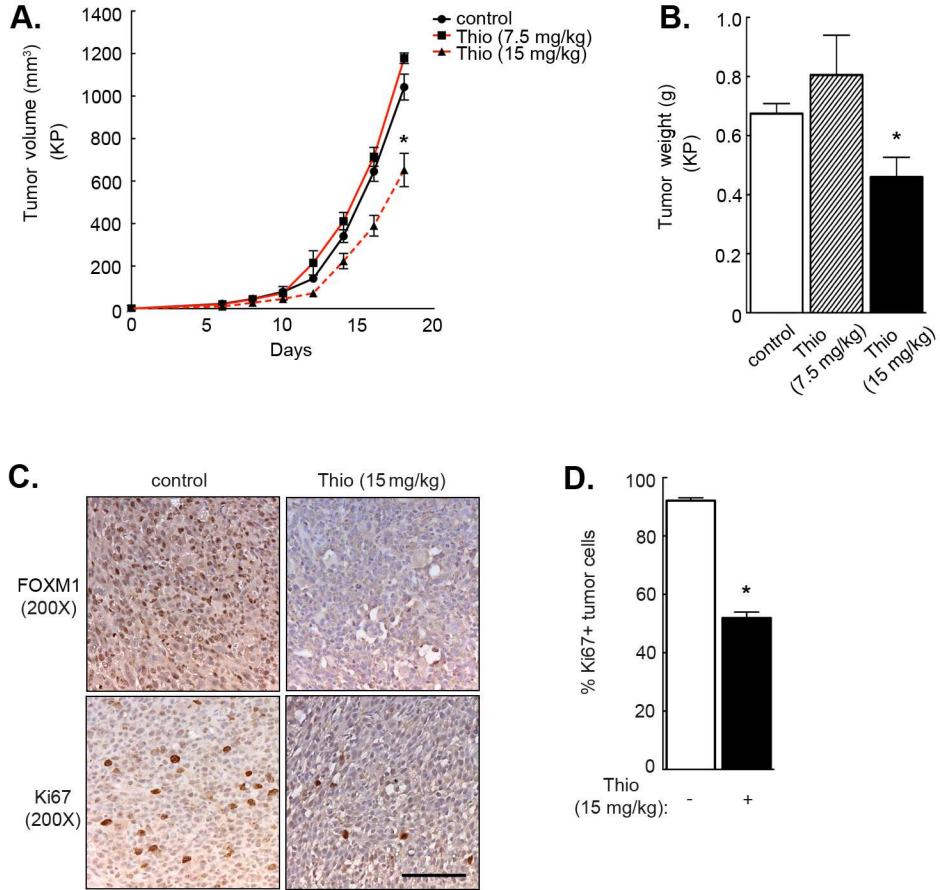
48

Figure 18. Thiostrepton-mediated FOXM1 inhibition decreases proliferation *in vivo.* A) Tumor volume in a subcutaneous xenograft of KP cells treated with PBS control and 7.5 mg/kg or 15 mg/kg micelle-encapsulated Thiostrepton. n = 9 mice for control tumors; n = 2 mice for 7.5 mg/kg treatment; n = 7 mice for 15 mg/kg treatment. B) Tumor weights of KP xenografts from micelle-encapsulated Thiostrepton treatment in A). 15 mg/kg Thiostrepton treatment resulted in significant decrease in tumor weight compared to control treated xenografts (P = 0.0083). C) Immunohistochemical staining for FOXM1 and Ki67 in control and Thiostrepton (15 mg/kg) treated tumors from A) at day 18. D) Quantification of Ki67 positive cells in control and Thiostrepton (15 mg/kg) treated tumors P=2.5X10^{-22}. Scale bar=100 μM. *Karin Eisinger and Kevin Biju contributed to this figure.*

49

data indicate that FOXM1 inhibitors may be valuable tools for the treatment of sarcomas.

Discussion

The Hippo pathway has been extensively studied both during development and in epithelial tumorigenesis. Substantially less is known about the role of Hippo and its downstream effector YAP in mesenchymal tumors. Previous studies evaluating the role of YAP in STS have focused on alvelolar and embryonal rhabdomyosarcoma (aRMS and eRMS), two rare STS subtypes that affect children and adolescents (Parham and Ellison, 2006). Compared to many other STS, aRMS and eRMS are relatively well understood: their tissue of origin is known to be skeletal muscle, and for aRMS, the underlying oncogenic chromosomal translocation has been identified (e.g. *PAX7/FOXO1*), and histologically they appear less pleomorphic in comparison to the more aggressive, molecularly complex subtypes discussed here, including UPS, fibrosarcoma, and de-differentiated liposarcoma. We investigated the expression of key upstream Hippo pathway modulators like NF2, SAV1, MST1/2, and LATS1/2 in sarcoma patient samples and found that several genomic loci encoding essential factors are at least partially lost in STS. While it is currently unclear whether or not these genes are completely or partially deleted, we have shown that YAP expression and nuclear localization is stabilized in human UPS and an autochthonous mouse model of UPS. YAP activation is known to promote tumor growth via increased transcription of pro-proliferative and anti-apoptotic factors, as a TEAD cofactor. Moreover, YAP/TEAD – mediated FOXM1 expression is crucial for this process. However, over-expression does not guarantee that FOXM1 is transcriptionally active in sarcomas. FOXM1 activation is controlled by oncogenic stimuli (i.e. Ras) and loss of tumor suppressors (i.e. p53, Arf) (Wierstra, 2013). Perturbation of the Mitogen-activated protein kinase (MAPK) pathway and loss of p53 are commonly observed in sarcomas (Sasaki et al., 2011; Taylor et al., 2011). Therefore, the KP mouse model of UPS is an appropriate system to query the function and regulation of FOXM1 in STS. Conditional *Foxm1* deletion in the KP model dramatically reduces tumor burden, suggesting that FOXM1 serves as a transcriptional node connecting Hippo pathway inactivation

with oncogenic stimuli/tumor suppressor loss in sarcoma (Fig.19). Furthermore, we observed that FOXM1 functions not only downstream of YAP, but can also interact directly with the YAP/TEAD complex to facilitate proliferation (Fig.19). Together these findings suggest that inhibiting the YAP/TEAD1/FOXM1 complex is an attractive avenue for therapeutic intervention in these mesenchymal tumors.

Pharmacologic inhibition of transcription factor/coactivator complexes has been a challenge due to a lack of druggable pockets in DNA-transcription factor binding. However, several proof-of concept small molecules and peptides have been shown to inhibit FOXM1 or YAP. Due to biologic inhibition by ARF, FOXM1 can be inhibited by a small synthetic ARF peptide (Gusarova et al., 2007). Additionally, FOXM1 can be inhibited by a class of thiopeptide antibiotics, including Thiostrepton. Thiostrepton efficacy against FOXM1 has been shown both *in vitro* and *in vivo* (Wang and Gartel, 2011). While less is known about small molecules effective at inhibiting YAP or TEAD, a 2012 screen for molecules disrupting the YAP/TEAD complex yielded the benzophyrin class of molecules as promising inhibitors. Among these, Verteporfin (VP) was shown to inhibit YAP/TEAD function both *in vitro* and *in vivo*, possibly by binding YAP and changing its structure so as to inhibit YAP/TEAD direct association (Liu-Chittenden et al., 2012).

Currently there are no anti-cancer treatments specifically targeting YAP or FOXM1 in the clinic. VP is being used to treat macular degeneration under the trade name Visudyne™, but the mechanism of action involves generation of reactive oxygen species (ROS) for photodynamic therapy (Michels and Schmidt-Erfurth, 2001) rather than YAP inhibition. It may be worthwhile to investigate the use of VP, or related benzophyrin molecules, in YAP-driven tumors. However, it is generally accepted that inhibition of a major upstream regulator can have a variety of unrelated targets and undesired outcomes leading to cytotoxicity and patient side effects. Therefore, we focused on inhibition of an essential downstream target that controls many YAP-dependent phenotypes, FOXM1. Thiostrepton successfully inhibited FOXM1 and reduced tumorigenesis, in an allograft sarcoma model, even at a relatively low dose of 15 mg/kg. This result shows that FOXM1 inhibition is a promising approach for sarcoma treatment, warranting further study and

preclinical assessment. While Thiostrepton is not specific for FOXM1, our findings suggest that an unbiased screen to identify more selective inhibitors would expand therapeutic opportunities for sarcoma. Previous studies have shown that injection of cell permeable Arf peptides can effectively inhibit FOXM1 and tumorigenesis in a model of HCC (Gusarova et al., 2007). Targeting these peptides for delivery to sarcoma cells may also be an effective, additional therapeutic approach.

One limitation of the current study is that primary sarcomagenesis, investigated in this study, is seldom responsible for poor patient outcome as is the case for a variety of cancers. In many, if not most, sarcoma cases metastatic disease burden is the principal cause of mortality. Importantly, sarcoma metastasis is directly linked to primary tumor hyperproliferation and resulting changes in intratumoral microenvironments (Eisinger-Mathason et al., 2013). While targeting the primary tumor should prevent metastatic progression in those patients diagnosed prior to micrometastatic dissemination, metastatic cells arising from YAP-driven FOXM1 expressing sarcomas may also be sensitive to inhibition of this pathway. Further analysis of metastatic tissue is required to determine if metastatic cells rely on YAP/FOXM1 to assess whether inhibition of this complex would target both the primary and metastatic tumor sites. Of note, it has been shown that YAP and FOXM1 play a role in migration/invasion and metastasis in other contexts (Lamar et al., 2012; Lok et al., 2011; Mo et al., 2012). Importantly, human FOXM1 has been associated specifically with UPS metastasis (Mito et al., 2009). Further study would determine if YAP and FOXM1 co-regulate metastatic progression beyond their control of proliferation in the primary tumor.

Although sarcomas comprise a heterogeneous and histopathologically diverse set of malignancies, our work indicates that one frequently occurring genetic alteration in a subset of these tumor types is in the Hippo pathway. We have found that this pathway is inactivated in nearly half of reported sarcomas in the TCGA database, spanning diverse STS tumors. In parallel we have observed that *FOXM1* expression is elevated in multiple STS subtypes including, de-

52

differentiated liposarcoma, fibrosarcoma, leiomyosarcoma, and UPS, suggesting that some mechanisms may cross histological classifications. However, this finding cannot be universally applied to sarcoma. For example synovial sarcoma patient samples express heterogeneous levels of *FOXM1*. Together our data lead us to conclude that sarcoma classification based on molecular signatures, rather than solely on histopathology, would allow the development of therapeutics (i.e. FOXM1 inhibitors) that benefit the broadest possible, yet most accurate, cohort of patients.
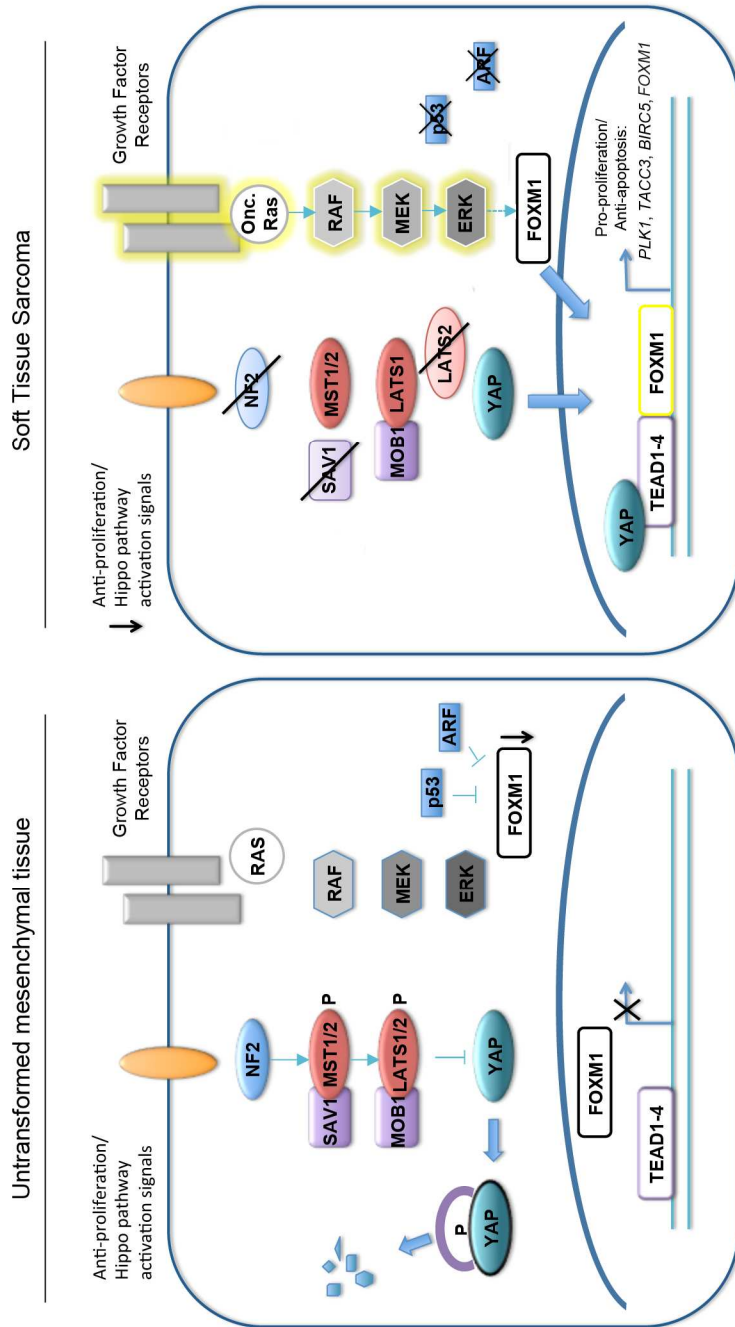
53

Figure 19. Model depicting the mechanism governing YAP-mediated control of FOXM1 and other pro-proliferation downstream targets.

54

CHAPTER 3

MiR-124 counteracts pro-survival stress responses in glioblastoma

SUMMARY

Glioblastomas are aggressive adult brain tumors, characterized by inadequately organized vasculature and consequent nutrient and oxygen (O_2)-depleted areas. Adaptation to low nutrients and hypoxia supports glioblastoma cell survival, progression, and therapeutic resistance. However, specific mechanisms promoting cellular survival under nutrient and O_2 deprivation remain incompletely understood. In this chapter, I show that *miR-124* expression is negatively correlated with a hypoxic gene signature in glioblastoma patient samples, suggesting that low *miR-124* levels contribute to pro-survival adaptive pathways in this disease. Since *miR-124* expression is repressed in various cancers (including glioblastoma), we quantified *miR-124* abundance in normoxic and hypoxic regions in glioblastoma patient tissue, and investigated whether ectopic *miR-124* expression compromises cell survival during tumor ischemia. Our results indicate that *miR-124* levels are further diminished in hypoxic/ischemic regions within individual glioblastoma patient samples, compared to regions replete in O_2 and nutrients. Importantly, we also show that increased *miR-124* expression affects the ability of tumor cells to survive under O_2 and/or nutrient deprivation. Moreover, *miR-124* re-expression increases cell death *in vivo*, and enhances the survival of mice bearing intracranial xenograft tumors. *miR-124* exerts this phenotype in part by directly regulating *TEAD1*, *MAPK14*/p38α and *SERP1*, factors involved in cell proliferation and survival under stress. Collectively, among the many pro-tumorigenic properties of *miR-124* repression in glioblastoma, we delineated a novel role in promoting tumor cell survival under stressful microenvironments, thereby supporting tumor progression.

55

INTRODUCTION

Glioblastoma Multiforme (GBM) is the most aggressive adult brain tumor. At only 12 months, median GBM patient survival is one of the lowest for all cancers (Krex et al., 2007). The standard of care for GBM treatment is surgery, followed by radiation and chemotherapy (Stupp et al., 2005). However, glioblastomas rapidly become resistant to these therapies, thereby making them ineffective at significantly improving prognosis. GBM tumors are considered Grade IV (the most aggressive gliomas) and occur either *de novo* or as a progression from lower grade lesions (Louis et al., 2007). In both instances, the key feature of GBM, as compared with lower grade gliomas, is the presence of severely hypoxic/ischemic regions (Amberger-Murphy, 2009). Low oxygen tension (hypoxia) is defined as less than 2% O_2 and occurs in most solid tumors due to rapid proliferation, or aberrant angiogenesis, resulting in poor perfusion. The presence of hypoxic/ischemic areas is detrimental to GBM patients, as it positively correlates with recurrence and negatively correlates with patient survival (Evans et al., 2010; Spence et al., 2008). Therefore, identifying factors mediating cellular adaptation to nutrient deprivation and hypoxia is crucial for improving therapeutic approaches to GBM.

Recent studies, such as the Cancer Genome Atlas (TCGA), have elucidated genetic aberrations associated with glioblastomas. In addition to deregulated oncoproteins and tumor suppressors (such as EGFR, PDGFR, PI3K, PTEN, NF1, etc.) (2008; Verhaak et al., 2010), numerous micro-RNAs (miRNAs) are differentially expressed in GBMs relative to adjacent non-neoplastic tissue (Silber et al., 2008a; Wu et al., 2012). miRNAs are ~22 nucleotide small RNAs that function as post-transcriptional negative regulators of ~30% of all mammalian genes (Ambros, 2004; Bartel, 2009). While the inhibition of any single miRNA target is relatively modest, each miRNA impacts the expression of numerous genes. Thus, by targeting genes involved in multiple pathways, a single miRNA can significantly influence systems involved in cell cycle progression, differentiation, and cell death, as well as broad responses to stress (Esquela-Kerscher and Slack, 2006a).

56

Previous studies have measured miRNA levels in glioblastoma and compared them to adjacent non-neoplastic tissues, or to lower-grade gliomas. In particular, *miR-124* levels were shown to be significantly reduced in glioblastomas as compared to both adjacent non-neoplastic tissues (Silber et al., 2008a) and lower-grade tumors (Ben-Hamo and Efroni, 2011; Koivunen et al., 2012). *miR-124* is a brain-enriched miRNA critical for regulating neuronal differentiation (Gao, 2010; Lim et al., 2005; Makeyev et al., 2007b; Visvanathan et al., 2007; Yoo et al., 2011). As *miR-124* levels are differentially expressed in distinct brain cell types, low *miR-124* levels in glioblastoma may be a result of the cellular heterogeneity between glioma and adjacent tissue (Nelson et al., 2006; Sonntag et al., 2012). Alternatively, it is possible that *miR-124* functions as a tumor suppressor in GBM. This has been suggested in the context of other tumors (Hatziapostolou et al., 2011; Hunt et al., 2011; Wu et al., 2012) and the abundance of known *miR-124* targets negatively correlates with *miR-124* levels in brain tumor patient samples (Koivunen et al., 2012; Sonntag et al., 2012), leaving open the possibility that glioblastoma cells expressing low *miR-124* levels exhibit a selective growth or survival advantage.

Hypoxic glioblastoma cells are often found in perinecrotic areas, where surviving cells experience low levels of O_2 in addition to diminished nutrient and growth factor availability (Rong et al., 2006). Such cells must therefore adapt to steep O_2 and nutrient gradients, and these adaptive responses are partly mediated by the Hypoxia Inducible Factors (HIFs) (Kaelin and Ratcliffe, 2008). Recent studies have shown that miRNAs also play a key role in modulating cellular survival or death under limiting O_2 and nutrient availability. For example, *miR-210* is elevated in hypoxic regions and promotes survival under low O_2 (Huang et al., 2009). Additionally, we have shown that restoring *miR-218* levels in glioblastoma opposes a Receptor-Tyrosine Kinase/HIF signaling pathway necessary for glioblastoma progression, particularly in the Mesenchymal subtype (Mathew et al., 2014b).

Here, we show that *miR-124* levels inversely correlate with a hypoxic signature in TCGA patient samples. Moreover, *miR-124* levels are diminished in pseudopalisading regions within

57

individual glioblastoma patient tissues, when compared to relatively well-perfused regions. We demonstrate that increased *miR-124* expression in glioblastoma cells experiencing nutrient and O_2 deprivation promotes cell death, suggesting that *miR-124* targets factors important for glioblastoma survival under stressful microenvironments. Moreover, *miR-124* expression leads to increased cell death *in vivo*, in a doxycycline-induced tumor xenograft model that faithfully recapitulates hypoxic/ischemic regions in GBM. We identify three factors, TEAD1, p38α (MAPK14) and SERP1, as direct *miR-124* targets, and show that they are overexpressed in hypoxic/ischemic conditions. Combined inhibition of these targets recapitulates the increased cell death observed under low nutrient/O_2 stress, upon *miR-124* expression. In addition, SERP1 re-expression reverses the *miR-124* cell death phenotype in glioblastoma cells grown under hypoxia. Finally, we show that *miR-124* restoration confers increased mouse overall survival in an intracranial orthotopic xenograft model. These data suggest further investigation of *miR-124* and its targets, in particular SERP1, is strongly warranted.

MATERIALS AND METHODS

Cell Culture conditions, reagents, and lentiviral transduction

U87MG, U373, LN18 and HEK 293T cells were obtained from ATCC (Manassas, VA, USA), and cultured in DMEM containing 10% FBS, glutamine, non-essential amino-acids, Penicillin/Streptomyicin antibiotics and HEPES buffer, and passaged on average every three days. Cells cultured in the nutrient deprived media were grown in glucose-free DMEM containing glutamine, non-essential amino-acids, antibiotics and HEPES buffer, without the addition of FBS. Cells were grown under hypoxic incubation in a Ruskinn invivO$_2$ 400 workstation. Patient-derived glioblastoma tumor spheres were a gift from Dr. Jeremy Rich (Cleveland Clinic, Cleveland, OH, USA). These cells were maintained in Neurobasal medium, supplemented 1:50 with B27 (Invitrogen, Carlsbad, CA, USA), Epidermal Growth Factor (Sigma, St. Louis, MO, USA) at 20 ng/mL, and basic Fibroblast Growth Factor at 20 ng/mL. Non-targeting and miR-124 mimics were obtained from Dharmacon (Lafayette, CO, USA). microRNA mimic transfection was performed

using HiPerFect transfection reagent (Qiagen, Germantown, MD, USA). 100 mM miRNA mimics were used for all experiments. Tunicamycin (Sigma) was diluted in DMSO was administered at 1 µg/mL for 24 hours. All viruses were packaged using the third generation lentivector system (Invitrogen) and expressed in HEK 293T cells. Supernatant containing virus was collected at 24 hr and 48 hr timepoints and concentrated using 10-kDa Amicon Ultra-15 centrifugal filter units (Millipore, Billerica, MA, USA). Overexpression of SERP1 Open Reading Frame was achieved by cloning into the pCDH-CMV-MCS-EF1-Puro vector (Systems Biosciences, Mountain View, CA, USA) via *Eco*RI and *Not*I restriction sites.

Immunoblots

Lysates were collected using a whole cell elution buffer previously described. 20 or 40 μg protein was loaded in 12% or 15% SDS-PAGE gels, transferred to nitrocellulose and blotted with various antibodies for TEAD1 (Novus, St. Charles, MI, USA), p38α (Cell Signaling, Danvers, MA, USA), SERP1 (Genetex, Irvine, CA, USA), β-tubulin, PARP, cleaved PARP, (Cell Signaling). Primary antibodies were diluted 1:1000 in 5% non-fat milk TBST.

Cell death assays

Cell death was assessed using Annexin-PI staining on Flow Cytometry, using the FITC Annexin V Apoptosis Detection Kit I from BD Pharmingen (San Jose, CA, USA). For nutrient deprivation/hypoxia experiments, cells were kept under stress conditions for 48 hours before cell death was assayed. For tunicamycin experiments, cells were kept under stress conditions for 24 hours.

In vivo *xenograft assays*

All experiments were performed in accordance with NIH guidelines and approved by the University of Pennsylvania Institutional Animal Care and Use Committee (IACUC). Sub-cutaneous xenografts were performed on Nu/Nu mice (Charles River, Burlington, MA, USA) as

59

previously described. 1,000,000 U87-MG cells expressing the empty pCDH-EF1-copGFP lentivector or the pCDH-EF1-copGFP-pre-*miR-124* lentivector were injected on flanks of nude mice and the tumors were subsequently measured by caliper over the period of a month. Additionally, sub-cutaneous xenografts were performed with U87-MG cells expressing: Scr shRNA, TEAD1 shRNA, SERP1 shRNA, doxycycline-inducible miR-124 and doxycycline inducible control. Tumor volume was measured using the calculation: $(X \bullet Y^2)\pi/6$, where X is the longest caliper measurement, Y is the shortest, and π=3.14. For the doxycycline-inducible experiments, mice were fed 2 mg/mL doxycycline and 5% glucose in their drinking water for 7 days.

Orthotopic xenograft injections were performed by stereotactically injecting 500,000 U87-MG glioblastoma cells in 5 uL PBS, 5mm in the right cerebral hemisphere in 8-week-old Nu/Nu mice. As in the sub-cutaneous xenograft experiment, the U87-MG cells were expressing either the empty pCDH-EF1-copGFP, or the pCDH-EF1-copGFP-pre-*miR-124* lentivector. Prior to injection, the mouse was prepared as previously described. The animals were sacrificed at the first sign of neurological symptoms.

Immunohistochemistry (IHC) and Immunofluorescence (IF) assays

IHC and IF were performed on 5 μm sections according to standard protocols. Antibody concentrations are the following: HIF1α: 1:100 (Abcam, Cambridge, UK), GFP: 1:100 (Cell Signaling). Images were taken using a Leica 500 microscope (Leica, Solms, Germany) at 10X magnification. Paraffin embedded sections were stained for TUNEL using an ApopTag Plus Fluorescein In situ Apoptosis Detection Kit (Chemicon, Temecula, CA, USA) according to the manufacturer's instructions. Images were taken at 20X magnification using an Olympus IX81 microscope (Olympus, Center Valley, PA, USA).

Laser Capture Microdissection

60

FFPE slides were lightly stained with Hematoxylin and Eosin and immediately subjected to laser capture under RNase-Free conditions. For pseudopalisading regions, the internal necrotic core was initially cut and discarded, before the pseudopalisading region was collected for testing. Microdissection was performed using a Leica microscope and the Leica LMD software. Upon collection, RNA was extracted using the Qiagen miRNeasy FFPE kit.

Patient samples

LCM tissue: At the Hospital of the University of Pennsylvania, we searched the departmental surgical pathology database for cases with the diagnosis of "Glioblastoma, WHO grade IV" over a two year period (2011-2013). Only primary glioblastomas that had not received prior radiation or chemotherapy were included. Subsequently, the cases were screened by a neuropathologist (P.P.G) for adequate areas of both pseudopalisading necrosis and solid tumor, and whether it was possible to obtain ten 10 um unstained tissue sections from the archived paraffin embedded formalin fixed tissue blocks.   mRNA extraction from whole patient sample: the formalin-fixed, paraffin-embedded (FFPE) patient samples were obtained from the University of Pennsylvania Department of Pathology and Laboratory Medicine (Philadelphia, PA). GBM blocks were screened by a neuropathologist (S.V) contained > 95% tumor cells. Controls (temporal lobectomy tissue obtained from intractable epilepsy patients) showed histopathologic evidence of mild to focally moderate gliosis, but no lesions. GBM patients age range: 24 to 89 years, (Median: 63 years). Control patients age range: 22 to 61 years, (Median: 38 years). RNA was obtained from FFPE samples using the RecoverAll™ Total Nucleic Acid Isolation kit (Ambion, Austin, TX, USA).

Bioinformatic analyses

mRNA expression data were downloaded from the TCGA Data Portal (https://tcga-data.nci.nih.gov/tcga/). Data generated on the Affymetrix microarray platform HT_HG-U133A for 385 tumor and 10 normal samples was subjected to GCRMA normalization (GCRMA background

61

correction, quantile normalization, log2 transformation and Median polish probeset summarization) was used to determine mRNA expression. To obtain expression, previously normalized TCGA Level2 data from 426 tumor samples and 10 normal samples run on Agilent's miRNA microarray was utilized. Data were analyzed using the Partek software (Partek Inc., St. Louis, MO, USA). To determine the association between *miR-124* and expression of the HIF signature, we utilized the Gene Set Analysis (GSA) implementation (version 1.03) of Gene Set Enrichment Analysis (GSEA). We defined the HIF signature by using previously - established HIF regulated genes (Koivunen et al., 2012). To create a single value that represents the expression of the HIF signature (HIF metagene), the average expression of all the genes in the HIF signature was calculated for each tumor sample (using TCGA GBM data). This HIF metagene was then used as a continuous variable for various comparisons between groups. Analysis was performed using the R language and environment for statistical computing.

Statistics

All statistical analysis was performed using the GraphPad Prism™software (La Jolla, CA, USA). All data are represented as mean $\pm$ S.E.M. To establish whether a difference between two values is statistically significant, we performed Student's t-test, where $p < 0.05$ defines statistical significance.

RESULTS

miR-124 *levels inversely correlate with hypoxia signatures in glioblastoma patients and are further decreased in pseudopalisading necrotic regions within patient tissues.*

While several studies have shown that *miR-124* levels are low in glioblastomas as compared to adjacent non-neoplastic tissues, little is known about how *miR-124* levels correlate with low O_2 microenvironments. We took advantage of the large TCGA glioblastoma dataset (2008), and compared *miR-124* levels to a "hypoxia" signature identified in the GBM patients' expression profile. We defined a Hypoxia Inducible Factor (HIF) metagene by averaging the

62

expression of known HIF-regulated genes (Koivunen et al., 2012) from each TCGA patient into a single expression value. A high HIF metagene score positively correlates with high levels of hypoxia in each patient sample. Interestingly, *miR-124* levels negatively correlated with the HIF metagene, suggesting that GBM tissues experiencing highly hypoxic microenvironments have even lower *miR-124* levels (Fig. 20A, Fig. 21). Furthermore, we stratified TCGA patients based on *miR-124* levels (high vs. low) and observed that patients expressing the lowest levels of *miR-124* exhibited a higher correlation with the HIF metagene. To validate our analysis, we also queried the levels of *miR-210*, a known miRNA stimulated by hypoxia, which positively correlated with the HIF metagene (Fig. 20B).

While the TCGA contains a large repository of patient samples, it does not compare normoxic and hypoxic regions of glioblastoma within the same tumor. To determine whether *miR-124* levels were changing in hypoxic/ischemic domains within an individual glioblastoma patient sample, we performed laser-capture microdissection, collected regions of pseudopalisading necrosis, and compared them to non-necrotic, better-perfused areas. (Fig. 22A,B). We compared *miR-124* and *GLUT1* levels between the perfused ("normoxic") and hypoxic regions of each individual patient, and showed that, while *miR-124* levels are already low in glioblastoma tissue, they are further diminished in domains experiencing hypoxia/ischemia (Fig. 22C, left panel). Conversely, *GLUT1*, a hypoxically induced HIF target gene, was elevated in the hypoxic regions (Fig. 22C, right panel). Taken together, these findings suggest the possibility that *miR-124* levels may be further decreased in hypoxic/ischemic domains, potentially to confer a survival advantage within a stressful microenvironment.

miR-124 *expression increases cell death in glioblastoma cells grown under limiting nutrients and oxygen.*

63

A.

Correlation to HIF Metagene

B.

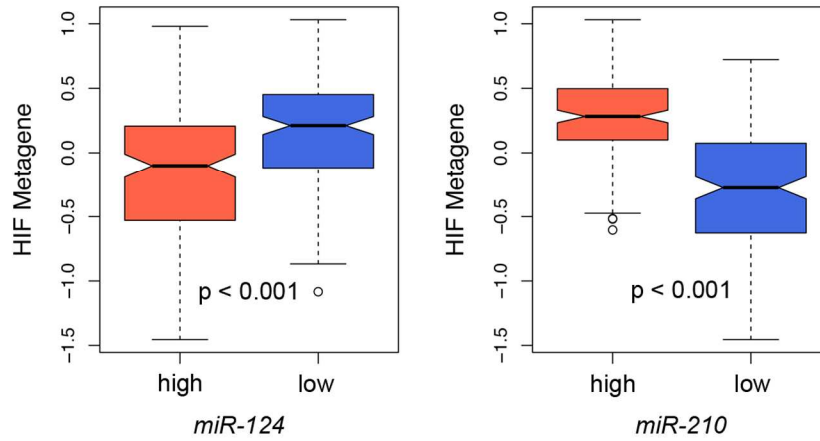*miR-124*   *miR-210*
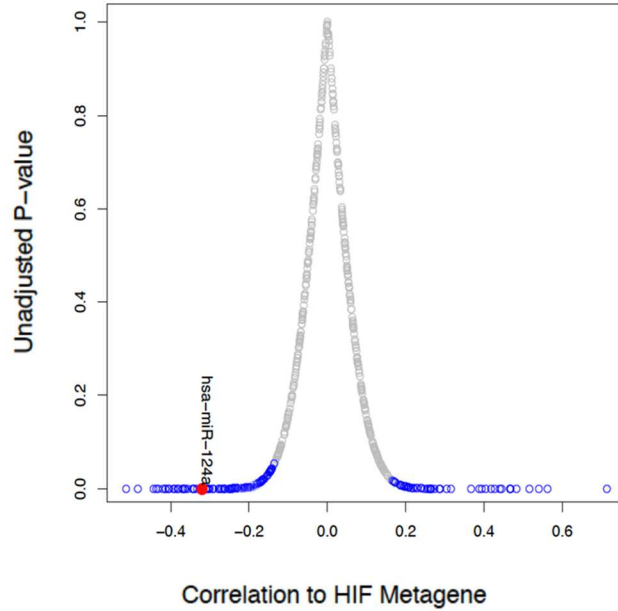
Figure 20. Correlation between miRNA levels and hypoxic metagene in TCGA patient samples. A) Hypoxia Inducible Factor (HIF) metagene correlation to miRNA levels. MiRNAs that are positively and negatively correlated with the metagene are indicated blue = p - value < 0.05. Red dot = *miR-124*. B) HIF metagene in TCGA GBM patient samples divided into high and low *miR-124* / *miR-210* levels. *Andy Minn assisted with the completion of this figure.*
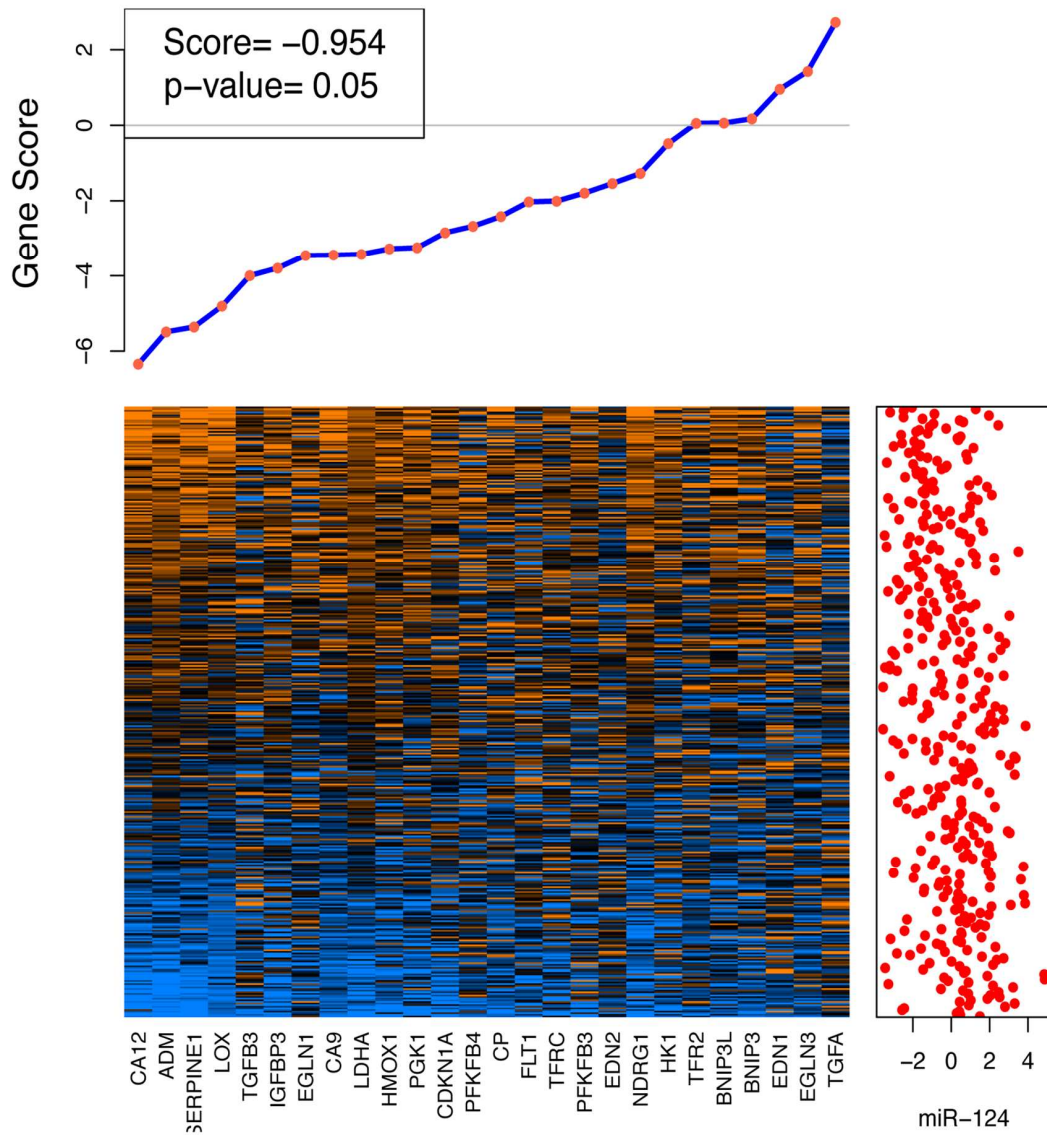
64

Figure 21. Correlation between *miR-124* levels and individual hypoxia/HIF signature targets. Gene Set Enrichment Analysis showing a negative correlation between a hypoxic gene signature and *miR-124* levels. Red dots = *miR-124* levels for each individual TCGA patient (log scale). Heatmap shows individual levels of each patient sample. Orange = high level of mRNA expression. Blue = low level of mRNA expression. *Andy Minn assisted with the completion of this figure.*
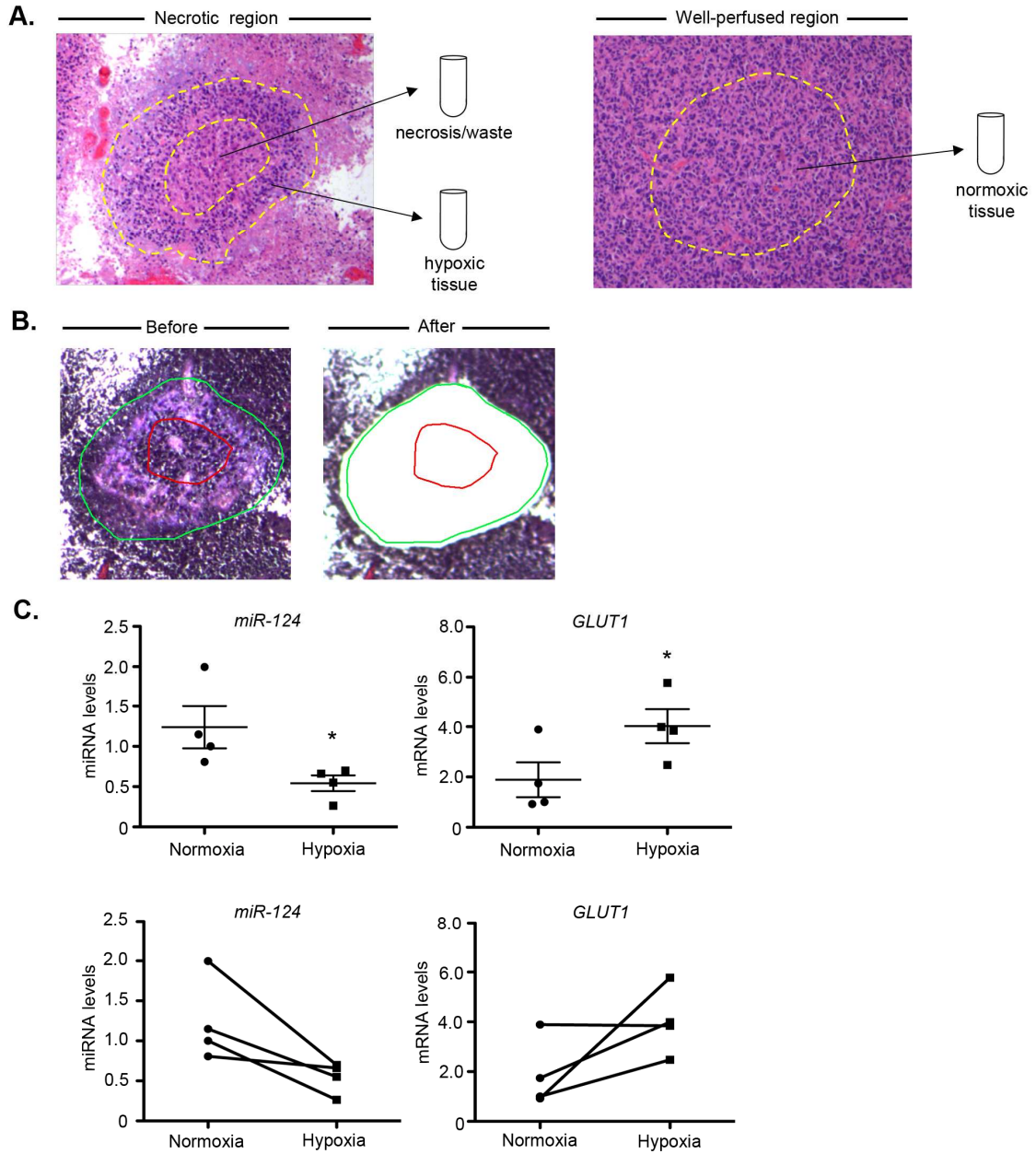
Figure 22. *miR-124* is decreased in pseudopalisading regions within patient tumors. A) Schematic of Laser-Capture Microdissection. Left: region of pseudopalisading necrosis. The inner necrotic region is discarded, while the pseudopalisade is collected as "hypoxic tissue". Right: Non-necrotic region, collected as the perfused ("normoxic") tissue counterpart. B) Laser-Capture microdissection images before and after microdissection. Red line indicates necrotic sample that was discarded as waste. Green line indicates perinecrotic area that was collected after disposal of necrotic sample. C) *miR-124* and *GLUT1* mRNA levels in perfused or "normoxic" and hypoxic regions in patient samples. Top: averages; bottom: paired representation (each pair is from an individual patient). * p - value = 0.047 (*miR-124* changes); p - value = 0.035 (*GLUT1* changes). n = 4 patients.

To determine whether *miR-124* levels affect glioblastoma cells during stress, we increased *miR-124* expression in U87MG and LN18 glioblastoma cells and incubated them for 48 hours under nutrient deprivation (no glucose, no serum) or hypoxia (0.5% O_2). Interestingly, we found that *miR-124* re-expression resulted in a significant increase in cell death in glioblastoma cells cultured under nutrient or O_2 deprivation, as measured by Annexin/PI staining and flow cytometry (Fig. 23A,C). Consequently, a slight increase in cleaved PARP accumulation was observed (Fig. 23B). As shown previously, no significant change in cell viability was observed in glioblastoma cells grown under replete O_2 and nutrients upon *miR-124* expression (Fig. 23A), suggesting that cell death is due to *miR-124* negatively regulating factors responsible for pro-survival, adaptive responses specifically during stress. We confirmed these results by modulating serum and O_2 levels in U373-MG cells and imaging *miR-124*-dependent cell death (Fig. 24). Of note, *miR-124* enhanced cell death was also observed when cells were treated with tunicamycin, a small molecule that induces ER stress (Fig. 23D-F). Based on these results, we hypothesized that *miR-124* may be targeting factors that are active under stress conditions, and subsequently their pro-survival effects.

TEAD1*,* MAPK14*/p38*α*, and* SERP1 *are* miR-124 *direct targets.*

To identify potential *miR-124* targets promoting survival during stress, we queried various miRNA target prediction bioinformatic databases, including TargetScan™, miRBase™ and DIANA-LAB, as well as previously published microarrays of genes modulated by *miR-124* overexpression (Lim et al., 2005; Makeyev et al., 2007b), and identified three putative *miR-124* targets that may play a role in pro-survival stress responses: *MAPK14*/p38α, *TEAD1* and *SERP1.*

TEAD1 (TEA Domain 1) is a transcription factor regulated by the Hippo pathway, which controls the expression of many pro-proliferation genes (Zhao et al., 2008a). Interestingly, a recent study has shown that TEAD1 overexpression leads to an anti-apoptotic phenotype in HeLa cells (Malt et al., 2012). p38α (also known as MAPK14, MAP kinase 14) is a kinase typically
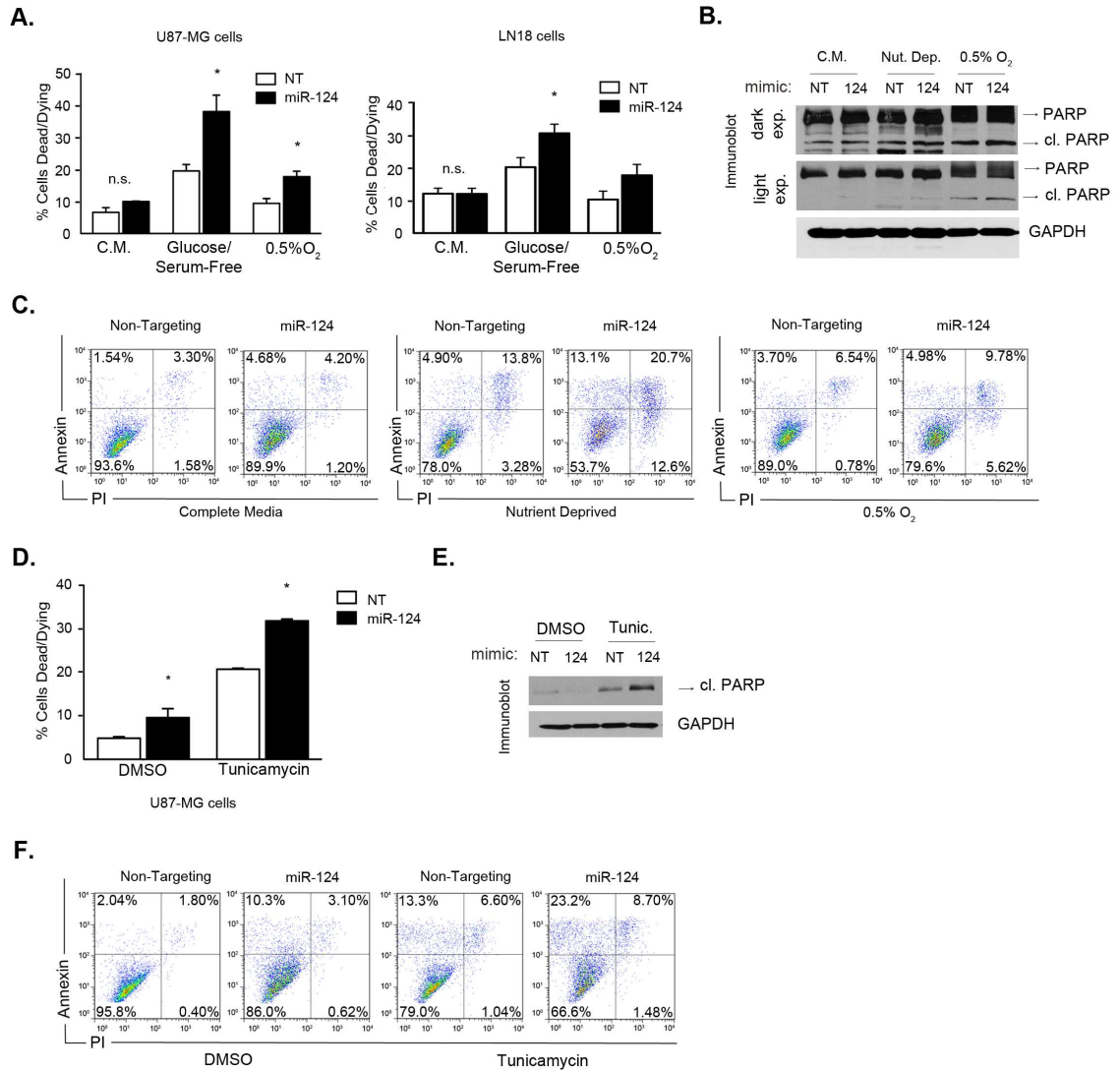
67

Figure 23. *miR-124* **expression increases cell death in glioblastoma cells grown under limiting nutrients and oxygen.** A) U87-MG and LN18 cells were grown under the following conditions: Complete Media (C.M.), Glucose/Serum-Free, and Hypoxia (0.5% O_2). Cells were transfected with either a Non-Targeting (NT) or *miR-124* mimic (miR-124) for 48 hours, followed by Annexin/PI staining and flow cytometry for cell death analysis. B) Immunoblots of cleaved (cl.) PARP in cells treated as described in (A) (lysates probed with total PARP antibody which shows both PARP and cleaved PARP). C) Representative Annexin – PI flow cytometry plots of U87MG cells corresponding to (A). D) U87-MG cells were treated with tunicamycin or DMSO control, and transfected with either a NT or *miR-124* mimic for 24 hours, followed by Annexin/PI staining and cell death analysis by flow cytometry. E) Immunoblot of cleaved PARP in cells described in (D). F) Representative Annexin – PI flow cytometry plots from (D). * p - value < 0.05.

68
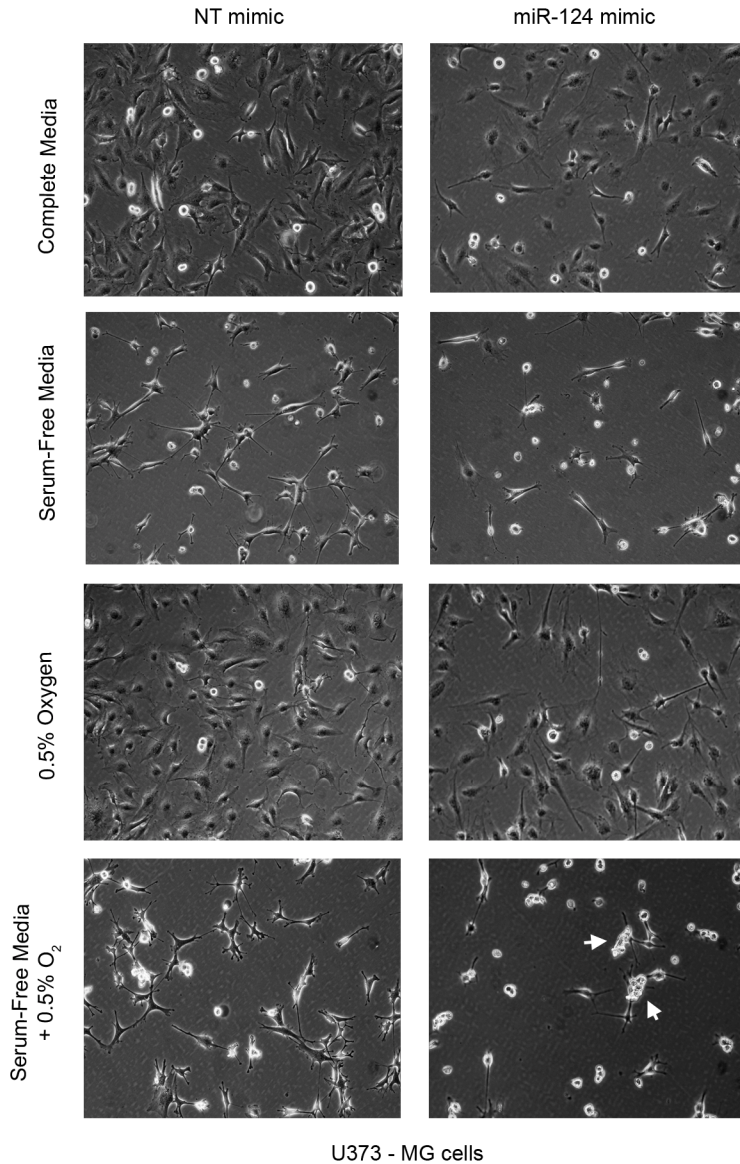
Figure 24. *miR-124* **elicits increased cell death under stress.** Descriptive images of U373-MG cells transfected with NT or *miR-124* mimics and grown in complete media, serum-free media, 0.5% O_2, or a combination of serum-free media and 0.5% O_2 and imaged for viability. In particular, *miR-124*-treated cells grown in the Serum-Free Media + 0.5% O_2 condition exhibit a crumpled, detached phenotype, with missing cellular protrusions (white arrows).

69

activated as a response to upstream stress signaling. Although p38α is thought to be tumor suppressive in some settings (Wagner and Nebreda, 2009), it may have a pro-tumorigenic role in GBM: an activated p38-MAPK pathway signature correlates with poor survival in glioblastoma (Ben-Hamo and Efroni, 2011), and increased glioblastoma invasion (Demuth et al., 2007). Interestingly, a recent study demonstrated that *miR-124* can decrease MAPK14 levels, to counteract p38α signaling in neurons (Lawson et al., 2013). TEAD1 and p38α are upregulated in several cancers, including colon, prostate, lung and pancreatic cancer (Malt et al., 2012; Paillas et al., 2012), suggesting a pro-tumorigenic role for these proteins. SERP1 (stress-associated endoplasmic reticulum protein, also known as RAMP4) is a 7 kD peptide located within the sec61 ER translocon protein complex. While very little is known about SERP1 biological functions, it has been proposed that this peptide is critical for the folding of newly synthesized proteins under stress conditions: SERP1 was originally identified as a peptide exhibiting increased expression during hypoxia and hypoglycemia (Yamaguchi et al., 1999b), and *Serp1$^{-/-}$* mice are more susceptible to ER stress (Hori et al., 2006a).

According to TargetScan™, *MAPK14* harbors a putative conserved *miR-124* binding site in its 3' Untranslated Region (UTR), while *TEAD1* and *SERP1* have two putative conserved binding sites each (Fig. 25A). We ectopically increased Non-Targeting (NT) and *miR-124* levels in U87MG and LN18 cell lines, and assessed target mRNA levels by quantitative RT-PCR (Fig. 25B) and protein levels in U87MG, U373 and LN18 cell lines by immunoblot (Fig. 25C). In all cases, *miR-124* expression led to decreased levels of each of the three mRNA and protein targets, respectively. We then transduced lentiviruses expressing either a Non-Targeting or a pre-*miR-124* vector into human glioblastoma "stem like cells" grown as tumor spheres and again showed that *miR-124* overexpression leads to decreased levels of target mRNA (Fig. 25D). To investigate whether *MAPK14*, *TEAD1* and *SERP1* are direct *miR-124* targets, we employed a 3' UTR luciferase assay comparing luciferase levels in cells transfected with plasmids expressing wild type 3' UTRs or those harboring mutations in the *miR-124* seed binding sites (see **Table 4**

70
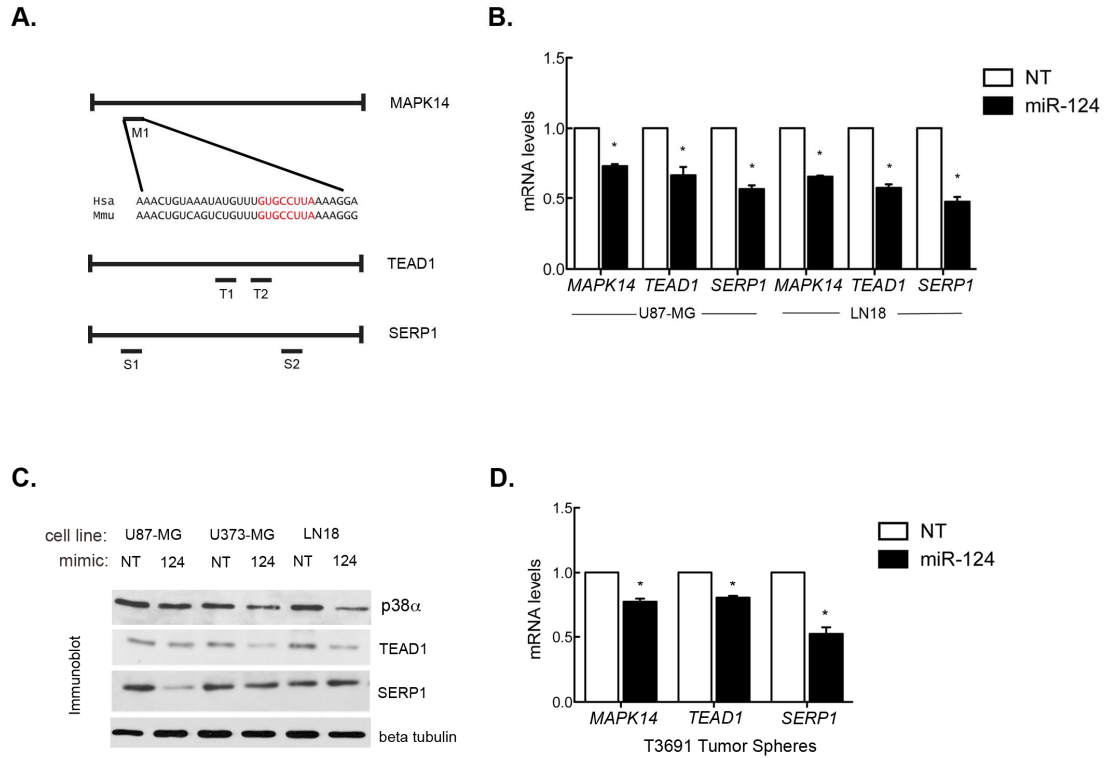
Figure 25. *TEAD1*, *MAPK14*/p38α, and *SERP1* levels decrease upon miR-124 transfection.
A) Schematic of *miR-124* seed sequence binding sites in the 3' untranslated regions of the three putative targets. B) *MAPK14*/p38, *TEAD1* and *SERP1* mRNA levels in U87-MG and LN18 cells treated either with a Non-Targeting (NT) or a *miR-124* mimic after 12 hours of transfection. C) p38, TEAD1 and SERP1 protein levels in U87-MG, U373-MG, and LN18 cells treated either with a Non-Targeting (NT) or *miR-124* mimic after 72 hours of transfection. D) mRNA levels of glioblastoma stem like cells grown as tumor spheres transduced with either an empty control or pre-*miR-124* expressing virus.

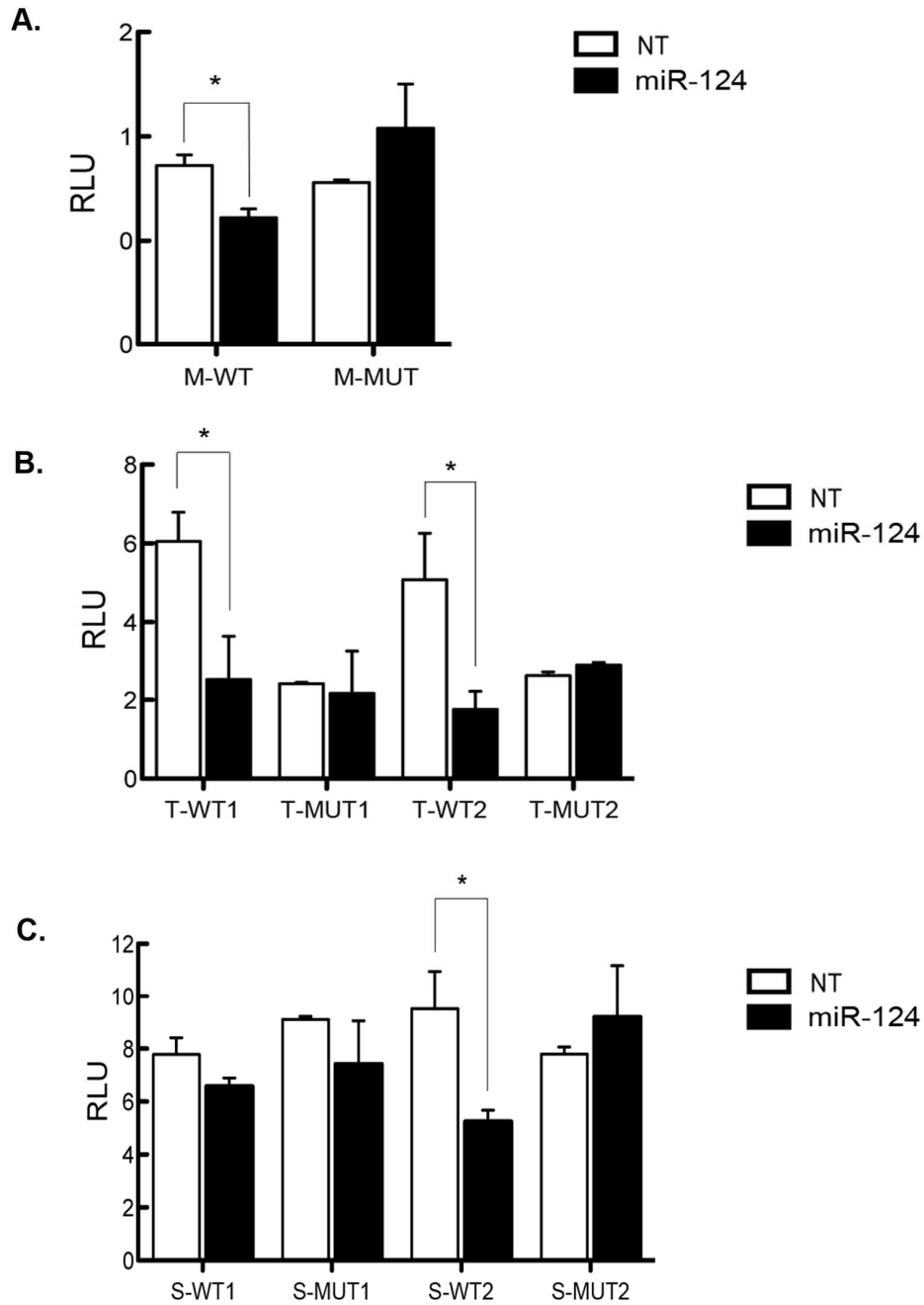**Figure 26.** *TEAD1*, *MAPK14*/p38α, **and** *SERP1* **are direct** *miR-124* **targets.** T98G cells transfected with pMIR-REPORT with intact or mutated seed sequences were tested for luciferase activity in the presence of stable *miR-124* expression. Luciferase levels for A) *MAPK14,* B) *TEAD1* and C) *SERP1* 3'UTR constructs. RLU: Relative Luciferase Units.

Name	Oligonucleotide Sequence
MAPK14 WT1 F	GGCACTAGTtatggttctcagatcttgacagtatatttgaaactgtaaatatgtttgtgccttaaaggagagagagagaaagtgtagatagAAGCTTGGC
MAPK14 WT1 R	GCCAAGCTTctatctacactttcttctctccttttaaggcacaaacatatttacagtttcaaatatactgtcaagatctgagaaccataACTAGTGCC
MAPK14 MUT1 F	GGCACTAGTtatggttctcagatcttgacagtatatttgaaactgtaaatatgttGCCAGCAGaaaggagagagaaagtgtagatagAAGCTTGGC
MAPK14 MUT1 R	GCCAAGCTTctatctacactttctttctctccttCTGCTGGCaaacatatttacagtttcaaatatactgtcaagatctgagaaccataACTAGTGCC
TEAD1 WT1 F	GGCACTAGTtgttcccgtaagcagtgccttagtaaccttagtcatgccgccagcctttttacaccAAGCTTGGC
TEAD1 WT1 R	GCCAAGCTTggtgtaagaaaaggctggcgtggcgcatgactaaggtattactaaggcactgcttacgggaacaACTAGTGCC
TEAD1 MUT1 F	GGCACTAGTtgttcccgtaagcaGCCAGCAGgtaataccttagtcatgccgccagcctttttacaccAAGCTTGGC
TEAD1 MUT1 R	GCCAAGCTTggtgtaagaaaaggctggcgtggcgcatgactaaggtattacCTGCTGGCtgcttacgggaacaACTAGTGCC
TEAD1 WT2 F	GGCACTAGTttctgcactctagcatgaaaagtgccatttgtttgagattccagcttagaaaagtgtgccAAGCTTGGC
TEAD1 WT2 R	GCCAAGCTTggcagcactttctaagctggaatctcaaaccaaaggcactttcatgctagagtgcagaaACTAGTGCC
TEAD1 MUT2 F	GGCACTAGTttctgcactctagcatgaaaGCCAGCAtgtttgagattccagcttagaaaagtgccAAGCTTGGC
TEAD1 MUT2 R	GCCAAGCTTggcagcactttctaagctggaatctcaaaccaTGCTGGCtttcatgctagagtgcagaaACTAGTGCC
SERP1 WT1 F	GGCACTAGTaggttcttcatgagtcattccaagttttctagtccataccacagtgccttgcaaaaaccaccacagtgaataaagcaataAAGCTTGGC
SERP1 WT1 R	GCCAAGCTTtattgctttattcatgtggttgtttttgcaaggcactgtgtatggactagaaaaacttggaatgactcatgaagaaaacctACTAGTGCC
SERP1 MUT1 F	GGCACTAGTaggtttcttcatgagtcattccaagttttctagtccataccacaGCCAGCAgcaaaaaacaccacatgaataaagcaataAAGCTTGGC
SERP1 MUT1 R	GCCAAGCTTtattgctttattcatgtggtgttttttgcTGCTGGCtgtggtatggactagaaaacttggaatgactcatgaagaaacctACTAGTGCC
SERP1 WT2 F	GGCACTAGTttaactaattctgtttttatggttgtctaaattcatagcaggtgccttattctttgcttttagtcaaaccattccatatcAAGCTTGGC
SERP1 WT2 R	GCCAAGCTTgatatggaatggtttgactaaaagcaaagaataaggcacctgctatgaatttagccaaccataaaacagaattagttaaACTAGTGCC
SERP1 MUT2 F	GGCACTAGTttaactaattctgtttttatggttgtgtctaaattcatagcagGCCAGCAGttctttgcttttagtcaaaccattccatatcAAGCTTGGC
SERP1 MUT2 R	GCCAAGCTTgatatggaatggtttgactaaaagcaaagaaCTGCTGGCctgctatgaattagcacaaccataaaacagaattagttaaACTAGTGCC

Table 4. Oligonucleotide primer sequences of *TEAD1*, *SERP1* and *MAPK14* partial 3'UTRs containing *miR-124* binding sites. WT: Wildtype. MUT: Mutated seed sequence binding site (in red). MAPK14 has only one *miR-124* binding site, whereas TEAD1 and SERP1 have two *miR-124* biding sites each.

73

for 3' UTR oligo sequences used). We determined that all three targets are directly regulated by *miR-124*, as luciferase levels decreased upon *miR-124* expression in cells expressing the wild type 3'UTR regions, but not in cells expressing 3'UTR regions with mutated *miR-124* seed sequences (Fig. 26A-C). (Note: only one *SERP1* seed sequence binding [S2] site appears to be a bona fide *miR-124* binding site [Fig. 26C]).

TEAD1*,* MAPK14 *and* SERP1 *promote glioblastoma progression.*

To assess whether *MAPK14*, *TEAD1*, and *SERP1* play a role in glioblastoma tumorigenesis, we obtained RNA from formalin-fixed, paraffin embedded (FFPE) glioblastoma patient samples, procured from the University of Pennsylvania Department of Pathology. A comparison of average *miR-124* levels between glioblastoma RNA versus normal brain tissue RNA showed that *miR-124* levels are greatly diminished in GBM, relative to normal brain, as previously shown (Silber et al., 2008a) (Fig. 27A). Of note, *MAPK14*, *TEAD1* and *SERP1* mRNA levels exhibited the opposite result: mRNA levels of these targets were higher in GBM samples compared to normal brain tissue (Fig. 27B-D). These data suggest an important role for all three genes in glioblastoma. In order to verify whether they promote glioblastoma cell survival, we employed short hairpin RNAs (shRNAs) to inhibit *TEAD1*, *MAPK14*, and *SERP1* individually (Fig. 28A; Fig. 28B shows resulting mRNA levels**)** and as part of a combined triple depletion (Fig. 28C; Fig. 28D depicts corresponding protein levels**)**. Decreased expression of each *miR-124* target partially enhanced cell death under nutrient or O_2 deprivation (Fig. 28A); in contrast, combined loss of *TEAD1*, *MAPK14* and *SERP1* fully recapitulated the increased apoptosis (Fig. 28C) observed in *miR-124* expressing cells (see Fig. 23).

Finally, we treated U87-MG cells with scrambled or *pre-miR-124* lentivirus and subjected them to low O_2 or serum-free/low O_2 conditions for 24 hours. Upon stress, particularly the serum-free/low O_2 conditions, a marked increase in all three targets was observed (6-8 fold) (Fig. 29A-C). *miR-124* treatment counteracted this increase, bringing target levels closer to baseline. At the

74
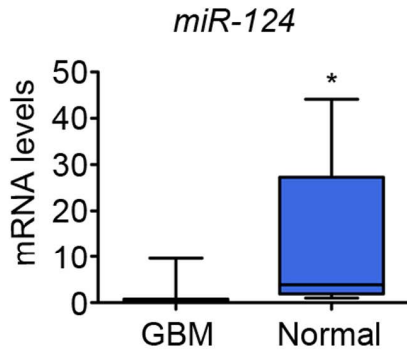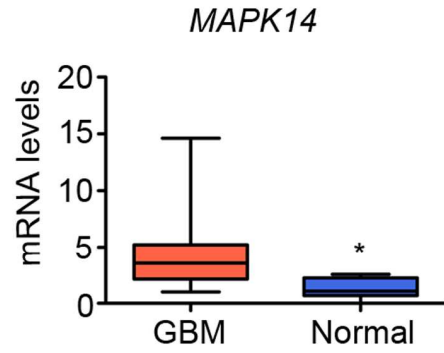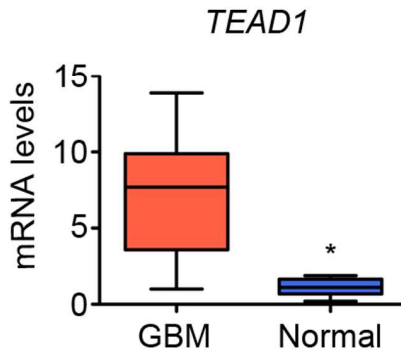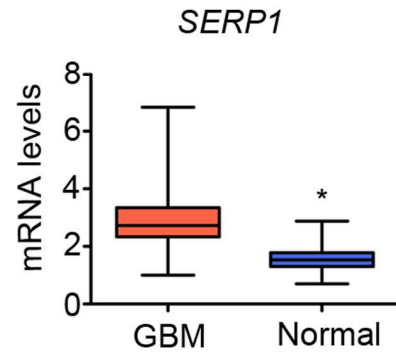
Figure 27. *miR-124* **and target levels in normal brain and glioblastoma in RRFPE patient samples.** A) *miR-124*, B) *MAPK14*, C) *TEAD1*, and D) *SERP1* levels in GBM (n=30) and normal brain samples (n=10). * p value < 0.05. GBM: Glioblastoma tissue. Normal: Normal brain tissue.
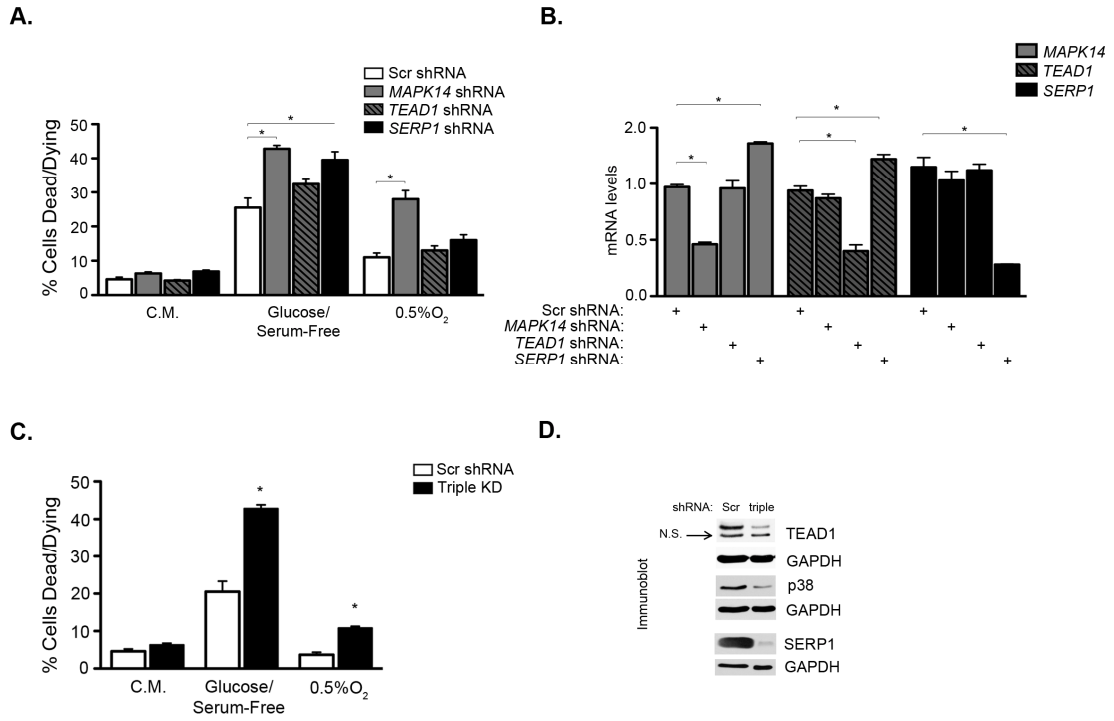
Figure 28. *TEAD1 MAPK14* and *SERP1* recapitulate miR-124 cell death phenotype. A) shRNA-mediated inhibition of individual targets partially recapitulates the cell death phenotype observed in Figure 2a. * p value < 0.05. B) Transcript levels of all three targets, upon shRNA-mediated inhibition of any single target. C) Cell death levels after shRNA-mediated depletion of all three targets combined (Triple KD). D) Immunoblot showing target protein levels upon triple ablation. Scr = Scrambled control shRNA, triple = shRNAs for all three targets. *Dion Giannoukos assisted with the completion of this figure.*
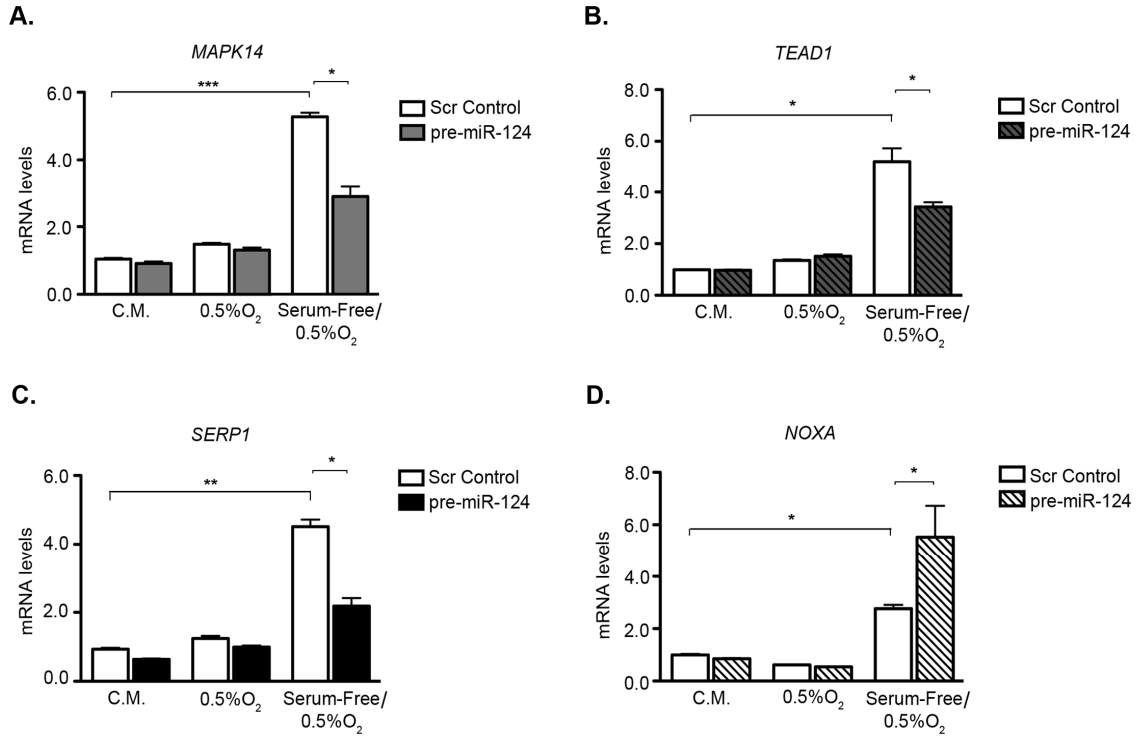
Figure 29. *miR-124* counteracts target increase under stress. mRNA levels of A) *MAPK14*, B) *TEAD1*, and C) *SERP1* under the following conditions: Complete Media (C.M.), Hypoxia (0.5% O_2), and Serum Free + Hypoxia (0.5% O_2). U87-MG cells were transduced with scrambled control (Scr) or pre-*miR-124*-expressing lentivirus and subjected to these conditions for 24 hours. D) *NOXA* levels from same experiment. * p - value < 0.05; ** p - value < 0.001, *** p - value < 0.0001.

same time, ectopic *miR-124* expression under serum-free/low O_2 conditions significantly increased *NOXA* levels, a marker of apoptotic cell death (Fig. 29D).

miR-124 *expression affects glioblastoma cell proliferation and survival* in vivo*.

In order to establish a role for *miR-124* re-expression/target gene downregulation *in vivo*, we transduced U87-MG cells with control or pre-*miR-124* – GFP, and assessed growth both *in vitro* (cell counts) and *in vivo* (subcutaneous xenografts). Additionally, we performed the same experiments comparing non-targeting shRNA vs. *TEAD1*, *SERP1*, or *MAPK14* shRNAs. As previously established (Silber et al., 2008a), *miR-124* re-expression leads to decreased cell proliferation *in vitro* (Fig. 30A) and subcutaneous tumor growth *in vivo* (Fig. 30E). *TEAD1* and *MAPK14*/p38α inhibition also resulted in decreased *in vitro* proliferation when U87-MG cells were grown under replete media (Fig. 30B,C). *SERP1* knockdown did not result in significant differences in *in vitro* proliferation under replete media, but resulted in decreased proliferation when cells were grown under 0.5% O_2. (Fig. 30D). *TEAD1* and *SERP1* inhibition led to decreased tumor growth *in vivo* (Fig. 30F,G; p38α modulation has been previously shown to lead to decreased tumor growth in glioblastoma growth *in vivo* (Cloninger et al., 2011), thus not shown here).

Since increased *miR-124* expression led to a significant difference in tumor size (Fig. 30A), it was difficult to determine whether increased cell death occurred in areas experiencing limited nutrient and O_2 availability, since smaller tumors exhibit fewer hypoxic/ischemic regions. In order to mitigate this scenario, we devised a doxycycline-inducible system where *miR-124* expression is regulated by doxycycline administration. Briefly, we created stable U87-MG cell lines expressing either a doxycycline-inducible control or *miR-124*, along with GFP, to assess the robustness of the system. As shown in the schematic in Fig. 31A, subcutaneous tumors were allowed to grow for 20 days in nude mice, so that they achieved a size sufficient for the natural generation of O_2/nutrient gradients. At day 20, doxycycline was administered, thereby activating expression of *miR-124*-GFP, or the control-GFP construct. The doxycycline-inducible system was

78
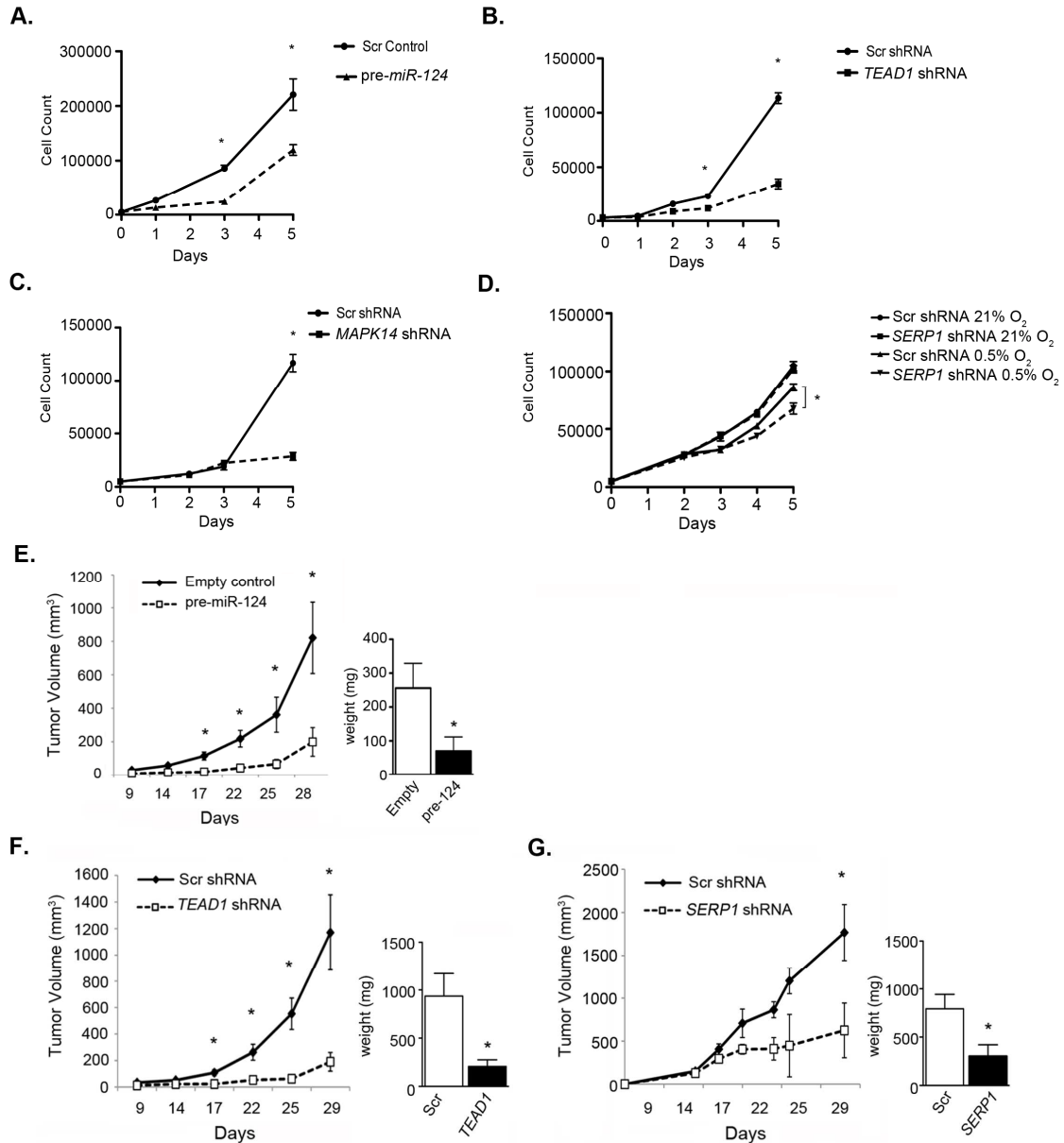
Figure 30. *miR-124* and target modulation affects proliferation *in vitro* and *in vivo*. A) Cell count of U87-MG cells expressing *miR-124* or a control scrambled miRNA. Cell count of U87-MG cells expressing control or B) *TEAD1* shRNA, C) *MAPK14* shRNA and D) *SERP1* shRNA. Growth curves and tumor weights of subcutaneous xenografts of U87-MG cells expressing *miR-124* (E, n=9), *TEAD1* shRNA **(**F, n=9**)**, and *SERP1* shRNA **(**G, n=6**)**. *Dion Giannoukos and Michael Nakazawa assisted with the completion of this figure.*

www.manaraa.com

validated *in vitro* as described in Fig. 32A,B. Surprisingly, no statistically significant difference in tumor size was observed after doxycycline treatment (Fig. 31B). Subcutaneous tumor architecture was similar in both control and *miR-124* expressing tumors, and both showed regions of hypoxia as demonstrated by HIF-1α staining (Fig. 31C). However, when we stained for GFP (the proxy for expression of either the control or the *miR-124* construct), a significant loss of GFP-expressing cells was detected in the tumor tissues expressing the *miR-124* construct (Fig. 31D,E), even though both constructs expressed GFP in a doxycycline-dependent manner *in vitro* (Fig. 32A). We then quantified cell death using the terminal deoxynucleotidyl transferase dUTP nick end-labeling (TUNEL) assay, and observed increased apoptosis in tissues expressing *miR-124*, compared to those expressing the control construct (Fig. 31F,G). While there are many possible explanations for these observations, increased TUNEL staining in *miR-124* expressing tumors, coupled with decreased numbers of GFP-expressing cells, suggest that *miR-124* expressing cells may be selected against in the seven days of doxycycline treatment, due to their inability to survive O_2 and nutrient deprivation.

SERP1 is an important pro-survival target in glioblastoma.

Since SERP1 has been shown to be elevated during brain ischemia , we focused on dissecting the role for SERP1 in survival under stress. We decreased *SERP1* levels via an shRNA-mediated lentivirus in U87-MG cells and subjected them to low O_2 or serum-free/low O_2 conditions for 24 hours. Just as we observed in Fig. 29C, *SERP1* transcripts are elevated under stress (Fig. 33A). Importantly, we demonstrate that shRNA treatment recapitulates the *miR-124* phenotype by eliciting increased *NOXA* levels (Fig. 33B). We therefore determined if re-expression of the *SERP1* Open Reading Frame (lacking the 3'UTR) reverses *miR-124*-mediated cell death. Increased *miR-124* expression led to enhanced cell death under hypoxia, while SERP1 re-expression almost completely abrogated *miR-124*-mediated cell death under hypoxia (Fig. 33C). This underscores a previously unappreciated role for SERP1 in glioblastoma. As observed with our FFPE patient samples in Fig. 27D, TCGA patient data also

80
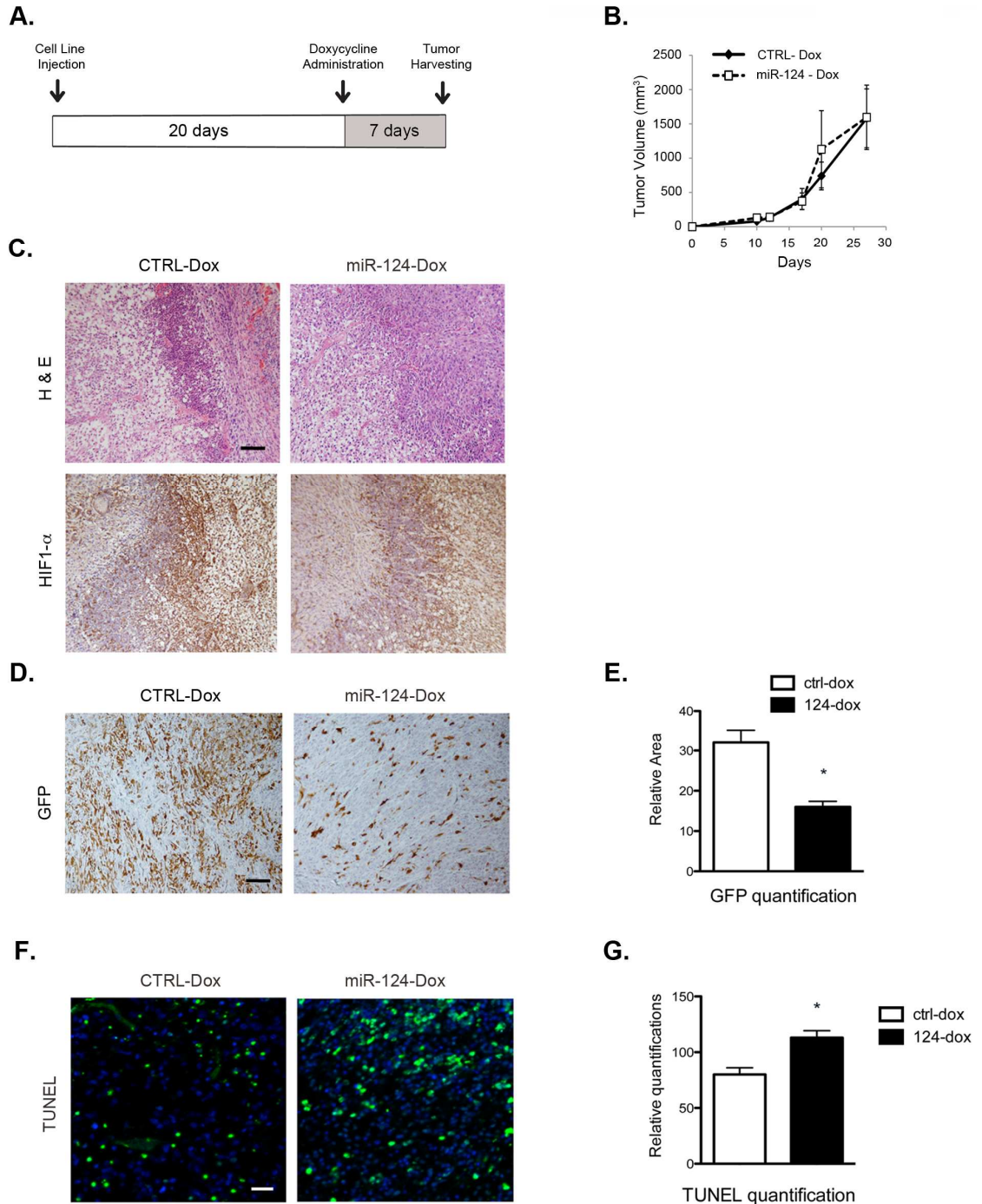
Figure 31. Doxycycline-Inducible xenograft assay. A) Schematic of assay. B) Growth curve of doxycycline inducible subcutaneous xenografts after expressing control or *miR-124* for seven days. C) H&E and HIF-1α IHC staining of doxycycline-inducible subcutaneous xenograft tumor sections. Scale bar is 200 μm. (D, E) GFP IHC staining and quantification, (F, G) TUNEL staining and quantification of doxycycline-inducible subcutaneous xenograft tumor sections. Scale bar is 100 μm. * p - value < 0.05.
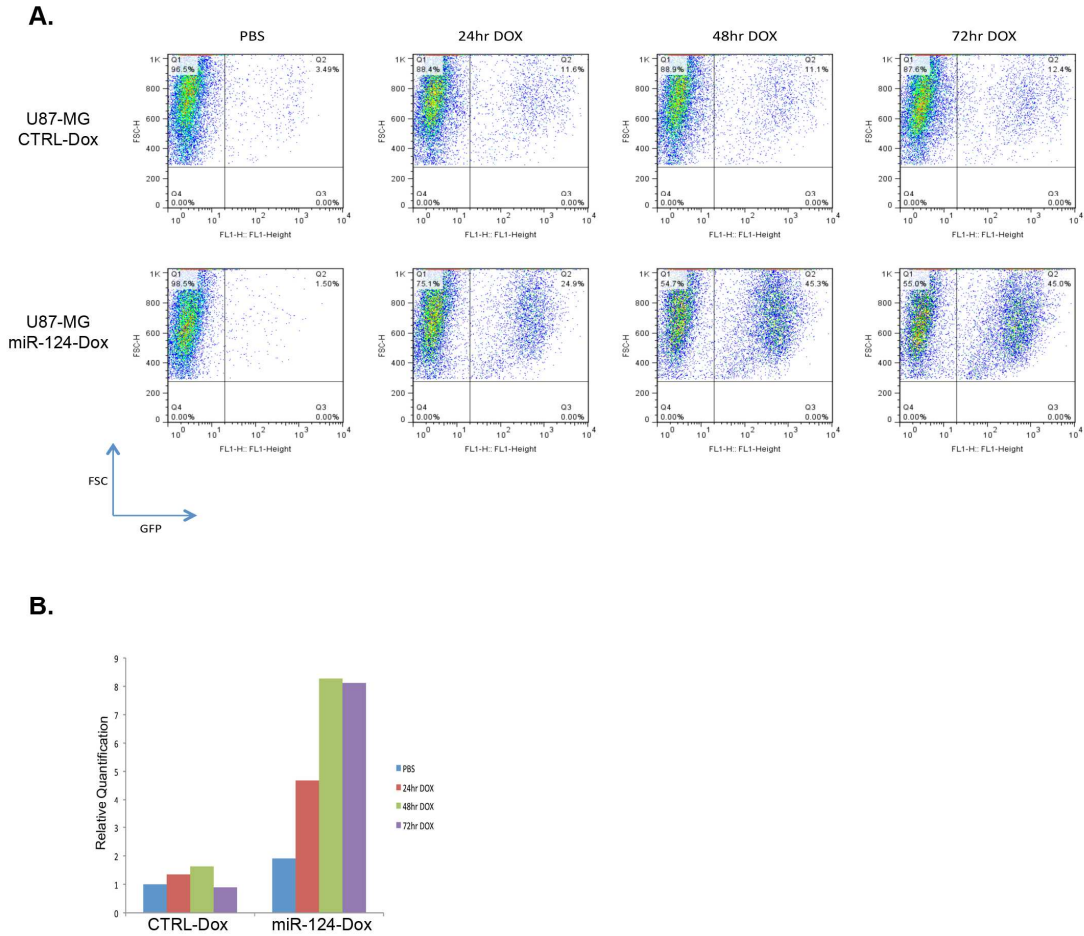
Figure 32. Determination of lentiviral and doxycycline-inducible systems *in vitro*. A) Flow cytometry analysis of Green Fluorescent Protein expression in Control-Dox expressing and 124-Dox expressing U87-MG cells. Time lapse of doxycycline administration up to 72 hours. FSC = Forward Scattering; Dox = Doxycycline. B) qRT-PCR measuring *miR-124* levels upon doxycycline induction for a 72 hour time course. *Bo Qiu assisted with the completion of this figure.*
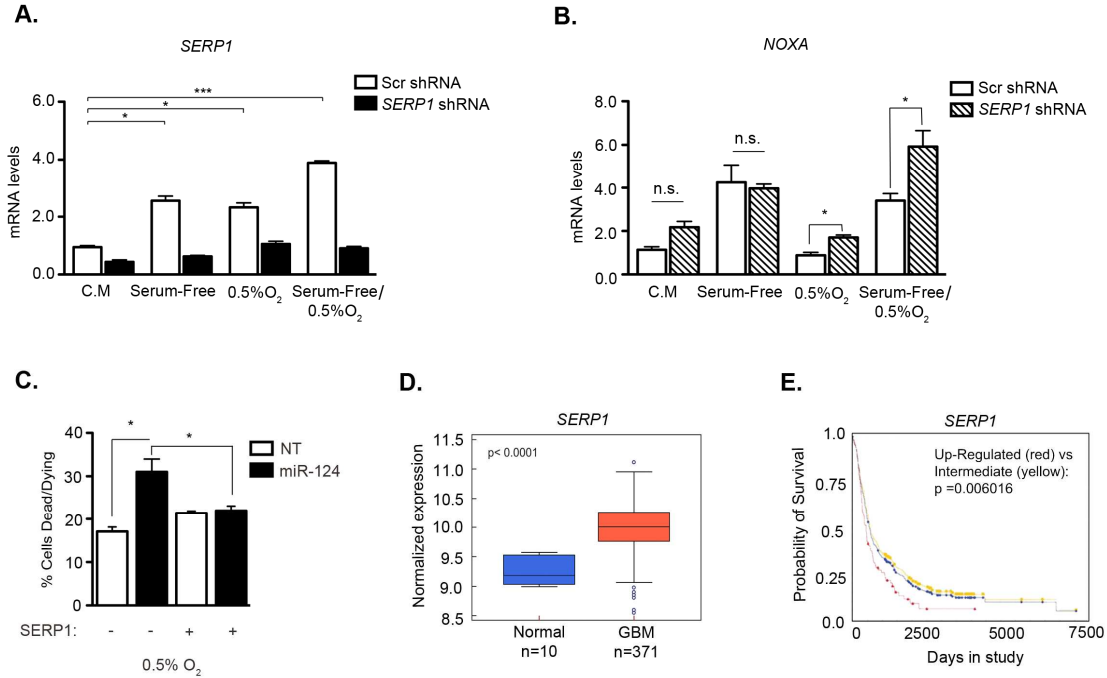
Figure 33. SERP1 is an important factor in glioblastoma. A) *SERP1* and B) *NOXA* mRNA levels in U87-MG cells grown under the following conditions: Complete Media (C.M.), Serum-Free, Hypoxia (0.5% O_2), and Serum Free + Hypoxia (0.5% O_2). Cells were transduced with scrambled (Scr) or *SERP1* shRNA and subjected to these conditions for 24 hours. * p - value < 0.05; ** p - value < 0.001, C) *SERP1* Open Reading Frame re-expression leads to rescue of cell death in U87-MG expressing *miR-124* under hypoxia. D) SERP1 levels in normal brain and GBM tissues from the TCGA dataset (p - value < 0.0001). E) Kaplan – Meier survival curve of patients from the REMBRANDT database, stratified by SERP1 expression levels (p - value = 0.006).

suggest that *SERP1* mRNA levels are elevated in glioblastoma samples, as compared to normal brain tissue (p - value < 0.0001) (Fig. 33D). Additionally, a query into the REMBRANDT database (https://caintegrator.nci.nih.gov/rembrandt/) showed that patients with increased *SERP1* mRNA exhibit lower overall survival, compared to patients with low or intermediate levels (p - value = 0.006) (Fig. 33E). Taken together, these data suggest that SERP1 may be an attractive target for further evaluation in glioblastoma survival.

miR-124 *expression increases overall survival in an orthotopic intracranial mouse model.*

While several studies have investigated the role for *miR-124* in glioblastoma (Li et al., 2011; Silber et al., 2008a), the impact of *miR-124* expression on glioblastoma cell survival *in vivo* is unclear. To test whether *miR-124* expression led to a change in tumor cell survival, we performed an intracranial orthotopic experiment in Nu/Nu mice expressing either control or pre-*miR-124* construct, as well as GFP. *miR-124* levels were increased only ~50 fold (data not shown), similar to the difference in *miR-124* levels between GBM and adjacent non-neoplastic tissue measured in patients (Godlewski et al., 2008; Silber et al., 2008a). GFP levels were similar between control and *miR-124* constructs **(**Fig. 34C**)**. Mice were sacrificed upon showing neurological symptoms associated with tumor burden. We observed that *miR-124* re-expression conferred mice with a higher survival rate (p - value < 0.0001) (Fig. 34A, 34B shows brain sections upon sacrifice), suggesting the importance of silencing *miR-124* during GBM tumor progression.

DISCUSSION

Glioblastomas are difficult to treat, primarily due to their resistance to standard of care therapy and eventual tumor recurrence. Both resistance to therapy and recurrence are closely associated with the frequent occurrence of hypoxic/ischemic regions in grade IV gliomas. The ability of glioblastoma cells to survive under nutrient and O_2 deprivation ensures the opportunity for glioblastoma recurrence. Many factors are over - and underexpressed to promote cellular

84

A.

B.

C.
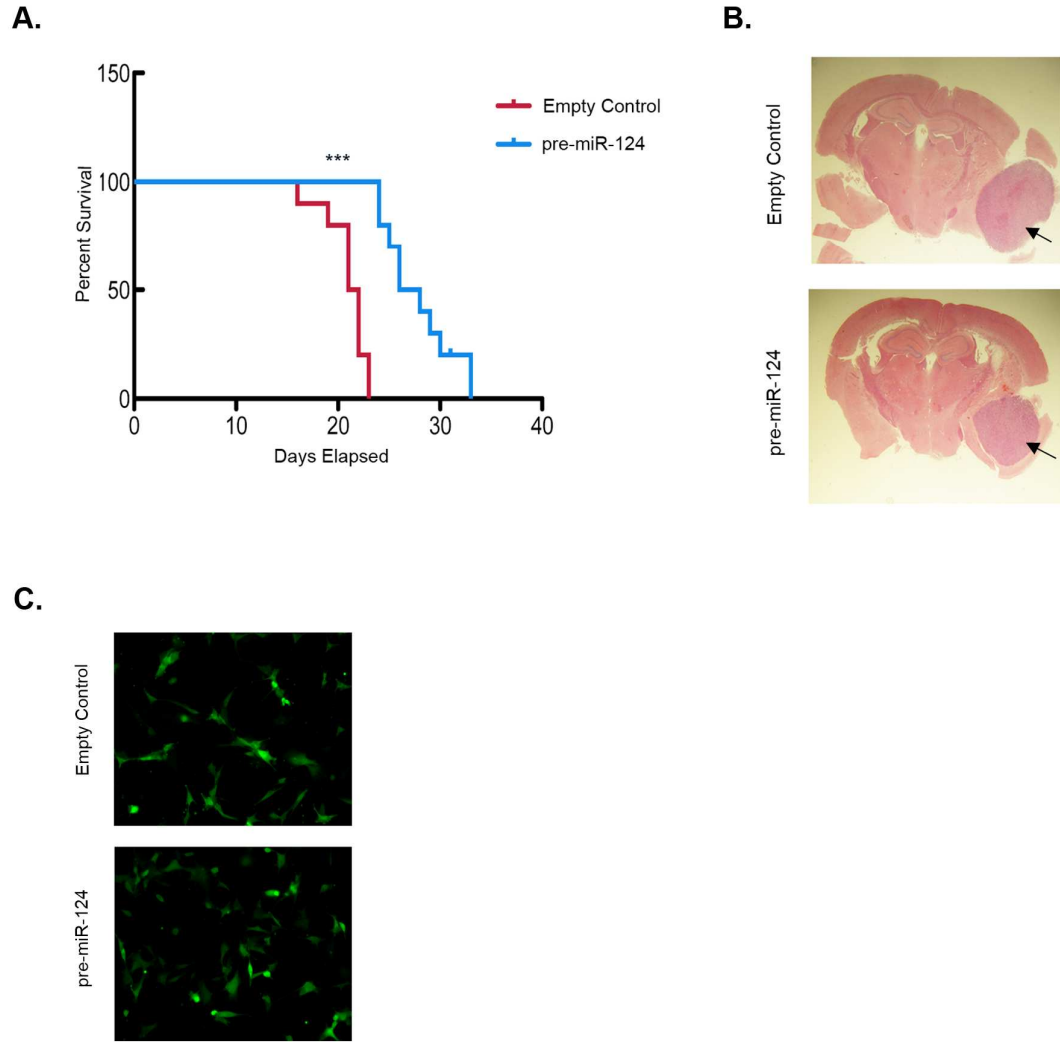
Figure 34. *miR-124* expression increases overall survival in an orthotopic intracranial mouse model. A) U87-MG cells transduced with either an empty control or pre-*miR-124* expressing virus were injected into nude mice, subsequently surveyed for survival. Kaplan-Meier curve, *** p - value < 0.0001. B) Representative H&E images of xenografts in the brain showing tumor lesions (arrows) at the time of sacrifice. C) GFP levels in control/pre-miR-124 transduced U87-MG cells, 48 hours after transduction.
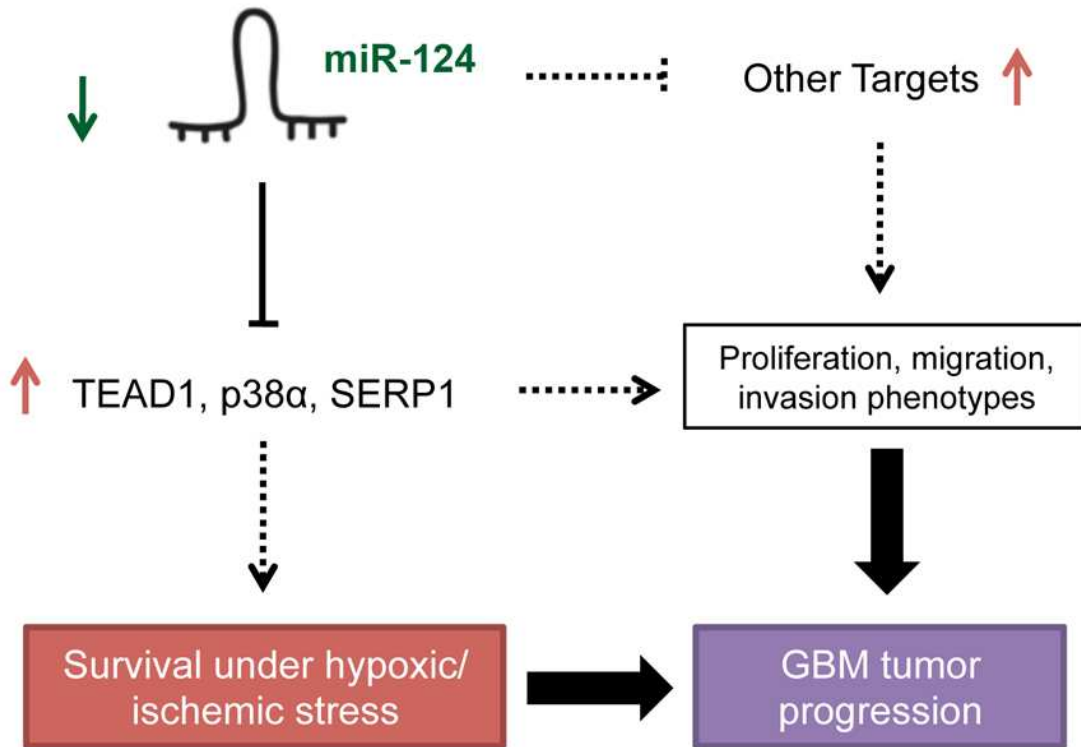
Figure 35. Model for *miR-124* role in glioblastoma. *miR-124* loss contributes to glioblastoma tumorigenesis by promoting the elevated expression of cell proliferation factors, as well as pro-survival factors, especially in regions experiencing nutrient and oxygen deprivation.

survival, and a majority have yet to be elucidated. Several micro-RNAs have been demonstrated to promote survival under stress. Here, we show that *miR-124* loss in glioblastoma allows for survival during nutrient and O_2 deprivation, as *miR-124* re-expression in glioblastoma cells increased cell death under these conditions.

miRNAs function by targeting and modestly inhibiting a vast array of mRNAs and proteins. Given that miRNAs can inhibit up to 30% of the mammalian genome (Esquela-Kerscher and Slack, 2006a), differentially expressed miRNAs are a powerful discovery tool in cellular processes impacting development, physiology and disease. While a single miRNA inhibits any given mRNA or protein only ~10-20%, global pathway changes can be significant. Additionally, modulating miRNA levels often reveals new targets or pathways that have been under-investigated or not well understood. Previous studies have identified an anti-proliferative role for *miR-124* in glioblastoma (Silber et al., 2008a), but no consistent evidence has linked *miR-124* to cell death under limiting O_2 and nutrient conditions in the context of glioblastoma. A recently published study showed that *miR-124* levels are downregulated in pulmonary artery smooth muscle cells (PASMC) subjected to hypoxia, implying that *miR-124* expression could be utilized in the future to target effectors of pulmonary arterial hypertension (Kang et al., 2013). In this paper, we show that *miR-124* levels (while decreased in glioblastoma compared to normal brain tissue) are further diminished in pseudopalisading necrotic/hypoxic regions as compared to better-perfused tissue. Based on TCGA data, the more patient samples express a hypoxic signature, the lower *miR-124* levels become. While the observation that *miR-124* levels anti-correlate with hypoxic regions and hypoxic signatures in patients (Fig. 20) does not necessarily imply that *miR-124* has been selectively inhibited to confer survival, endogenous *miR-124* expression has a significant effect in inhibiting cell survival in hypoxic/ischemic glioblastoma tissue. We demonstrate for the first time how *miR-124* controls cell death through inhibition of various pro-survival targets elevated under low nutrients, growth factors and O_2, making *miR-124* an attractive target for further investigation in glioblastoma. Our current model suggests that, due to lack of *miR-124* expression, tumor cells acquire the ability to uncontrollably proliferate, as these

87

cells express high levels of pro-proliferation factors including CDK-6 (Silber et al., 2008a), and TEAD1 **(**Fig. 25**)**. During growth and expansion, glioblastoma tissues invariably experience gradients of nutrient and O_2 availability, and in many cases, regions where nutrients and O_2 are significantly depleted. Our study suggests that lack of *miR-124* allows cells in these regions to upregulate pro-survival factors (such as SERP1, a novel *miR-124* target). Taken together, lack of *miR-124* expression allows glioblastoma cells to proliferate, but also survive under stress conditions (Fig. 35, model). While at the present time miRNA-based therapeutics await further development, investigating miRNA targets should lead to insights into the biological processes of glioblastoma, as well as potential new therapeutic modalities.

One interesting novel *miR-124* target described here is SERP1. No previous connection has been made between SERP1 and glioblastoma progression, and very little is known about the biological roles for SERP1 in the endoplasmic reticulum. So far, SERP1 appears to have a role in modulating responses to ER stress (Hori et al., 2006a) and protecting proteins from degradation while promoting consequent glycosylation (Yamaguchi et al., 1999a). Additionally, it was shown that SERP1 levels are elevated in astrocytes during rat brain ischemia (Yamaguchi et al., 1999a). Since *miR-124* re-expression led to increased cell death under tumor ischemic and ER stress conditions, we hypothesized that *miR-124* counteracts pro-survival stress responses in glioblastoma, in part by targeting SERP1. Here, we identify SERP1 as an important factor in glioblastoma patient survival. Additionally, we show that SERP1 overexpression rescues the cell death phenotype conferred by *miR-124*, suggesting that SERP1 may provide a pro-survival (hence, pro-tumorigenic) role *in vivo*.

Liu et al. have recently shown that *miR-124* levels decrease in the sub-ventricular zone when mice are subjected to cerebral ischemia, in a model of stroke (Liu et al., 2011). The authors suggest that decreased *miR-124* allows for increased proliferation in the ischemic region during stroke-induced neurogenesis. We demonstrate that, in addition to allowing for cellular proliferation, the decrease in *miR-124* may also be permissive for cellular survival during stroke,

88

potentially by allowing for SERP1 upregulation under low nutrients and O_2, as described by Yamaguchi and colleagues (Yamaguchi et al., 1999b). Thus, more research regarding the connection between *miR-124*, SERP1, and hypoxia/ischemia is warranted, in the settings of stroke and glioblastoma tumorigenesis.

In summary, we have shown glioblastoma cells undergo apoptosis under hypoxic/ischemic conditions, upon *miR-124* reintroduction. This increase in cell death may be partially mediated by direct *miR-124* inhibition of TEAD1, *MAPK14*/p38α and SERP1, in addition to numerous other factors. Further research on *miR-124* targets involved in survival under nutrient and O_2 deprivation may lead to novel glioblastoma therapeutics.

89

CHAPTER 4

Concluding Remarks

The previous two chapters described experiments that asked how cancer cells control proliferation and survival under stress, particularly in tumors expressing a mesenchymal phenotype. First, what pathways are aberrantly regulated for tumor progression in mesenchymal tumors? Secondly, how do tumors experiencing limited nutrient and O_2 levels upregulate pro-survival factors? The models used to answer these questions were soft tissue sarcoma (Chapter 2) and glioblastoma (Chapter 3). In chapter 2, I demonstrated that the Hippo pathway is aberrantly inhibited in multiple aggressive STS subtyptes, leading to elevated YAP and FOXM1 activity. These factors, in turn, activate a potent pro-proliferation set of targets. Additionally, I demonstrated that YAP and FOXM1 may co-operate in the nucleus, and that pharmacologic inhibition of either YAP or FOXM1 can lead to decreased tumorigenesis. In chapter 3, I showed that *miR-124* expression in glioblastoma cells experiencing hypoxia/ischemia results in increased cell death. I identified three key miR-124 targets which are upregulated under limited nutrients and O_2. I verified that *miR-124*-mediated negative regulation of these targets (particularly of SERP1) is responsible for the cell death associated with *miR-124* expression. Taken together, these studies add to our understanding of mesenchymal tumor progression. Here, I will attempt to address some of the implications that arise from these bodies of work. In addition, I will suggest several future directions to build on these stories.

HIPPO PATHWAY IN SARCOMA

The data presented in chapter II of this dissertation comprise one of the first attempts to define a role for Hippo pathway loss in high-grade sarcomas. Our work suggests that genetic aberrations in key upstream members of the Hippo pathway cause YAP overexpression and hyperproliferation. Moreover, we identify for the first time a functional interaction between

90

YAP/TEAD and another potent transcription factor, FOXM1. Mizuno and colleagues had previously identified FOXM1 as a direct YAP/TEAD target (Mizuno et al., 2012). Taken together, these findings suggest that YAP/TEAD/FOXM1 may cooperate as a complex that is also a positive feed-forward loop for FOXM1 regulation. However, these findings are preliminary and further work needs to biochemically address how FOXM1 interacts with the YAP/TEAD complex. We have shown that TEAD immunoprecipitates with FOXM1 but YAP does not. This was surprising, as YAP has been shown to directly interact with FOXO1, another forkhead transcription factor (Shao et al., 2014). It will be interesting to see how exactly TEAD and FOXM1 bind, and whether this complex enhances TEAD/YAP association or weakens it. In addition, we took advantage of ENCODE data to delineate a few targets that may be co-transcribed from TEAD and FOXM1. However the data presented there is acquired from ChIP-seq analyses in different cell lines, under different conditions. In the future, it will be important to identify all the common and disparate FOXM1 and TEAD targets, in the context of sarcoma, but also in normal cells. It is possible, for example, that TEAD and FOXM1 cooperate towards the transcription of factors involved in cell cycle progression, but target completely different factors implicated in migration, invasion, or cell survival. Comparing a FOXM1 ChIP-seq analysis to a TEAD1 ChIP-seq analysis from the same cells would allow us to elucidate that question. Moreover, it will be important to learn how TEAD1 and FOXM1 behave in the context of normal cells. Do they interact during normal development (e.g. in embryonic stem cells) or is this interaction specific to sarcoma? If the former is true, then FOXM1 can be considered a downstream effector of the Hippo pathway, and it will be important to evaluate how, if at all, FOXM1 is controlled by upstream Hippo pathway members. If the latter is the case, and the YAP/TEAD/FOXM1 complex is a property of tumors but not normal cells, then that finding would provide a powerful tool for novel targeted therapies. Regardless, the observation that YAP/TEAD/FOXM1 may interact in a complex needs to be followed up with more extensive experiments and should be a goal of future work.

91

Using an autochthonous model of sarcoma, we have shown that FOXM1 is a key target for sarcoma tumor progression, as FOXM1 deletion ablated tumor formation. Currently, we are addressing whether Yap ablation induces the same phenotype, by generating $Kras^{G12D/+}$; $Trp53^{fl/fl}$; $Yap^{fl/fl}$ animals. Based on the remaining *in vitro* and *in vivo* data presented in chapter II, I hypothesize that Yap deletion will result in ablated tumor formation as well. In addition, the availability of genetic models to dissect the Hippo pathway allows the field to further probe whether Yap is necessary for sarcoma formation. Similar to experiments performed by Tremblay and colleagues, wildtype Yap, or YAP S112A (mouse equivalent of S127) overexpressing mice crossed to *LSL Kras*$^{G12D/+}$ or *Trp53*$^{fl/fl}$, or *LSL Kras*$^{G12D/+}$; *Trp53*$^{fl/fl}$ can be queried to address those questions. Alternatively, *Nf2*, or *Mst1/Mst2*, or *Sav1* deletion would address the same question, while at the same time mimic genetic changes in the Hippo pathway that are observed in sarcoma patients (Fig. 20).

As mentioned in chapter II, our TCGA query of sarcoma patients yielded copy number variations for NF2, LATS2, and SAV1. We limited our analysis to the core kinase cassette players and a few upstream factors. However as discussed in chapter I, we consider many factors to be upstream of the core Hippo pathway (Fig. 1, Table 1). It would be interesting to evaluate every upstream member of the Hippo pathway for copy number variation and gene expression changes. In particular, Fat4 and Dchs1 PCP members (mammalian counterparts of Ft and Ds) are highly expressed in a variety of mesenchymal cells (Mao et al., 2011). It is possible that key members of apico-basal and planar cell polarity complexes are aberrantly regulated in sarcoma. However, one caveat of TCGA data is that, as of the time this document was written, sample banking and pathologic descriptions are still a work in progress. It was difficult for us to assess mRNA expression data from the currently accessible samples, as, while there were more than a hundred sarcoma samples for comparison, only two normal tissue samples were made available. In addition, almost half of the sarcoma samples present in the database were not defined by subgroup. Thus, it was not possible to compare mRNA expression data or CNV data between different sarcoma subtypes. These technical difficulties however are likely to dissipate in the near

future. It will be very interesting to query both CNV changes and mRNA expression levels for all key players of the Hippo pathway, and ask whether certain subtypes track with pathway perturbations. This could become crucial information, should clinical treatments against YAP become available in the near future.

Another direction of future research will be to investigate other YAP/TEAD targets and their roles in sarcomagenesis. Calvo and colleagues demonstrated that YAP can act downstream of mechanotransduction signals to regulate the expression of ANLN and DIAPH3, two regulators of cytoskeleton function (Calvo et al., 2013). In this paper, the authors argue that activated YAP in Cancer-Associated Fibroblasts (CAFs) is necessary for CAF maintenance. Being mesenchymal in nature, sarcomas don't necessarily have to rely on CAFs for tumor progression. In fact, we have previously shown that in our mouse models, more than 90% of the fibroblast-like cells originate from the primary tumor, and not the microenvironment, and suggested that sarcoma cells modify their microenvironment to promote metastatic progression in a cell autonomous manner. Although it will be challenging to dissect proliferation-related phenotypes form events promoting metastasis, it would be interesting to investigate the role of YAP (or of a downstream factor that does not display a proliferation phenotype when ablated) in sarcoma metastasis formation.

Finally, as sarcomas are characterized by high levels of intratumoral hypoxia/ischemia, it will be interesting to evaluate how YAP expression and localization is affected by limited nutrients and O_2. Some of my preliminary data in fibroblasts has shown that YAP phosphorylation increases when cells are grown in limited O_2 levels, and that eventually YAP levels diminish as cells are exposed to low O_2 for periods longer than 24 hours. One hypothesis is that cells may restrict YAP function when experiencing a lack of nutrients and O_2, similarly to the ways glioblastoma cells potentially engage in pro-survival stress response by elevating pro-survival *SERP1* and diminishing *miR-124* levels. Restricting YAP function could be beneficial in a pathologic setting such as tissue injury, before revascularization has allowed for replete

93

nutrient/O_2 conditions, as proliferation under nutrient deprivation or hypoxia could lead to further cell death and tissue damage. In fact, some further evidence to support this hypothesis comes from a mouse testis model, where HIF2α deletion results in downregulation of tight junction proteins such as ZO1 and ZO2 . Since YAP may interact with ZO1 and ZO2 via its PDZ motif, it is possible that YAP could be sequestered away from the nucleus under hypoxia in a HIF-dependent manner. However, YAP restriction at tight and adherens junctions as a method of inactivation is controversial, as further evidence has shown that YAP can freely shuttle from the adherens junction to the nucleus, at least in the context of YAP/Angiomotin interaction (Yi et al., 2013). Thus, more work needs to be done to assess whether this is a viable hypothesis.

Interestingly, hypoxia has been shown to affect cell shape, as hypoxic cells secrete and modify extracellular matrix components, possibly in order to create a "highway" for metastatic dissemination. In sarcoma, our lab has shown that HIF-1α - mediated PLOD2 expression results in collagen modifications that create a stiffer ECM (Eisinger-Mathason et al., 2013). Similar results have been described in other tumor models (Erler et al., 2006; Gilkes et al., 2013; Wong et al., 2011; Wong et al., 2012). Taken together with the evidence that mechanotransduction signaling resulting from changes in stiffness can affect YAP function (Dupont et al., 2011), it is possible that the Hippo and the Hypoxia inducible Factors cross-talk through cell stiffness changes. In fact, our preliminary observations from IHC experiments have shown that YAP expression is more nuclear and more intense at the migratory edge of tumors, as compared to more intratumoral regions. As upstream factors affecting the Hippo pathway remain incompletely understood, it would be interesting to query whether a crosstalk between the Hippo pathway and O_2 sensing does in fact occur.

MIR-124 AND GLIOBLASTOMA

In chapter III, I identify three novel *miR-124* targets (*MAPK14*, *TEAD1* and *SERP1*) and suggest that negative regulation of these targets by *miR-124* causes cell death, specifically when glioblastoma cells are experiencing low nutrients and O_2, the experimental equivalent to

intratumoral hypoxia and ischemia. Our work suggests that inhibiting these targets could be a way to target glioblastoma cells that survive in hypoxic/ischemic regions of the tumor, cells that have been difficult to target by our current treatment modalities. However, it would be more beneficial to identify a pathway, or a series of common factors that get differentially expressed under hypoxic/ischemic conditions. *miR-124* could still serve as an interesting tool for identifying such factors, as we already know that *miR-124* expression will induce cell death under stress, thereby affecting many factors important for survival. An RNA-seq analysis of the global targets differentially modulated by *miR-124* ectopic expression in cells experiencing hypoxia, nutrient deprivation, or both, would be important towards the identification of pathways and key factors implicated in survival under stress conditions. Cells grown under hypoxia, nutrient deprivation, or a combination of both might lead to different top hits upon miR-124 modulation. Regardless, that information could be useful in identifying what factors are important for survival under nutrient deprivation vs. O_2 deprivation. Equally important, factors that are upregulated under all the aforementioned conditions could be considered lynchpins in glioblastoma survival under ischemia. SERP1 might be such a factor, as we and others have now shown that it can be upregulated both under low O_2, limiting nutrients/growth factors, and under ER stress (Hori et al., 2006b; Mucaj et al., 2014; Yamaguchi et al., 1999b). Therefore, further studies on the mechanism by which SERP1 affects cell survival under stress are warranted.

As mentioned in chapter III, two different studies show evidence for SERP1 upregulation and *miR-124* deregulation in mouse and rat models of ischemia (Liu et al., 2011; Yamaguchi et al., 1999b). It is tempting to speculate that *miR-124* is downregulated in stroke regions so that pro-survival factors like SERP1 can become elevated. However, this needs to be experimentally tested. If that hypothesis is validated, then it would be intriguing to test whether one of the explanations for why there is increased neuronal cell death in stroke patients is that high *miR-124* levels in differentiated neurons is inhibiting the upregulation of factors like SERP1, TEAD1, p38α and other proteins necessary for adaptation under stress. However, ischemic induced neuronal

95

cell death is a multifaceted process that requires more sophisticated explanations outside of *miR-124* expression in neurons.

One caveat of the glioblastoma work described in chapter III is that *in vivo* experiments were performed in xenograft models, which, even when injected orthotopically, do not recapitulate the full microenvironment experienced by glioblastoma tumors. For example, while our models showed evidence for intratumoral hypoxia, they do not exhibit the same migratory and invasive phenotypes seen in patient glioblastoma tissues. In addition, they do not allow for the proper recruitment of the immune system. A 2011 paper described a role for *miR-124* in inducing microglia quiescence in the brain (Ponomarev et al., 2011). As microglia comprise a large portion of glioblastoma mass (Charles et al., 2012), it is important to understand how *miR-124* expression affects their function within the glioma tumor microenviroment. Additionally, by directly targeting STAT3, *miR-124* can counteract T-cell mediated immunosuppression in a glioblastoma model. This would suggest that a potential *miR-124* treatment could affect glioblastoma mass threefold. First, it could decrease tumor size by targeting factors such as CDK6 and TEAD1 and inhibiting proliferation. Secondly, it could target cells residing in hypoxic/ischemic regions by inhibiting SERP1 and MAPK14 expression. And lastly it could enhance T-cell mediated immune clearance (Wei et al., 2013). Performing this experiment however would require an efficient way of targeting miRNAs to the brain, which is currently a technical challenge. A genetic model crossing a glioblastoma tumor model (such as GFAP-Cre, *NF1*$^{fl/fl}$; *Trp53*$^{fl/fl}$ mouse) to a mouse with conditional deletions of *miR-124* would also be technically challenging, as there are three intergenic *miR-124* loci in mammalian genomes (Visvader, 2011) (Clark et al., 2010). In fact, as of right now, the only *miR-124* knockdown has been accomplished in *C. elegans,* as they possess only one copy of *miR-124*. In the future, it might be more feasible to deliver *miR-124* mimics to analyze the role of ectopic expression of this miRNA in inhibiting glioblastoma progression.

96

BIBLIOGRAPHY

(2008). Comprehensive genomic characterization defines human glioblastoma genes and core pathways. Nature Epub 0906 *455*, 1061-1068.

Amberger-Murphy, V. (2009). Hypoxia helps glioma to fight therapy. Current cancer drug targets *9*, 381-390.

Ambros, V. (2004). The functions of animal microRNAs. Nature *431*, 350-355.

Avruch, J., Zhou, D., and Bardeesy, N. (2012). YAP oncogene overexpression supercharges colon cancer proliferation. Cell Cycle *11*, 1090-1096.

Badouel, C., Gardano, L., Amin, N., Garg, A., Rosenfeld, R., Le Bihan, T., and McNeill, H. (2009). The FERM-domain protein Expanded regulates Hippo pathway activity via direct interactions with the transcriptional activator Yorkie. Dev Cell *16*, 411-420.

Bao, Y., Nakagawa, K., Yang, Z., Ikeda, M., Withanage, K., Ishigami-Yuasa, M., Okuno, Y., Hata, S., Nishina, H., and Hata, Y. (2011). A cell-based assay to screen stimulators of the Hippo pathway reveals the inhibitory effect of dobutamine on the YAP-dependent gene transcription. Journal of biochemistry *150*, 199-208.

Bartel, D.P. (2009). MicroRNAs: target recognition and regulatory functions. Cell *136*, 215-233.

Baumgartner, R., Poernbacher, I., Buser, N., Hafen, E., and Stocker, H. (2010). The WW domain protein Kibra acts upstream of Hippo in Drosophila. Developmental cell *18*, 309-316.

Ben-Hamo, R., and Efroni, S. (2011). Gene expression and network-based analysis reveals a novel role for hsa-miR-9 and drug control over the p38 network in glioblastoma multiforme progression. Genome medicine *3*, 77.

Bennett, F.C., and Harvey, K.F. (2006). Fat cadherin modulates organ size in Drosophila via the Salvador/Warts/Hippo signaling pathway. Current biology : CB *16*, 2101-2110.

Bertout, J.A., Patel, S.A., and Simon, M.C. (2008). The impact of O2 availability on human cancer. Nat Rev Cancer *8*, 967-975.

Bhat, U.G., Halasi, M., and Gartel, A.L. (2009). FoxM1 is a general target for proteasome inhibitors. PLoS One *4*, e6593.

Bossuyt, W., Chen, C.L., Chen, Q., Sudol, M., McNeill, H., Pan, D., Kopp, A., and Halder, G. (2014). An evolutionary shift in the regulation of the Hippo pathway between mice and flies. Oncogene *33*, 1218-1228.

Callus, B.A., Verhagen, A.M., and Vaux, D.L. (2006). Association of mammalian sterile twenty kinases, Mst1 and Mst2, with hSalvador via C-terminal coiled-coil domains, leads to its stabilization and phosphorylation. FEBS J *273*, 4264-4276.

Calvo, F., Ege, N., Grande-Garcia, A., Hooper, S., Jenkins, R.P., Chaudhry, S.I., Harrington, K., Williamson, P., Moeendarbary, E., Charras, G.*, et al.* (2013). Mechanotransduction and YAP-dependent matrix remodelling is required for the generation and maintenance of cancer-associated fibroblasts. Nat Cell Biol *15*, 637-646.

Camargo, F.D., Gokhale, S., Johnnidis, J.B., Fu, D., Bell, G.W., Jaenisch, R., and Brummelkamp, T.R. (2007). YAP1 increases organ size and expands undifferentiated progenitor cells. Current biology : CB *17*, 2054-2060.

Cao, X., Pfaff, S.L., and Gage, F.H. (2008). YAP regulates neural progenitor cell number via the TEA domain transcription factor. Genes Dev *22*, 3320-3334.

Carmeliet, P., and Jain, R.K. (2011). Principles and mechanisms of vessel normalization for cancer and other angiogenic diseases. Nature reviews Drug discovery *10*, 417-427.

Chan, E.H., Nousiainen, M., Chalamalasetty, R.B., Schafer, A., Nigg, E.A., and Sillje, H.H. (2005). The Ste20-like kinase Mst2 activates the human large tumor suppressor kinase Lats1. Oncogene *24*, 2076-2086.

Chan, Y.C., Banerjee, J., Choi, S.Y., and Sen, C.K. (2012). miR-210: the master hypoxamir. Microcirculation *19*, 215-223.

Charles, N.A., Holland, E.C., Gilbertson, R., Glass, R., and Kettenmann, H. (2012). The brain tumor microenvironment. Glia *60*, 502-514.

Cheong, H., Lu, C., Lindsten, T., and Thompson, C.B. (2012). Therapeutic targets in cancer cell metabolism and autophagy. Nature biotechnology *30*, 671-678.

Chitnis, N.S., Pytel, D., Bobrovnikova-Marjon, E., Pant, D., Zheng, H., Maas, N.L., Frederick, B., Kushner, J.A., Chodosh, L.A., Koumenis, C.*, et al.* (2012). miR-211 is a prosurvival microRNA that regulates chop expression in a PERK-dependent manner. Mol Cell *48*, 353-364.

Clark, A.M., Goldstein, L.D., Tevlin, M., Tavare, S., Shaham, S., and Miska, E.A. (2010). The microRNA miR-124 controls gene expression in the sensory nervous system of Caenorhabditis elegans. Nucleic acids research *38*, 3780-3793.

Clay, M.R., and Halloran, M.C. (2011). Regulation of cell adhesions and motility during initiation of neural crest migration. Current opinion in neurobiology *21*, 17-22.

Cloninger, C., Bernath, A., Bashir, T., Holmes, B., Artinian, N., Ruegg, T., Anderson, L., Masri, J., Lichtenstein, A., and Gera, J. (2011). Inhibition of SAPK2/p38 enhances sensitivity to mTORC1 inhibition by blocking IRES-mediated translation initiation in glioblastoma. Molecular cancer therapeutics *10*, 2244-2256.

Cockman, M.E., Masson, N., Mole, D.R., Jaakkola, P., Chang, G.W., Clifford, S.C., Maher, E.R., Pugh, C.W., Ratcliffe, P.J., and Maxwell, P.H. (2000). Hypoxia inducible factor-alpha binding and ubiquitylation by the von Hippel-Lindau tumor suppressor protein. J Biol Chem *275*, 25733-25741.

Crose, L.E., Galindo, K.A., Kephart, J.G., Chen, C., Fitamant, J., Bardeesy, N., Bentley, R.C., Galindo, R.L., Chi, J.T., and Linardic, C.M. (2014). Alveolar rhabdomyosarcoma-associated PAX3-FOXO1 promotes tumorigenesis via Hippo pathway suppression. J Clin Invest *124*, 285-296.

Dayan, F., Roux, D., Brahimi-Horn, M.C., Pouyssegur, J., and Mazure, N.M. (2006). The oxygen sensor factor-inhibiting hypoxia-inducible factor-1 controls expression of distinct genes through the bifunctional transcriptional character of hypoxia-inducible factor-1alpha. Cancer Res *66*, 3688-3698.

Demuth, T., Reavie, L.B., Rennert, J.L., Nakada, M., Nakada, S., Hoelzinger, D.B., Beaudry, C.E., Henrichs, A.N., Anderson, E.M., and Berens, M.E. (2007). MAP-ing glioma invasion: mitogen-activated protein kinase kinase 3 and p38 drive glioma invasion and progression and predict patient survival. Molecular cancer therapeutics *6*, 1212-1222.

den Bakker, M.A., Tascilar, M., Riegman, P.H., Hekman, A.C., Boersma, W., Janssen, P.J., de Jong, T.A., Hendriks, W., van der Kwast, T.H., and Zwarthoff, E.C. (1995). Neurofibromatosis type 2 protein co-localizes with elements of the cytoskeleton. Am J Pathol *147*, 1339-1349.

Detwiller, K.Y., Fernando, N.T., Segal, N.H., Ryeom, S.W., D'Amore, P.A., and Yoon, S.S. (2005). Analysis of hypoxia-related gene expression in sarcomas and effect of hypoxia on RNA interference of vascular endothelial cell growth factor A. Cancer Res *65*, 5881-5889.

Dong, J., Feldmann, G., Huang, J., Wu, S., Zhang, N., Comerford, S.A., Gayyed, M.F., Anders, R.A., Maitra, A., and Pan, D. (2007). Elucidation of a universal size-control mechanism in Drosophila and mammals. Cell *130*, 1120-1133.

Dupont, S., Morsut, L., Aragona, M., Enzo, E., Giulitti, S., Cordenonsi, M., Zanconato, F., Le Digabel, J., Forcato, M., Bicciato, S.*, et al.* (2011). Role of YAP/TAZ in mechanotransduction. Nature *474*, 179-183.

Eisinger-Mathason, T.S., Zhang, M., Qiu, Q., Skuli, N., Nakazawa, M.S., Karakasheva, T., Mucaj, V., Shay, J.E., Stangenberg, L., Sadri, N.*, et al.* (2013). Hypoxia-dependent modification of collagen networks promotes sarcoma metastasis. Cancer Discov *3*, 1190-1205.

Erler, J.T., Bennewith, K.L., Nicolau, M., Dornhofer, N., Kong, C., Le, Q.T., Chi, J.T., Jeffrey, S.S., and Giaccia, A.J. (2006). Lysyl oxidase is essential for hypoxia-induced metastasis. Nature *440*, 1222-1226.

Esquela-Kerscher, A., and Slack, F.J. (2006a). Oncomirs - microRNAs with a role in cancer. Nature reviews Cancer *6*, 259-269.

Esquela-Kerscher, A., and Slack, F.J. (2006b). Oncomirs - microRNAs with a role in cancer. Nat Rev Cancer *6*, 259-269.

Evans, S.M., Jenkins, K.W., Chen, H.I., Jenkins, W.T., Judy, K.D., Hwang, W.-T., Lustig, R.A., Judkins, A.R., Grady, M.S., Hahn, S.M.*, et al.* (2010). The Relationship among Hypoxia, Proliferation, and Outcome in Patients with De Novo Glioblastoma: A Pilot Study. Translational oncology *3*, 160-169.

Fan, R., Kim, N.G., and Gumbiner, B.M. (2013). Regulation of Hippo pathway by mitogenic growth factors via phosphoinositide 3-kinase and phosphoinositide-dependent kinase-1. Proc Natl Acad Sci U S A *110*, 2569-2574.

Feng, Y., and Irvine, K.D. (2007). Fat and expanded act in parallel to regulate growth through warts. Proc Natl Acad Sci U S A *104*, 20362-20367.

Fernandez, L.A., Northcott, P.A., Dalton, J., Fraga, C., Ellison, D., Angers, S., Taylor, M.D., and Kenney, A.M. (2009). YAP1 is amplified and up-regulated in hedgehog-associated medulloblastomas and mediates Sonic hedgehog-driven neural precursor proliferation. Genes Dev *23*, 2729-2741.

Folkman, J. (2002). Role of angiogenesis in tumor growth and metastasis. Seminars in oncology *29*, 15-18.

Gao, F.-B. (2010). Context-dependent functions of specific microRNAs in neuronal development. Neural development *5*, 25.

Genevet, A., Wehr, M.C., Brain, R., Thompson, B.J., and Tapon, N. (2010). Kibra is a regulator of the Salvador/Warts/Hippo signaling network. Developmental cell *18*, 300-308.

Gilkes, D.M., Chaturvedi, P., Bajpai, S., Wong, C.C., Wei, H., Pitcairn, S., Hubbi, M.E., Wirtz, D., and Semenza, G.L. (2013). Collagen Prolyl Hydroxylases Are Essential for Breast Cancer Metastasis. Cancer Res.

Godlewski, J., Nowicki, M.O., Bronisz, A., Nuovo, G., Palatini, J., De Lay, M., Van Brocklyn, J., Ostrowski, M.C., Chiocca, E.A., and Lawler, S.E. (2010). MicroRNA-451 regulates LKB1/AMPK signaling and allows adaptation to metabolic stress in glioma cells. Mol Cell *37*, 620-632.

Godlewski, J., Nowicki, M.O., Bronisz, A., Williams, S., Otsuki, A., Nuovo, G., Raychaudhury, A., Newton, H.B., Chiocca, E.A., and Lawler, S. (2008). Targeting of the Bmi-1 oncogene/stem cell renewal factor by microRNA-128 inhibits glioma proliferation and self-renewal. Cancer research *68*, 9125-9130.

Gros, J., Serralbo, O., and Marcelle, C. (2009). WNT11 acts as a directional cue to organize the elongation of early muscle fibres. Nature *457*, 589-593.

Grusche, F.A., Richardson, H.E., and Harvey, K.F. (2010). Upstream regulation of the hippo size control pathway. Current biology : CB *20*, R574-582.

Gumbiner, B.M., and Kim, N.G. (2014). The Hippo-YAP signaling pathway and contact inhibition of growth. Journal of cell science *127*, 709-717.

Gusarova, G.A., Wang, I.C., Major, M.L., Kalinichenko, V.V., Ackerson, T., Petrovic, V., and Costa, R.H. (2007). A cell-penetrating ARF peptide inhibitor of FoxM1 in mouse hepatocellular carcinoma treatment. J Clin Invest *117*, 99-111.

Halasi, M., and Gartel, A.L. (2009). A novel mode of FoxM1 regulation: positive auto-regulatory loop. Cell Cycle *8*, 1966-1967.

Halasi, M., and Gartel, A.L. (2013). FOX(M1) news--it is cancer. Mol Cancer Ther *12*, 245-254.

Hamaratoglu, F., Willecke, M., Kango-Singh, M., Nolo, R., Hyun, E., Tao, C., Jafar-Nejad, H., and Halder, G. (2006). The tumour-suppressor genes NF2/Merlin and Expanded act through Hippo signalling to regulate cell proliferation and apoptosis. Nat Cell Biol *8*, 27-36.

Hanahan, D., and Weinberg, R.A. (2000). The hallmarks of cancer. Cell *100*, 57-70.

Hanahan, D., and Weinberg, R.A. (2011). Hallmarks of cancer: the next generation. Cell *144*, 646-674.

Hao, Y., Chun, A., Cheung, K., Rashidi, B., and Yang, X. (2008). Tumor suppressor LATS1 is a negative regulator of oncogene YAP. J Biol Chem *283*, 5496-5509.

Harvey, K.F., Pfleger, C.M., and Hariharan, I.K. (2003). The Drosophila Mst ortholog, hippo, restricts growth and cell proliferation and promotes apoptosis. Cell *114*, 457-467.

Harvey, K.F., Zhang, X., and Thomas, D.M. (2013). The Hippo pathway and human cancer. Nat Rev Cancer *13*, 246-257.

Hatziapostolou, M., Polytarchou, C., Aggelidou, E., Drakaki, A., Poultsides, G.A., Jaeger, S.A., Ogata, H., Karin, M., Struhl, K., Hadzopoulou-Cladaras, M.*, et al.* (2011). An HNF4α-miRNA inflammatory feedback circuit regulates hepatocellular oncogenesis. Cell *147*, 1233-1247.

Hergovich, A., Schmitz, D., and Hemmings, B.A. (2006). The human tumour suppressor LATS1 is activated by human MOB1 at the membrane. Biochemical and biophysical research communications *345*, 50-58.

Hetz, C., Chevet, E., and Harding, H.P. (2013). Targeting the unfolded protein response in disease. Nature reviews Drug discovery *12*, 703-719.

101

Hori, O., Miyazaki, M., Tamatani, T., Ozawa, K., Takano, K., Okabe, M., Ikawa, M., Hartmann, E., Mai, P., Stern, D.M.*, et al.* (2006a). Deletion of SERP1/RAMP4, a component of the endoplasmic reticulum (ER) translocation sites, leads to ER stress. Molecular and cellular biology *26*, 4257-4267.

Hori, O., Miyazaki, M., Tamatani, T., Ozawa, K., Takano, K., Okabe, M., Ikawa, M., Hartmann, E., Mai, P., Stern, D.M.*, et al.* (2006b). Deletion of SERP1/RAMP4, a component of the endoplasmic reticulum (ER) translocation sites, leads to ER stress. Mol Cell Biol *26*, 4257-4267.

Huang, J., Wu, S., Barrera, J., Matthews, K., and Pan, D. (2005). The Hippo signaling pathway coordinately regulates cell proliferation and apoptosis by inactivating Yorkie, the Drosophila Homolog of YAP. Cell *122*, 421-434.

Huang, X., Ding, L., Bennewith, K.L., Tong, R.T., Welford, S.M., Ang, K.K., Story, M., Le, Q.-T., and Giaccia, A.J. (2009). Hypoxia-inducible mir-210 regulates normoxic gene expression involved in tumor initiation. Molecular cell *35*, 856-867.

Hunt, S., Jones, A.V., Hinsley, E.E., Whawell, S.A., and Lambert, D.W. (2011). MicroRNA-124 suppresses oral squamous cell carcinoma motility by targeting ITGB1. FEBS letters *585*, 187-192.

Jaakkola, P., Mole, D.R., Tian, Y.M., Wilson, M.I., Gielbert, J., Gaskell, S.J., von Kriegsheim, A., Hebestreit, H.F., Mukherji, M., Schofield, C.J.*, et al.* (2001). Targeting of HIF-alpha to the von Hippel-Lindau ubiquitylation complex by O2-regulated prolyl hydroxylation. Science *292*, 468-472.

Ji, M., Yang, S., Chen, Y., Xiao, L., Zhang, L., and Dong, J. (2012). Phospho-regulation of KIBRA by CDK1 and CDC14 phosphatase controls cell-cycle progression. The Biochemical journal *447*, 93-102.

Jia, J., Zhang, W., Wang, B., Trinko, R., and Jiang, J. (2003). The Drosophila Ste20 family kinase dMST functions as a tumor suppressor by restricting cell proliferation and promoting apoptosis. Genes Dev *17*, 2514-2519.

Jiao, S., Wang, H., Shi, Z., Dong, A., Zhang, W., Song, X., He, F., Wang, Y., Zhang, Z., Wang, W.*, et al.* (2014). A peptide mimicking VGLL4 function acts as a YAP antagonist therapy against gastric cancer. Cancer Cell *25*, 166-180.

Johnson, R., and Halder, G. (2014). The two faces of Hippo: targeting the Hippo pathway for regenerative medicine and cancer treatment. Nature reviews Drug discovery *13*, 63-79.

Kaelin, W.G., and Ratcliffe, P.J. (2008). Oxygen sensing by metazoans: the central role of the HIF hydroxylase pathway. Molecular cell *30*, 393-402.

Kalinichenko, V.V., Major, M.L., Wang, X., Petrovic, V., Kuechle, J., Yoder, H.M., Dennewitz, M.B., Shin, B., Datta, A., Raychaudhuri, P.*, et al.* (2004). Foxm1b transcription factor

is essential for development of hepatocellular carcinomas and is negatively regulated by the p19ARF tumor suppressor. Genes Dev *18*, 830-850.

Kalinichenko, V.V., Zhou, Y., Bhattacharyya, D., Kim, W., Shin, B., Bambal, K., and Costa, R.H. (2002). Haploinsufficiency of the mouse Forkhead Box f1 gene causes defects in gall bladder development. J Biol Chem *277*, 12369-12374.

Kang, K., Peng, X., Zhang, X., Wang, Y., Zhang, L., Gao, L., Weng, T., Zhang, H., Ramchandran, R., Raj, J.U.*, et al.* (2013). MicroRNA-124 suppresses the transactivation of nuclear factor of activated T cells by targeting multiple genes and inhibits the proliferation of pulmonary artery smooth muscle cells. J Biol Chem *288*, 25414-25427.

Keith, B., Johnson, R.S., and Simon, M.C. (2012). HIF1alpha and HIF2alpha: sibling rivalry in hypoxic tumour growth and progression. Nat Rev Cancer *12*, 9-22.

Keith, B., and Simon, M.C. (2007). Hypoxia-inducible factors, stem cells, and cancer. Cell *129*, 465-472.

Kelleher, F.C., and Viterbo, A. (2013). Histologic and genetic advances in refining the diagnosis of "undifferentiated pleomorphic sarcoma". Cancers (Basel) *5*, 218-233.

Kim, J.E., Finlay, G.J., and Baguley, B.C. (2013). The role of the hippo pathway in melanocytes and melanoma. Front Oncol *3*, 123.

Kirsch, D.G., Dinulescu, D.M., Miller, J.B., Grimm, J., Santiago, P.M., Young, N.P., Nielsen, G.P., Quade, B.J., Chaber, C.J., Schultz, C.P.*, et al.* (2007). A spatially and temporally restricted mouse model of soft tissue sarcoma. Nat Med *13*, 992-997.

Koivunen, P., Lee, S., Duncan, C.G., Lopez, G., Lu, G., Ramkissoon, S., Losman, J.A., Joensuu, P., Bergmann, U., Gross, S.*, et al.* (2012). Transformation by the (R)-enantiomer of 2-hydroxyglutarate linked to EGLN activation. Nature *483*, 484-488.

Krex, D., Klink, B., Hartmann, C., von Deimling, A., Pietsch, T., Simon, M., Sabel, M., Steinbach, J.P., Heese, O., Reifenberger, G.*, et al.* (2007). Long-term survival with glioblastoma multiforme. Brain : a journal of neurology *130*, 2596-2606.

Lamar, J.M., Stern, P., Liu, H., Schindler, J.W., Jiang, Z.G., and Hynes, R.O. (2012). The Hippo pathway target, YAP, promotes metastasis through its TEAD-interaction domain. Proc Natl Acad Sci U S A *109*, E2441-2450.

Lamouille, S., Xu, J., and Derynck, R. (2014). Molecular mechanisms of epithelial-mesenchymal transition. Nature reviews Molecular cell biology *15*, 178-196.

Lawson, S.K., Dobrikova, E.Y., Shveygert, M., and Gromeier, M. (2013). p38alpha mitogen-activated protein kinase depletion and repression of signal transduction to translation machinery by miR-124 and -128 in neurons. Mol Cell Biol *33*, 127-135.

Lee, R.C., Feinbaum, R.L., and Ambros, V. (1993). The C. elegans heterochronic gene lin-4 encodes small RNAs with antisense complementarity to lin-14. Cell *75*, 843-854.

Li, D., Chen, P., Li, X.-Y., Zhang, L.-Y., Xiong, W., Zhou, M., Xiao, L., Zeng, F., Li, X.-L., Wu, M.-H.*, et al.* (2011). Grade-specific expression profiles of miRNAs/mRNAs and docking study in human grade I-III astrocytomas. Omics : a journal of integrative biology *15*, 673-682.

Lim, L.P., Lau, N.C., Garrett-Engele, P., Grimson, A., Schelter, J.M., Castle, J., Bartel, D.P., Linsley, P.S., and Johnson, J.M. (2005). Microarray analysis shows that some microRNAs downregulate large numbers of target mRNAs. Nature *433*, 769-773.

Linehan, D.C., Lewis, J.J., Leung, D., and Brennan, M.F. (2000). Influence of biologic factors and anatomic site in completely resected liposarcoma. J Clin Oncol *18*, 1637-1643.

Liu, X.S., Chopp, M., Zhang, R.L., Tao, T., Wang, X.L., Kassis, H., Hozeska-Solgot, A., Zhang, L., Chen, C., and Zhang, Z.G. (2011). MicroRNA profiling in subventricular zone after stroke: MiR-124a regulates proliferation of neural progenitor cells through Notch signaling pathway. PloS one *6*, e23461.

Liu-Chittenden, Y., Huang, B., Shim, J.S., Chen, Q., Lee, S.J., Anders, R.A., Liu, J.O., and Pan, D. (2012). Genetic and pharmacological disruption of the TEAD-YAP complex suppresses the oncogenic activity of YAP. Genes Dev *26*, 1300-1305.

Lok, G.T., Chan, D.W., Liu, V.W., Hui, W.W., Leung, T.H., Yao, K.M., and Ngan, H.Y. (2011). Aberrant activation of ERK/FOXM1 signaling cascade triggers the cell migration/invasion in ovarian cancer cells. PLoS One *6*, e23790.

Louis, D.N., Ohgaki, H., Wiestler, O.D., Cavenee, W.K., Burger, P.C., Jouvet, A., Scheithauer, B.W., and Kleihues, P. (2007). The 2007 WHO classification of tumours of the central nervous system. Acta neuropathologica *114*, 97-109.

Lu, L., Li, Y., Kim, S.M., Bossuyt, W., Liu, P., Qiu, Q., Wang, Y., Halder, G., Finegold, M.J., Lee, J.S.*, et al.* (2010). Hippo signaling is a potent in vivo growth and tumor suppressor pathway in the mammalian liver. Proc Natl Acad Sci U S A *107*, 1437-1442.

Majmundar, A.J., Wong, W.J., and Simon, M.C. (2010). Hypoxia-inducible factors and the response to hypoxic stress. Mol Cell *40*, 294-309.

Makeyev, E.V., Zhang, J., Carrasco, M.A., and Maniatis, T. (2007a). The MicroRNA miR-124 promotes neuronal differentiation by triggering brain-specific alternative pre-mRNA splicing. Mol Cell *27*, 435-448.

Makeyev, E.V., Zhang, J., Carrasco, M.A., and Maniatis, T. (2007b). The MicroRNA miR-124 promotes neuronal differentiation by triggering brain-specific alternative pre-mRNA splicing. Molecular cell *27*, 435-448.

Malt, A., Cagliero, J., Legent, K., Silber, J., Zider, A., Flagiello, D., and S. (2012). Landin Alteration of TEAD1 expression levels confers apoptotic resistance through the transcriptional up-regulation of Livin. PLo e45498 Epub 1003 *7*.

Mao, Y., Mulvaney, J., Zakaria, S., Yu, T., Morgan, K.M., Allen, S., Basson, M.A., Francis-West, P., and Irvine, K.D. (2011). Characterization of a Dchs1 mutant mouse reveals requirements for Dchs1-Fat4 signaling during mammalian development. Development *138*, 947-957.

Mathew, L.K., Lee, S.S., Skuli, N., Rao, S., Keith, B., Nathanson, K.L., Lal, P., and Simon, M.C. (2014a). Restricted expression of miR-30c-2-3p and miR-30a-3p in clear cell renal cell carcinomas enhances HIF2alpha activity. Cancer Discov *4*, 53-60.

Mathew, L.K., Skuli, N., Mucaj, V., Lee, S.S., Zinn, P.O., Sathyan, P., Imtiyaz, H.Z., Zhang, Z., Davuluri, R.V., Rao, S.*, et al.* (2014b). miR-218 opposes a critical RTK-HIF pathway in mesenchymal glioblastoma. Proc Natl Acad Sci U S A *111*, 291-296.

Matsuura, K., Nakada, C., Mashio, M., Narimatsu, T., Yoshimoto, T., Tanigawa, M., Tsukamoto, Y., Hijiya, N., Takeuchi, I., Nomura, T.*, et al.* (2011). Downregulation of SAV1 plays a role in pathogenesis of high-grade clear cell renal cell carcinoma. BMC Cancer *11*, 523.

McCaffrey, L.M., and Macara, I.G. (2011). Epithelial organization, cell polarity and tumorigenesis. Trends in cell biology *21*, 727-735.

McCartney, B.M., Kulikauskas, R.M., LaJeunesse, D.R., and Fehon, R.G. (2000). The neurofibromatosis-2 homologue, Merlin, and the tumor suppressor expanded function together in Drosophila to regulate cell proliferation and differentiation. Development *127*, 1315-1324.

McClatchey, A.I., Saotome, I., Mercer, K., Crowley, D., Gusella, J.F., Bronson, R.T., and Jacks, T. (1998). Mice heterozygous for a mutation at the Nf2 tumor suppressor locus develop a range of highly metastatic tumors. Genes Dev *12*, 1121-1133.

Michels, S., and Schmidt-Erfurth, U. (2001). Photodynamic therapy with verteporfin: a new treatment in ophthalmology. Semin Ophthalmol *16*, 201-206.

Miller, E., Yang, J., DeRan, M., Wu, C., Su, A.I., Bonamy, G.M., Liu, J., Peters, E.C., and Wu, X. (2012). Identification of serum-derived sphingosine-1-phosphate as a small molecule regulator of YAP. Chemistry & biology *19*, 955-962.

Mito, J.K., Riedel, R.F., Dodd, L., Lahat, G., Lazar, A.J., Dodd, R.D., Stangenberg, L., Eward, W.C., Hornicek, F.J., Yoon, S.S.*, et al.* (2009). Cross species genomic analysis identifies a mouse model as undifferentiated pleomorphic sarcoma/malignant fibrous histiocytoma. PLoS One *4*, e8075.

Mizuno, T., Murakami, H., Fujii, M., Ishiguro, F., Tanaka, I., Kondo, Y., Akatsuka, S., Toyokuni, S., Yokoi, K., Osada, H.*, et al.* (2012). YAP induces malignant mesothelioma cell

proliferation by upregulating transcription of cell cycle-promoting genes. Oncogene *31*, 5117-5122.

Mlodzik, M. (2002). Planar cell polarization: do the same mechanisms regulate Drosophila tissue polarity and vertebrate gastrulation? Trends Genet *18*, 564-571.

Mo, J.S., Park, H.W., and Guan, K.L. (2014). The Hippo signaling pathway in stem cell biology and cancer. EMBO reports *15*, 642-656.

Mo, J.S., Yu, F.X., Gong, R., Brown, J.H., and Guan, K.L. (2012). Regulation of the Hippo-YAP pathway by protease-activated receptors (PARs). Genes Dev *26*, 2138-2143.

Mucaj, V., Lee, S.S., Skuli, N., Giannoukos, D.N., Qiu, B., Eisinger-Mathason, T.S., Nakazawa, M.S., Shay, J.E., Gopal, P.P., Venneti, S*., et al.* (2014). MicroRNA-124 expression counteracts pro-survival stress responses in glioblastoma. Oncogene.

Mucaj, V., Shay, J.E., and Simon, M.C. (2012). Effects of hypoxia and HIFs on cancer metabolism. Int J Hematol *95*, 464-470.

Muramatsu, T., Imoto, I., Matsui, T., Kozaki, K., Haruki, S., Sudol, M., Shimada, Y., Tsuda, H., Kawano, T., and Inazawa, J. (2011). YAP is a candidate oncogene for esophageal squamous cell carcinoma. Carcinogenesis *32*, 389-398.

Nakayama, R., Nemoto, T., Takahashi, H., Ohta, T., Kawai, A., Seki, K., Yoshida, T., Toyama, Y., Ichikawa, H., and Hasegawa, T. (2007). Gene expression analysis of soft tissue sarcomas: characterization and reclassification of malignant fibrous histiocytoma. Mod Pathol *20*, 749-759.

Nelson, P.T., Baldwin, D.A., Kloosterman, W.P., Kauppinen, S., Plasterk, R.H.A., and Mourelatos, Z. (2006). RAKE and LNA-ISH reveal microRNA expression and localization in archival human brain. RNA (New York, NY) *12*, 187-191.

Oh, H., Reddy, B.V., and Irvine, K.D. (2009). Phosphorylation-independent repression of Yorkie in Fat-Hippo signaling. Dev Biol *335*, 188-197.

Oka, T., Mazack, V., and Sudol, M. (2008). Mst2 and Lats kinases regulate apoptotic function of Yes kinase-associated protein (YAP). J Biol Chem *283*, 27534-27546.

Oka, T., Remue, E., Meerschaert, K., Vanloo, B., Boucherie, C., Gfeller, D., Bader, G.D., Sidhu, S.S., Vandekerckhove, J., Gettemans, J*., et al.* (2010). Functional complexes between YAP2 and ZO-2 are PDZ domain-dependent, and regulate YAP2 nuclear localization and signalling. Biochem J *432*, 461-472.

Overholtzer, M., Zhang, J., Smolen, G.A., Muir, B., Li, W., Sgroi, D.C., Deng, C.X., Brugge, J.S., and Haber, D.A. (2006). Transforming properties of YAP, a candidate oncogene on the chromosome 11q22 amplicon. Proc Natl Acad Sci U S A *103*, 12405-12410.

Paillas, S., Causse, A., Marzi, L., de Medina, P., Poirot, M., Denis, V., Vezzio-Vie, N., Espert, L., Arzouk, H., Coquelle, A.*, et al.* (2012). MAPK14/p38α confers irinotecan resistance to TP53-defective cells by inducing survival autophagy. Autophagy *8*, 1098-1112.

Pan, D. (2007). Hippo signaling in organ size control. Genes Dev *21*, 886-897.

Pan, D. (2010). The hippo signaling pathway in development and cancer. Developmental cell *19*, 491-505.

Pandit, B., Halasi, M., and Gartel, A.L. (2009). p53 negatively regulates expression of FoxM1. Cell Cycle *8*, 3425-3427.

Parham, D.M., and Ellison, D.A. (2006). Rhabdomyosarcomas in adults and children: an update. Arch Pathol Lab Med *130*, 1454-1465.

Park, H.J., Gusarova, G., Wang, Z., Carr, J.R., Li, J., Kim, K.H., Qiu, J., Park, Y.D., Williamson, P.R., Hay, N.*, et al.* (2011). Deregulation of FoxM1b leads to tumour metastasis. EMBO Mol Med *3*, 21-34.

Park, H.W., and Guan, K.L. (2013). Regulation of the Hippo pathway and implications for anticancer drug development. Trends Pharmacol Sci *34*, 581-589.

Ponomarev, E.D., Veremeyko, T., Barteneva, N., Krichevsky, A.M., and Weiner, H.L. (2011). MicroRNA-124 promotes microglia quiescence and suppresses EAE by deactivating macrophages via the C/EBP-alpha-PU.1 pathway. Nat Med *17*, 64-70.

Pouyssegur, J., Dayan, F., and Mazure, N.M. (2006). Hypoxia signalling in cancer and approaches to enforce tumour regression. Nature *441*, 437-443.

Praskova, M., Khoklatchev, A., Ortiz-Vega, S., and Avruch, J. (2004). Regulation of the MST1 kinase by autophosphorylation, by the growth inhibitory proteins, RASSF1 and NORE1, and by Ras. The Biochemical journal *381*, 453-462.

Reuven, N., Adler, J., Meltser, V., and Shaul, Y. (2013). The Hippo pathway kinase Lats2 prevents DNA damage-induced apoptosis through inhibition of the tyrosine kinase c-Abl. Cell death and differentiation *20*, 1330-1340.

Rong, Y., Durden, D.L., Van Meir, E.G., and Brat, D.J. (2006). 'Pseudopalisading' necrosis in glioblastoma: a familiar morphologic feature that links vascular pathology, hypoxia, and angiogenesis. J Neuropathol Exp Neurol *65*, 529-539.

Sasaki, K., Hitora, T., Nakamura, O., Kono, R., and Yamamoto, T. (2011). The role of MAPK pathway in bone and soft tissue tumors. Anticancer Res *31*, 549-553.

Schlegelmilch, K., Mohseni, M., Kirak, O., Pruszak, J., Rodriguez, J.R., Zhou, D., Kreger, B.T., Vasioukhin, V., Avruch, J., Brummelkamp, T.R.*, et al.* (2011). Yap1 acts downstream of alpha-catenin to control epidermal proliferation. Cell *144*, 782-795.

Sebe-Pedros, A., Zheng, Y., Ruiz-Trillo, I., and Pan, D. (2012). Premetazoan origin of the hippo signaling pathway. Cell reports *1*, 13-20.

Seidel, C., Schagdarsurengin, U., Blumke, K., Wurl, P., Pfeifer, G.P., Hauptmann, S., Taubert, H., and Dammann, R. (2007). Frequent hypermethylation of MST1 and MST2 in soft tissue sarcoma. Mol Carcinog *46*, 865-871.

Sekido, Y., Pass, H.I., Bader, S., Mew, D.J., Christman, M.F., Gazdar, A.F., and Minna, J.D. (1995). Neurofibromatosis type 2 (NF2) gene is somatically mutated in mesothelioma but not in lung cancer. Cancer Res *55*, 1227-1231.

Semenza, G.L. (2007). Life with oxygen. Science *318*, 62-64.

Shao, D., Zhai, P., Del Re, D.P., Sciarretta, S., Yabuta, N., Nojima, H., Lim, D.S., Pan, D., and Sadoshima, J. (2014). A functional interaction between Hippo-YAP signalling and FoxO1 mediates the oxidative stress response. Nat Commun *5*, 3315.

Shaw, R.J., McClatchey, A.I., and Jacks, T. (1998). Localization and functional domains of the neurofibromatosis type II tumor suppressor, merlin. Cell growth & differentiation : the molecular biology journal of the American Association for Cancer Research *9*, 287-296.

Silber, J., Lim, D.A., Petritsch, C., Persson, A.I., Maunakea, A.K., Yu, M., Vandenberg, S.R., Ginzinger, D.G., James, C.D., Costello, J.F.*, et al.* (2008a). miR-124 and miR-137 inhibit proliferation of glioblastoma multiforme cells and induce differentiation of brain tumor stem cells. BMC medicine *6*, 14.

Silber, J., Lim, D.A., Petritsch, C., Persson, A.I., Maunakea, A.K., Yu, M., Vandenberg, S.R., Ginzinger, D.G., James, C.D., Costello, J.F.*, et al.* (2008b). miR-124 and miR-137 inhibit proliferation of glioblastoma multiforme cells and induce differentiation of brain tumor stem cells. BMC Med *6*, 14.

Silva, E., Tsatskis, Y., Gardano, L., Tapon, N., and McNeill, H. (2006). The tumor-suppressor gene fat controls tissue growth upstream of expanded in the hippo signaling pathway. Current biology : CB *16*, 2081-2089.

Simons, M., and Mlodzik, M. (2008). Planar cell polarity signaling: from fly development to human disease. Annual review of genetics *42*, 517-540.

Sonntag, K.C., Woo, T.-U.W., and Krichevsky, A.M. (2012). Converging miRNA functions in diverse brain disorders: a case for miR-124 and miR-126. Experimental neurology *235*, 427-435.

Sorrentino, G., Ruggeri, N., Specchia, V., Cordenonsi, M., Mano, M., Dupont, S., Manfrin, A., Ingallina, E., Sommaggio, R., Piazza, S.*, et al.* (2014). Metabolic control of YAP and TAZ by the mevalonate pathway. Nat Cell Biol *16*, 357-366.

Spence, A.M., Muzi, M., Swanson, K.R., O'Sullivan, F., Rockhill, J.K., Rajendran, J.G., Adamsen, T.C.H., Link, J.M., Swanson, P.E., Yagle, K.J.*, et al.* (2008). Regional hypoxia in glioblastoma multiforme quantified with [18F]fluoromisonidazole positron emission tomography before radiotherapy: correlation with time to progression and survival. Clinical cancer research : an official journal of the American Association for Cancer Research *14*, 2623-2630.

St John, M.A., Tao, W., Fei, X., Fukumoto, R., Carcangiu, M.L., Brownstein, D.G., Parlow, A.F., McGrath, J., and Xu, T. (1999). Mice deficient of Lats1 develop soft-tissue sarcomas, ovarian tumours and pituitary dysfunction. Nat Genet *21*, 182-186.

Stanger, B.Z. (2012). Quit your YAPing: a new target for cancer therapy. Genes Dev *26*, 1263-1267.

Stupp, R., Mason, W.P., van den Bent, M.J., Weller, M., Fisher, B., Taphoorn, M.J.B., Belanger, K., Brandes, A.A., Marosi, C., Bogdahn, U.*, et al.* (2005). Radiotherapy plus concomitant and adjuvant temozolomide for glioblastoma. The New England journal of medicine *352*, 987-996.

Sudol, M. (1994). Yes-associated protein (YAP65) is a proline-rich phosphoprotein that binds to the SH3 domain of the Yes proto-oncogene product. Oncogene *9*, 2145-2152.

Sudol, M., and Harvey, K.F. (2010). Modularity in the Hippo signaling pathway. Trends in biochemical sciences *35*, 627-633.

Sudol, M., Shields, D.C., and Farooq, A. (2012). Structures of YAP protein domains reveal promising targets for development of new cancer drugs. Seminars in cell & developmental biology *23*, 827-833.

Tada, M., and Kai, M. (2012). Planar cell polarity in coordinated and directed movements. Curr Top Dev Biol *101*, 77-110.

Taylor, B.S., Barretina, J., Maki, R.G., Antonescu, C.R., Singer, S., and Ladanyi, M. (2011). Advances in sarcoma genomics and new therapeutic targets. Nat Rev Cancer *11*, 541-557.

Tremblay, A.M., Missiaglia, E., Galli, G.G., Hettmer, S., Urcia, R., Carrara, M., Judson, R.N., Thway, K., Nadal, G., Selfe, J.L.*, et al.* (2014). The Hippo Transducer YAP1 Transforms Activated Satellite Cells and Is a Potent Effector of Embryonal Rhabdomyosarcoma Formation. Cancer Cell *26*, 273-287.

Udan, R.S., Kango-Singh, M., Nolo, R., Tao, C., and Halder, G. (2003). Hippo promotes proliferation arrest and apoptosis in the Salvador/Warts pathway. Nat Cell Biol *5*, 914-920.

Varelas, X. (2014). The Hippo pathway effectors TAZ and YAP in development, homeostasis and disease. Development *141*, 1614-1626.

Varelas, X., Samavarchi-Tehrani, P., Narimatsu, M., Weiss, A., Cockburn, K., Larsen, B.G., Rossant, J., and Wrana, J.L. (2010). The Crumbs complex couples cell density sensing to Hippo-dependent control of the TGF-beta-SMAD pathway. Developmental cell *19*, 831-844.

Vartanian, A., Singh, S.K., Agnihotri, S., Jalali, S., Burrell, K., Aldape, K.D., and Zadeh, G. (2014). GBM's multifaceted landscape: highlighting regional and microenvironmental heterogeneity. Neuro Oncol *16*, 1167-1175.

Verhaak, R.G.W., Hoadley, K.A., Purdom, E., Wang, V., Qi, Y., Wilkerson, M.D., Miller, C.R., Ding, L., Golub, T., Mesirov, J.P., *et al.* (2010). Integrated genomic analysis identifies clinically relevant subtypes of glioblastoma characterized by abnormalities in PDGFRA, IDH1, EGFR, and NF1. Cancer cell *17*, 98-110.

Visvader, J.E. (2011). Cells of origin in cancer. Nature *469*, 314-322.

Visvanathan, J., Lee, S., Lee, B., Lee, J.W., and Lee, S.-K. (2007). The microRNA miR-124 antagonizes the anti-neural REST/SCP1 pathway during embryonic CNS development. Genes & development *21*, 744-749.

Wada, K., Itoga, K., Okano, T., Yonemura, S., and Sasaki, H. (2011). Hippo pathway regulation by cell morphology and stress fibers. Development *138*, 3907-3914.

Wagner, E.F., and Nebreda, A.R. (2009). Signal integration by JNK and p38 MAPK pathways in cancer development. Nature reviews Cancer *9*, 537-549.

Wang, M., and Gartel, A.L. (2011). Micelle-encapsulated thiostrepton as an effective nanomedicine for inhibiting tumor growth and for suppressing FOXM1 in human xenografts. Mol Cancer Ther *10*, 2287-2297.

Wang, W., Huang, J., Wang, X., Yuan, J., Li, X., Feng, L., Park, J.I., and Chen, J. (2012). PTPN14 is required for the density-dependent control of YAP1. Genes Dev *26*, 1959-1971.

Wei, J., Wang, F., Kong, L.Y., Xu, S., Doucette, T., Ferguson, S.D., Yang, Y., McEnery, K., Jethwa, K., Gjyshi, O., *et al.* (2013). miR-124 inhibits STAT3 signaling to enhance T cell-mediated immune clearance of glioma. Cancer Res *73*, 3913-3926.

Wierstra, I. (2013). FOXM1 (Forkhead box M1) in tumorigenesis: overexpression in human cancer, implication in tumorigenesis, oncogenic functions, tumor-suppressive properties, and target of anticancer therapy. Adv Cancer Res *119*, 191-419.

Wierstra, I., and Alves, J. (2006). Transcription factor FOXM1c is repressed by RB and activated by cyclin D1/Cdk4. Biol Chem *387*, 949-962.

Wong, C.C., Gilkes, D.M., Zhang, H., Chen, J., Wei, H., Chaturvedi, P., Fraley, S.I., Wong, C.M., Khoo, U.S., Ng, I.O., *et al.* (2011). Hypoxia-inducible factor 1 is a master regulator of breast cancer metastatic niche formation. Proc Natl Acad Sci U S A *108*, 16369-16374.

110

Wong, C.C., Zhang, H., Gilkes, D.M., Chen, J., Wei, H., Chaturvedi, P., Hubbi, M.E., and Semenza, G.L. (2012). Inhibitors of hypoxia-inducible factor 1 block breast cancer metastatic niche formation and lung metastasis. J Mol Med (Berl).

Wu, S., Huang, J., Dong, J., and Pan, D. (2003). hippo encodes a Ste-20 family protein kinase that restricts cell proliferation and promotes apoptosis in conjunction with salvador and warts. Cell *114*, 445-456.

Wu, Z., Sun, L., Wang, H., Yao, J., Jiang, C., Xu, W., and Yang, Z. (2012). MiR-328 expression is decreased in high-grade gliomas and is associated with worse survival in primary glioblastoma. PloS one *7*, e47270.

Yabuta, N., Okada, N., Ito, A., Hosomi, T., Nishihara, S., Sasayama, Y., Fujimori, A., Okuzaki, D., Zhao, H., Ikawa, M.*, et al.* (2007). Lats2 is an essential mitotic regulator required for the coordination of cell division. J Biol Chem *282*, 19259-19271.

Yamaguchi, A., Hori, O., Stern, D.M., Hartmann, E., Ogawa, S., and Tohyama, M. (1999a). Stress-associated endoplasmic reticulum protein 1 (SERP1)/Ribosome-associated membrane protein 4 (RAMP4) stabilizes membrane proteins during stress and facilitates subsequent glycosylation. The Journal of cell biology *147*, 1195-1204.

Yamaguchi, A., Hori, O., Stern, D.M., Hartmann, E., Ogawa, S., and Tohyama, M. (1999b). Stress-associated endoplasmic reticulum protein 1 (SERP1)/Ribosome-associated membrane protein 4 (RAMP4) stabilizes membrane proteins during stress and facilitates subsequent glycosylation. J Cell Biol *147*, 1195-1204.

Yi, C., Shen, Z., Stemmer-Rachamimov, A., Dawany, N., Troutman, S., Showe, L.C., Liu, Q., Shimono, A., Sudol, M., Holmgren, L.*, et al.* (2013). The p130 isoform of angiomotin is required for Yap-mediated hepatic epithelial cell proliferation and tumorigenesis. Science signaling *6*, ra77.

Yi, C., Troutman, S., Fera, D., Stemmer-Rachamimov, A., Avila, J.L., Christian, N., Persson, N.L., Shimono, A., Speicher, D.W., Marmorstein, R.*, et al.* (2011). A tight junction-associated Merlin-angiomotin complex mediates Merlin's regulation of mitogenic signaling and tumor suppressive functions. Cancer Cell *19*, 527-540.

Yi, R., and Fuchs, E. (2011). MicroRNAs and their roles in mammalian stem cells. Journal of cell science *124*, 1775-1783.

Yoo, A.S., Sun, A.X., Li, L., Shcheglovitov, A., Portmann, T., Li, Y., Lee-Messer, C., Dolmetsch, R.E., Tsien, R.W., and Crabtree, G.R. (2011). MicroRNA-mediated conversion of human fibroblasts to neurons. Nature *476*, 228-231.

Yoo, N.J., Park, S.W., and Lee, S.H. (2012). Mutational analysis of tumour suppressor gene NF2 in common solid cancers and acute leukaemias. Pathology *44*, 29-32.

Yu, F.X., and Guan, K.L. (2013). The Hippo pathway: regulators and regulations. Genes Dev *27*, 355-371.

Yu, F.X., Zhao, B., Panupinthu, N., Jewell, J.L., Lian, I., Wang, L.H., Zhao, J., Yuan, H., Tumaneng, K., Li, H.*, et al.* (2012). Regulation of the Hippo-YAP pathway by G-protein-coupled receptor signaling. Cell *150*, 780-791.

Yu, J., Zheng, Y., Dong, J., Klusza, S., Deng, W.M., and Pan, D. (2010). Kibra functions as a tumor suppressor protein that regulates Hippo signaling in conjunction with Merlin and Expanded. Developmental cell *18*, 288-299.

Zhang, J., Ji, J.Y., Yu, M., Overholtzer, M., Smolen, G.A., Wang, R., Brugge, J.S., Dyson, N.J., and Haber, D.A. (2009). YAP-dependent induction of amphiregulin identifies a non-cell-autonomous component of the Hippo pathway. Nat Cell Biol *11*, 1444-1450.

Zhang, N., Bai, H., David, K.K., Dong, J., Zheng, Y., Cai, J., Giovannini, M., Liu, P., Anders, R.A., and Pan, D. (2010). The Merlin/NF2 tumor suppressor functions through the YAP oncoprotein to regulate tissue homeostasis in mammals. Developmental cell *19*, 27-38.

Zhang, W., Nandakumar, N., Shi, Y., Manzano, M., Smith, A., Graham, G., Gupta, S., Vietsch, E.E., Laughlin, S.Z., Wadhwa, M.*, et al.* (2014). Downstream of mutant KRAS, the transcription regulator YAP is essential for neoplastic progression to pancreatic ductal adenocarcinoma. Science signaling *7*, ra42.

Zhao, B., Lei, Q.-Y., and Guan, K.-L. (2008a). The Hippo-YAP pathway: new connections between regulation of organ size and cancer. Current opinion in cell biology *20*, 638-646.

Zhao, B., Li, L., Lei, Q., and Guan, K.L. (2010a). The Hippo-YAP pathway in organ size control and tumorigenesis: an updated version. Genes Dev *24*, 862-874.

Zhao, B., Li, L., Lu, Q., Wang, L.H., Liu, C.Y., Lei, Q., and Guan, K.L. (2011a). Angiomotin is a novel Hippo pathway component that inhibits YAP oncoprotein. Genes Dev *25*, 51-63.

Zhao, B., Li, L., Tumaneng, K., Wang, C.Y., and Guan, K.L. (2010b). A coordinated phosphorylation by Lats and CK1 regulates YAP stability through SCF(beta-TRCP). Genes Dev *24*, 72-85.

Zhao, B., Li, L., Wang, L., Wang, C.Y., Yu, J., and Guan, K.L. (2012). Cell detachment activates the Hippo pathway via cytoskeleton reorganization to induce anoikis. Genes Dev *26*, 54-68.

Zhao, B., Tumaneng, K., and Guan, K.L. (2011b). The Hippo pathway in organ size control, tissue regeneration and stem cell self-renewal. Nat Cell Biol *13*, 877-883.

Zhao, B., Wei, X., Li, W., Udan, R.S., Yang, Q., Kim, J., Xie, J., Ikenoue, T., Yu, J., Li, L.*, et al.* (2007). Inactivation of YAP oncoprotein by the Hippo pathway is involved in cell contact inhibition and tissue growth control. Genes Dev *21*, 2747-2761.

Zhao, B., Ye, X., Yu, J., Li, L., Li, W., Li, S., Lin, J.D., Wang, C.Y., Chinnaiyan, A.M., Lai, Z.C.*, et al.* (2008b). TEAD mediates YAP-dependent gene induction and growth control. Genes Dev *22*, 1962-1971.

Zhao, B., Ye, X., Yu, J., Li, L., Li, W., Li, S., Yu, J., Lin, J.D., Wang, C.Y., Chinnaiyan, A.M.*, et al.* (2008c). TEAD mediates YAP-dependent gene induction and growth control. Genes Dev *22*, 1962-1971.

Zhou, D., Conrad, C., Xia, F., Park, J.S., Payer, B., Yin, Y., Lauwers, G.Y., Thasler, W., Lee, J.T., Avruch, J.*, et al.* (2009). Mst1 and Mst2 maintain hepatocyte quiescence and suppress hepatocellular carcinoma development through inactivation of the Yap1 oncogene. Cancer Cell *16*, 425-438.